The function of Copine 6

in the brain

Inauguraldissertation

zur
Erlangung der Würde eines Doktors der Philosophie
vorgelegt der
Philosophisch-Naturwissenschaftlichen Fakultät
der Universität Basel
von

Judith Reinhard

aus Horw LU

Basel, 2012

creative commons

Namensnennung-Keine kommerzielle Nutzung-Keine Bearbeitung 2.5 Schweiz

---

Sie dürfen:

das Werk vervielfältigen, verbreiten und öffentlich zugänglich machen

Zu den folgenden Bedingungen:

Namensnennung. Sie müssen den Namen des Autors/Rechteinhabers in der von ihm festgelegten Weise nennen (wodurch aber nicht der Eindruck entstehen darf, Sie oder die Nutzung des Werkes durch Sie würden entlohnt).

Keine kommerzielle Nutzung. Dieses Werk darf nicht für kommerzielle Zwecke verwendet werden.

Keine Bearbeitung. Dieses Werk darf nicht bearbeitet oder in anderer Weise verändert werden.

- Im Falle einer Verbreitung müssen Sie anderen die Lizenzbedingungen, unter welche dieses Werk fällt, mitteilen. Am Einfachsten ist es, einen Link auf diese Seite einzubinden.
- Jede der vorgenannten Bedingungen kann aufgehoben werden, sofern Sie die Einwilligung des Rechteinhabers dazu erhalten.
- Diese Lizenz lässt die Urheberpersönlichkeitsrechte unberührt.

Quelle: http://creativecommons.org/licenses/by-nc-nd/2.5/ch/ Datum: 3.4.2009

Genehmigt von der Philosophisch-Naturwissenschaftlichen Fakultät

auf Antrag von

Prof. Dr. Markus A. Rüegg

Prof. Dr. Bernhard Bettler

Basel, den 26.06.2012

Prof. Dr. Matin Spiess

Dekan

Table of Content

Summary

The formation of new or the remodeling of pre-existing synapses is thought to provide the cellular correlate of learning and memory processes. In the mammalian forebrain, the postsynaptic site of most excitatory synapses is located on dendritic spines. Even after their formation, dendritic spines remain plastic and undergo experience-dependent remodeling that correlates with adaptations in the synaptic strength. Hereby, changes in neuronal activity have to be translated into long- and short-term modifications of dendritic spines. Here, we identify Copine 6 as a novel activity sensor critically involved in these processes.

This project started with an initial characterization of Copine 6 *in vitro*. A shRNA-mediated knockdown of Copine 6 in primary hippocampal culture increases the number of dendritic spines and influences their maintenance upon changes in neuronal activity. The cytosolic Copine 6 is recruited into postsynaptic sites upon NMDA receptor activation. This translocation of Copine 6 upon increase in the intracellular calcium concentration influences the localization of its binding partner, the actin cytoskeleton modulator Rac1. We demonstrate that presence of Copine 6 affects not only the localization but also the activation state of Rac1. These data indicate that *in vitro* Copine 6 translates activity-induced calcium signals into morphological changes of the postsynapse through translocation and promotion of Rac1 activity in activated spines.

By the generation of mice deficient for Copine 6 we aimed to identify the role of Copine 6 *in vivo*. We found that Copine 6 expression is strongest in the hippocampus and starts postnatally when synapses are formed. In the hippocampus, Copine 6 expression is restricted to excitatory neurons. In line with its expression pattern, Copine 6 is dispensable for development. Copine 6 knockout mice thrive indistinguishable from their littermate controls and do not show an overt phenotype. In the hippocampus of adult Copine 6 knockout mice the spine density and morphology, and overall synaptic function is not changed, consistent with an unaffected Rac1 signaling. In contrast, loss of Copine 6 *in vivo* strongly affects synaptic plasticity. Copine 6 knockout mice are deficient in hippocampal long-term potentiation, suggesting that Copine 6 is dispensable for spine formation but essential for synaptic plasticity.

In a yeast-two hybrid screen we identified SIMPL as a novel Copine 6 interacting partner. We provide evidence that presence of Copine 6 anchors the NF-kappaB co-activator SIMPL in the cytoplasm and prevents its translocation into the nucleus. In consequence, absence of Copine 6 increases the transcriptional activity of NF-kappaB. These data indicate that Copine 6 may regulate long-term adaptations in neuronal functions that involve transcriptional regulations.

Taken together, this thesis identifies Copine 6 as an important player in the regulation of synaptic plasticity *in vitro* and *in vivo*.

CHAPTER 1

General introduction

Introduction

The human brain, the organ with which we learn and memorize consists of around 100 billion of nerve cells (neurons). The huge majorities of neurons are thought to be born within the first weeks of life and persist throughout lifetime. The ability of the brain to remain plastic after development is achieved by formation and remodeling of synaptic connections.

Synapses in the central nervous system

Synapses are the connections between neurons and manage the information transfer from one neuron to another. This connection consists of the information sending unit, the presynapse and the receiving one, the postsynapse. In the central nervous system (CNS) two kinds of synapses exist, the electrical and the chemical one. In electrical synapses, the signal from one neuron to another is transmitted via electrical current. This flow of ions is achieved by a very close proximity of pre- and postsynapse and its connection via gap junctions (paired channels in the pre- and postsynaptic membrane). This allows a very fast, also bidirectional information flow, but its simple architecture does not allow amplification (gain) of the signal transmitted. This is different for the chemical synapse, which prevails in the CNS. The space between pre- and postsynapse is substantially greater than in electrical synapses and is called the synaptic cleft. The transmission over this greater distance is achieved by the translation of the electrical signal (action potential) at the presynapse into a chemical signal that flows over the synaptic cleft and is reconverted at the postsynapse into an electrical signal. This information flow is achieved by a complex machinery at the pre- and postsynaptic site of the synapse. The chemical substance (neurotransmitter) has to be stored and secreted form the presynapse and is bound by specific receptors in the postsynaptic membrane. The properties of the receptors in the postsynapse determine whether a signal acts excitatory or inhibitory and thereby increases or decreases the probability of action potential generation in the postsynaptic neuron. The most abundant neurotransmitter in the brain is glutamate which is responsive for most of the excitatory neurotransmission. Glutamate binds to AMPA receptors, NMDA receptors and kainate receptors. All these receptors are nonselective cation channels, which means that binding of glutamate opens the channels and leads to a flux of positively charged ions (Na^+, K^+ and Ca^{2+}). The hereby caused depolarization of the postsynaptic neurons increases its probability to fire an action potential. In this way, information is transmitted from one neuron to another.

In the mammalian forebrain, the postsynaptic part of most glutamatergic synapses is located on small protrusions on dendrites called dendritic spines. Spines consist of two distinct basic compartments: the (bulbous) spine head contacting the axon and a constricted neck that connects the head to the dendritic shaft. The size and shapes of spines are very diverse. Based on microscopy studies three categories of spines based on their morphology have been identified; thin, filopodia-like protrusions (“thin spines”), short spines without well-defined spine neck (“stubby spines”) and spines with large bulbous heads and defined neck (“mushroom spines”) (Bourne and Harris, 2008). At the tip of the spine head attached to the postsynaptic membrane meshwork, electron microscopy reveals an electron dense region, the postsynaptic density (PSD). The PSD serves to cluster

neurotransmitter receptors, voltage-gated ion channels, adhesion molecules and a variety of signaling molecules of the postsynaptic machinery.

Synaptogenesis in the brain

Historically, most knowledge concerning synapse formation is based on studies on the neuromuscular junction (NMJ), a large peripheral synapse which is much more accessible than the very small neuron-neuron synapses in the brain. However, in recent years improvements in culture systems and microscopy facilitates to study the formation of neuronal synapses. Specifically, to elucidate the mechanism underlying the morphological development of synapses, i.e. the formation and maturation of dendritic spines, sheds light on the mechanisms of synaptogenesis. In the mammalian brain, synapses are formed during a protracted period during development, beginning in the embryo and expanding into early postnatal life (Ackermann and Matus, 2003), but synapses are also formed during some forms of plasticity during adulthood. During brain development, there occurs not only an increase in spine density, but also a transition of their morphology. In very young brains and immature cultures, one observes a high density of long, thin dendritic protrusions without head, termed filopodia (Fiala et al., 1998; Harris et al., 1992). These precursors of spines are gradually replaced by mature mushroom-shaped spines when a synapse matures (Ziv and Smith, 1996). Beside the sequence of morphological events during synapse assembly and maturation also some of its molecular events have been identified. Specifically, the morphological processes are accompanied by the accumulation of specific molecules in the pre- and postsynapse. The specificity of the initial axo-dendritic connection is thought to be guaranteed by the specific conjunction of adhesion molecules (Dalva et al., 2007), later on trans-synaptic signals coordinate the pre- and postsynaptic assembly. Several lines of evidence indicate that synaptic activity is required for some aspects of synapse maturations or the refinement (pruning) of synaptic connections (Cohen-Cory, 2002). However, it has been shown that blockage of synaptic activity by pharmacological or genetic manipulation does not impair the formation of central synapses (Varoqueaux et al., 2002; Verhage et al., 2000).

Synaptic plasticity

Even after their formation, synapses remain dynamic, rather than static, and are susceptible to remodeling according to the strength of the synaptic input. This input-specific strengthening or weakening of a synaptic connection is thought to be the cellular correlate of learning and memory (Bliss and Collingridge, 1993). According to the persistence of such changes one discriminates short- and long-term forms of synaptic plasticity. Short-term forms are often based on a change in the amount of neurotransmitter release from the presynaptic terminal. Long-term forms last for minutes to hours and are mainly based on signaling and structural changes at the postsynapse. Such long-term synaptic plasticity has been best studied at excitatory synapses in the hippocampus. The hippocampus has been shown to be essential for the formation and retrieval of some forms of memories. On the other hand the hippocampus consists of a densely packed and clearly defined layer of neurons connected in a well-organized manner. The layer of pyramidal neurons is divided into several distinct regions; the major ones are CA1 and CA3. The dendrites of the pyramidal

neurons in the CA1 region form a thick band, termed stratum radiatum, where they form synapses with the axons of the CA3 region (Schaffer collaterals). This arrangement of neurons and their connection allows the hippocampus to be sectioned such that the CA3-CA1 circuit stays intact. These features make the hippocampus a particularly favorable brain structure to study synaptic plasticity.

The best described form of synaptic plasticity is long-term potentiation (LTP), a process whereby a brief period of increased activity produces a long-lasting increase in synaptic strength, measured by an increase in the excitatory postsynaptic current (EPSC). *In vivo*, an LTP can last from hours to months and its blockade or restriction correlates with learning and memory deficiencies (Grant and Silva, 1994). The process of LTP can be induced at the CA1 synapses by a brief stimulation of high frequency at the presynapse. Glutamate that is released at the presynaptic terminals binds to AMPA and NMDA receptors at the postsynapse. In the best described form of LTP, the repetitive stimulation leads to a depolarization of the postsynapse that opens the voltage-dependent NMDA receptors. The NMDA receptor hereby acts as a "coincident-detector" that only opens by simultaneous presynaptic activity (release of glutamate) and postsynaptic activity (depolarization due to previous stimulus). An opening of NMDA receptors leads to calcium influx into the postsynapse that triggers the signaling cascade that leads to the increase in the EPSC. This increase in current is mainly achieved by the modulation of AMPA receptor conductance or the recruitment of additional AMPA receptors into the postsynaptic site. But the initiation, consolidation and maintenance of this postsynaptic modification demands a variety of molecular processes. The early phase of an LTP has been shown to be dependent on the activity of the Ca^{2+}/calmodulin-dependent protein kinase (CaMKII), which is directly activated by the influx of calcium into the postsynaptic site (Lisman et al., 2012). Among the downstream targets of CaMKII are subunits of the AMPA receptors and many other signaling molecules (Lisman et al., 2012). Whereas the early phase of an LTP is dependent on local signaling pathways, the later phase has been shown to demand protein synthesis and gene expression (Kandel, 2001; Klann and Dever, 2004).

If synapses continued to increase strength in response to LTP, they would reach a level of maximum activity and lose the ability to encode new information. Therefore the process of strengthening synaptic connections demands a converse process that guarantees the weakening of a synapse. Long-term depression (LTD) is such a process. In the hippocampus, LTD can be induced by low frequency stimulation. In the best characterized form of LTD, the stimulation pattern causes a low-amplitude rise in the postsynaptic calcium concentration, which in turn activates protein phosphatases (Collingridge et al., 2010). They cause an internalization of AMPA receptors, causing a long-lasting decrease in the EPSC (Collingridge et al., 2010).

Both LTP and also LTD are based on functional modification of the postsynapse and correlate with structural modifications. For example, it has been demonstrated, that LTP increases the spine volume whereas LTD causes spines to shrink (Matsuzaki et al., 2004; Okamoto et al., 2004).

Regulation of the actin cytoskeleton in dendritic spines

Numerous studies on postsynaptic signaling pathways demonstrated that the actin cytoskeleton plays a pivotal role in the formation and elimination, motility and stability, and size and shape of dendritic spines (Luo, 2002; Matus, 2000; Okamoto et al., 2004; Tada and Sheng, 2006). Within the

cell, actin exists in two states: the polymerized two-stranded helical filaments (F-actin) and the actin monomers (G-actin) that provide the building blocks for filament assembly. Whereas G-actin is uniformly distributed throughout dendrites and axons, F-actin is very concentrated in the head of mature dendritic spines. Therefore, the formation and maturation of dendritic spines involves pathways that regulate filament assembly. Among those, the best characterized one in neurons involves the Rho family of small GTPases with its family members Rac1, Cdc42 and RhoA. These GTPases can rapidly be switched on and off by exchange of their subunits GDP to GTP and vice versa. This subunit exchange is mediated by guanine nucleotide exchange factors (GEFs) and GTPase activating proteins (GAPs). The activated GTPases further promote signaling to downstream factors that control F-actin assembly, organization and stabilization. For example Rac1 signaling affects the actin cytoskeleton through several pathways, one of which involves the activation of Pak1, 2 and 3 (Figure 1). These kinases in turn phosphorylate LIMK1, which phosphorylates its downstream effector cofilin. Cofilin is an actin depolymerizing factor. In its inactive, phosphorylated form cofilin binds actin monomers and causes a stabilization of existing filaments. In contrast, active, non-phosphorylated cofilin induces depolymerization and filament remodeling (Hotulainen et al., 2009). In line with this, perturbation of the Rac1-Cofilin pathway results in altered spine number and morphology (Dietz et al., 2012; Haditsch et al., 2009; Meng et al., 2002). As changes in the spine morphology correlate with the synaptic strength, pathways that regulate the actin cytoskeleton play a role in spine formation and in synaptic plasticity. Several lines of evidence indicate that synaptic activity changes the equilibrium between F-actin and G-actin (Fukazawa et al., 2003; Okamoto et al., 2004). LTP induction causes an increase in filamentous actin and an increase in spine volume; in contrast, LTD induction shifts the ratio towards G-actin and results in spine shrinkage (Okamoto et al., 2004). The actin cytoskeleton in the dendritic spines contributes to its morphology but also plays important roles in synaptic activities that range from organizing the postsynaptic density (Sheng and Hoogenraad, 2007), anchoring postsynaptic receptors (Renner et al., 2008) and mediating the trafficking of proteins (Gu et al., 2010; Schlager and Hoogenraad, 2009; Zhou et al., 2001). This is all needed during the postsynaptic modifications induced by LTP or LTD. As depicted in Figure 2, the initiation and consolidation of LTP demands temporally controlled actin cytoskeleton modifications. The recruitment of additional AMPA receptors into the postsynaptic site is dependent on actin remodeling that is also responsible for the increase of spine volume. Later on, these synaptic modifications have to be stabilized and maintained, which requires the stabilization of existing filaments. It has been shown that the Rac1-

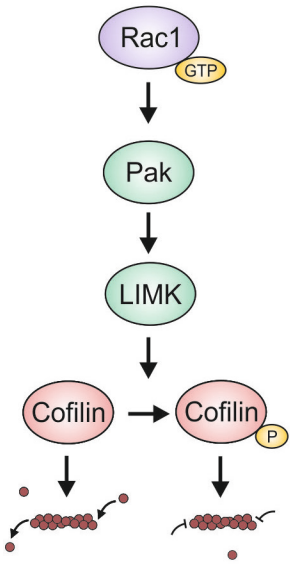

Figure 1. Rac1 signaling. Activated Rac1 (GTP-bound) activates Pak. This in turn increases the activity of LIMK1 which phosphorylates Cofilin. Non-phosphorylated, active Cofilin increases actin remodeling, whereas phosphorylated Cofilin causes stabilization of actin filaments.

Cofilin is involved in these steps. LTP induction elicits a temporal sequence of cofilin phosphorylation and dephosphorylation which are required for AMPA receptor trafficking and spine enlargement (Gu et al., 2010). Perturbation in this pathway causes LTP alterations (Haditsch et al., 2009; Meng et al., 2002; Rust et al., 2010). In humans, mutations in actin cytoskeleton molecules have been implicated with various neurological disorders (Penzes et al., 2011), indicating that unbalanced actin remodeling that causes changes in spine morphology and plasticity has strong implication on brain function.

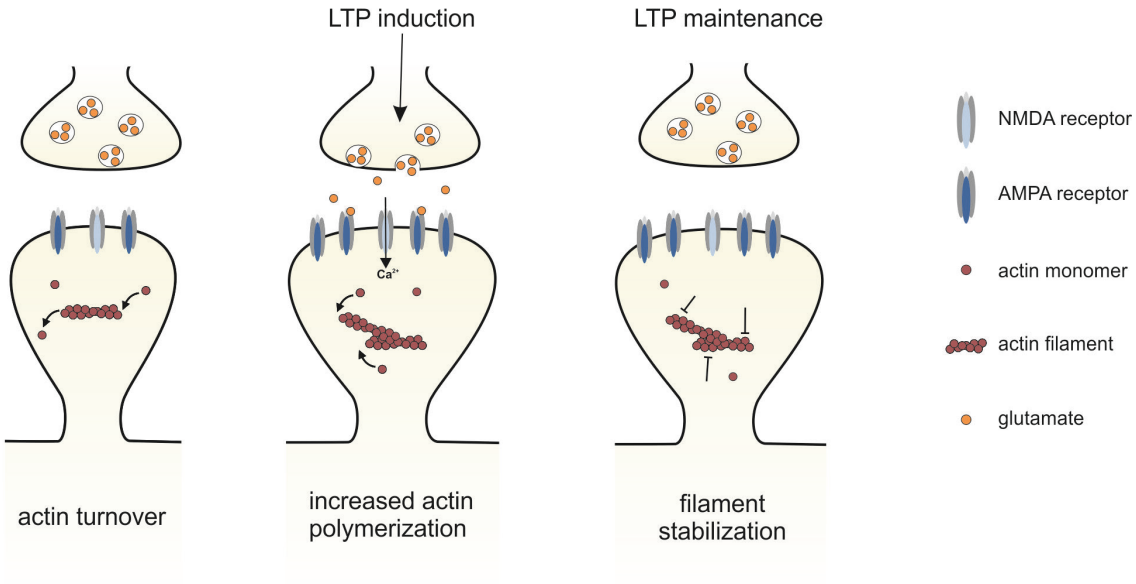

Figure 2. Actin remodeling during LTP. (Left) Under basal conditions, the actin filaments are maintained by balanced polymerization and depolymerization. (Middle) The induction of an LTP and subsequent calcium influx via NMDA receptors increases actin polymerization. This leads to an increase in spine head volume and recruitment of AMPA receptors into the postsynaptic site. (Right) LTP maintenance is achieved by the stabilization of existing actin filaments.

Copines

Copines are a family of cytosolic proteins with scarcely described function. The founding member was isolated from extracts of protozoa *Paramecium* by an attempt to identify novel proteins involved in membrane trafficking (Creutz et al., 1998). Since this protein has the ability to interact with membranes like a “companion” it was named Copine (Creutz et al., 1998). Copines are evolutionary conserved proteins found in protozoa to humans (Tomsig et al., 2003). They are characterized by the following domain architecture. At the amino-terminus they have two C2-domains, which are described to mediate a calcium-dependent interaction with phospholipids for example in synaptotagmins (Sutton et al., 1995). The C2-domains are followed by an A-domain which is known from integrins where it mediates interactions with other proteins of the extracellular matrix (Whittaker and Hynes, 2002). Copines are the first intracellular proteins identified to have A-domain, and therefore predictions of its functions do not exist. However, sequence database search reveals that A-domains are present in several other intracellular proteins present in eukaryotes (Whittaker and Hynes, 2002). As its C2-domains suggest a role of Copines in membrane trafficking, its role was

studied in the unicellular organism Dictyostelium, a model organism to study membrane trafficking. It has been shown that in Dictyostelium Copines associate with plasma membranes and intracellular vacuoles in a calcium-dependent manner (Damer et al., 2005). Copine mutants have been isolated in C. elegans and Arabidopsis. In Arabidopsis a loss of function Copine allele causes a reduction in size and affects regulation of apoptosis under certain environmental conditions (Hua et al., 2001; Jambunathan and McNellis, 2003; Jambunathan et al., 2001; Wang et al., 2011). In C. elegans a Copine homologue interacts with nicotinic acetylcholine receptors (nAChRs) and in Copine mutant worms the amount of synaptic nAChRs is reduced (Gottschalk et al., 2005).

In mammals, the Copine family consists of nine members of whom some are expressed ubiquitously and others show a tissue-specific expression pattern. In line with this variance in their expression, Copines are implicated in a variety of biological functions. On the cellular level, Copines have been found to be associated with the regulation of TNFα – NF-kappaB signaling (Ramsey et al., 2008; Tomsig et al., 2004) and therefore may play a role in the regulation of cell death. In line with this, deregulated Copine signaling or expression has been associated with certain cancer and tumor types in humans (Heinrich et al., 2010; Ramsey et al., 2003; Savino et al., 1999; Thomas et al., 2008).

Taken together the widespread distribution of Copines from unicellular organism over plants to humans and its high degree of conservation may indicate that Copines play a role in fundamental cellular processes. A very high degree of conservation among Copines is found in their C2-domains which indicates that a common feature of all Copines may be their calcium-dependent association with phospholipids. The calcium affinity in the micromolar range of its C2-domain and intracellular localization studies suggest that Copines may associate with membranes in stimulated rather than resting cells (Tomsig and Creutz, 2002). This suggests that Copines may have a conserved role in sensing and translating changes in intracellular calcium concentration. As different Copine family members require various calcium concentration to interact with membranes (Perestenko et al., 2010), different Copines may be responsive to distinct stimulations. In neurons, changes in the intracellular calcium concentration is the key signaling pathway to mediate neuronal plasticity. An indication that Copines play a role in neuron-specific processes is the existence of the neuron-specific Copine family member, Copine 6 (Nakayama et al., 1998). It has been shown that its expression correlates with neuronal activity, as its expression increases either upon LTP induction or kainate injection (Nakayama et al., 1998).

Aim of the thesis

In a screen to identify genes involved in synapse formation and maintenance Copines were discovered. The poorly described Copines have the ability to bind to phospholipids in a calcium-dependent manner, which makes them interesting candidates to play a role in synaptic plasticity. One Copine family members, Copine 6, is expressed exclusively in the central nervous system. We therefore decided to focus on Copine 6 and aimed to identify the function of Copine 6 in neurons. This work started with the functional characterization of Copine 6 *in vitro* using heterologous cells or cultured primary hippocampal neurons (Chapter 2). These *in vitro* data provide strong evidence that Copine 6 can sense neuronal activity and plays a role in spine formation and/or maintenance (Chapter 2). To study whether Copine 6 plays a role in synaptic plasticity *in vivo,* we generated

Copine 6-deficient mice and analyzed their phenotype (Chapter 3). Moreover, to identify novel Copine 6 interacting partners we performed a yeast-two hybrid screen and studied the functional consequences of the interaction of Copine 6 with its novel binding partner (Chapter 4).

References

Ackermann, M., and Matus, A. (2003). Activity-induced targeting of profilin and stabilization of dendritic spine morphology. Nat. Neurosci. *6*, 1194-1200.

Bliss, T.V., and Collingridge, G.L. (1993). A synaptic model of memory: long-term potentiation in the hippocampus. Nature *361*, 31-39.

Bourne, J.N., and Harris, K.M. (2008). Balancing structure and function at hippocampal dendritic spines. Annu. Rev. Neurosci. *31*, 47-67.

Cohen-Cory, S. (2002). The developing synapse: construction and modulation of synaptic structures and circuits. Science *298*, 770-776.

Collingridge, G.L., Peineau, S., Howland, J.G., and Wang, Y.T. (2010). Long-term depression in the CNS. Nat. Rev. Neurosci. *11*, 459-473.

Creutz, C.E., Tomsig, J.L., Snyder, S.L., Gautier, M.C., Skouri, F., Beisson, J., and Cohen, J. (1998). The copines, a novel class of C2 domain-containing, calcium-dependent, phospholipid-binding proteins conserved from Paramecium to humans. J. Biol. Chem. *273*, 1393-1402.

Dalva, M.B., McClelland, A.C., and Kayser, M.S. (2007). Cell adhesion molecules: signalling functions at the synapse. Nat. Rev. Neurosci. *8*, 206-220.

Damer, C.K., Bayeva, M., Hahn, E.S., Rivera, J., and Socec, C.I. (2005). Copine A, a calcium-dependent membrane-binding protein, transiently localizes to the plasma membrane and intracellular vacuoles in Dictyostelium. BMC cell biology *6*, 46.

Dietz, D.M., Sun, H., Lobo, M.K., Cahill, M.E., Chadwick, B., Gao, V., Koo, J.W., Mazei-Robison, M.S., Dias, C., Maze, I.*, et al.* (2012). Rac1 is essential in cocaine-induced structural plasticity of nucleus accumbens neurons. Nat. Neurosci.

Fiala, J.C., Feinberg, M., Popov, V., and Harris, K.M. (1998). Synaptogenesis via dendritic filopodia in developing hippocampal area CA1. J. Neurosci. *18*, 8900-8911.

Fukazawa, Y., Saitoh, Y., Ozawa, F., Ohta, Y., Mizuno, K., and Inokuchi, K. (2003). Hippocampal LTP is accompanied by enhanced F-actin content within the dendritic spine that is essential for late LTP maintenance in vivo. Neuron *38*, 447-460.

Gottschalk, A., Almedom, R.B., Schedletzky, T., Anderson, S.D., Yates, J.R., 3rd, and Schafer, W.R. (2005). Identification and characterization of novel nicotinic receptor-associated proteins in Caenorhabditis elegans. EMBO J. *24*, 2566-2578.

Grant, S.G., and Silva, A.J. (1994). Targeting learning. Trends Neurosci. *17*, 71-75.

Gu, J., Lee, C.W., Fan, Y., Komlos, D., Tang, X., Sun, C., Yu, K., Hartzell, H.C., Chen, G., Bamburg, J.R.*, et al.* (2010). ADF/cofilin-mediated actin dynamics regulate AMPA receptor trafficking during synaptic plasticity. Nat. Neurosci. *13*, 1208-1215.

Haditsch, U., Leone, D.P., Farinelli, M., Chrostek-Grashoff, A., Brakebusch, C., Mansuy, I.M., McConnell, S.K., and Palmer, T.D. (2009). A central role for the small GTPase Rac1 in hippocampal plasticity and spatial learning and memory. Mol. Cell. Neurosci. *41*, 409-419.

Harris, K.M., Jensen, F.E., and Tsao, B. (1992). Three-dimensional structure of dendritic spines and synapses in rat hippocampus (CA1) at postnatal day 15 and adult ages: implications for the maturation of synaptic physiology and long-term potentiation. J. Neurosci. *12*, 2685-2705.

Heinrich, C., Keller, C., Boulay, A., Vecchi, M., Bianchi, M., Sack, R., Lienhard, S., Duss, S., Hofsteenge, J., and Hynes, N.E. (2010). Copine-III interacts with ErbB2 and promotes tumor cell migration. Oncogene *29*, 1598-1610.

Hotulainen, P., Llano, O., Smirnov, S., Tanhuanpaa, K., Faix, J., Rivera, C., and Lappalainen, P. (2009). Defining mechanisms of actin polymerization and depolymerization during dendritic spine morphogenesis. J. Cell Biol. *185*, 323-339.

Hua, J., Grisafi, P., Cheng, S.H., and Fink, G.R. (2001). Plant growth homeostasis is controlled by the Arabidopsis BON1 and BAP1 genes. Genes Dev. *15*, 2263-2272.

Jambunathan, N., and McNellis, T.W. (2003). Regulation of Arabidopsis COPINE 1 gene expression in response to pathogens and abiotic stimuli. Plant Physiol. *132*, 1370-1381.

Jambunathan, N., Siani, J.M., and McNellis, T.W. (2001). A humidity-sensitive Arabidopsis copine mutant exhibits precocious cell death and increased disease resistance. The Plant cell *13*, 2225-2240.

Kandel, E.R. (2001). The molecular biology of memory storage: a dialogue between genes and synapses. Science *294*, 1030-1038.

Klann, E., and Dever, T.E. (2004). Biochemical mechanisms for translational regulation in synaptic plasticity. Nat. Rev. Neurosci. *5*, 931-942.

Lisman, J., Yasuda, R., and Raghavachari, S. (2012). Mechanisms of CaMKII action in long-term potentiation. Nat. Rev. Neurosci. *13*, 169-182.

Luo, L. (2002). Actin cytoskeleton regulation in neuronal morphogenesis and structural plasticity. Annu. Rev. Cell. Dev. Biol. *18*, 601-635.

Matsuzaki, M., Honkura, N., Ellis-Davies, G.C., and Kasai, H. (2004). Structural basis of long-term potentiation in single dendritic spines. Nature *429*, 761-766.

Matus, A. (2000). Actin-based plasticity in dendritic spines. Science *290*, 754-758.

Meng, Y., Zhang, Y., Tregoubov, V., Janus, C., Cruz, L., Jackson, M., Lu, W.Y., MacDonald, J.F., Wang, J.Y., Falls, D.L*., et al.* (2002). Abnormal spine morphology and enhanced LTP in LIMK-1 knockout mice. Neuron *35*, 121-133.

Nakayama, T., Yaoi, T., Yasui, M., and Kuwajima, G. (1998). N-copine: a novel two C2-domain-containing protein with neuronal activity-regulated expression. FEBS letters *428*, 80-84.

Okamoto, K., Nagai, T., Miyawaki, A., and Hayashi, Y. (2004). Rapid and persistent modulation of actin dynamics regulates postsynaptic reorganization underlying bidirectional plasticity. Nat. Neurosci. *7*, 1104-1112.

Penzes, P., Cahill, M.E., Jones, K.A., Vanleeuwen, J.E., and Woolfrey, K.M. (2011). Dendritic spine pathology in neuropsychiatric disorders. Nat. Neurosci. *14*, 285-293.

Perestenko, P.V., Pooler, A.M., Noorbakhshnia, M., Gray, A., Bauccio, C., and Jeffrey McIlhinney, R.A. (2010). Copines-1, -2, -3, -6 and -7 show different calcium-dependent intracellular membrane translocation and targeting. Febs J *277*, 5174-5189.

Ramsey, C.S., Yeung, F., Stoddard, P.B., Li, D., Creutz, C.E., and Mayo, M.W. (2008). Copine-I represses NF-kappaB transcription by endoproteolysis of p65. Oncogene *27*, 3516-3526.

Ramsey, H., Zhang, D.E., Richkind, K., Burcoglu-O'Ral, A., and Hromas, R. (2003). Fusion of AML1/Runx1 to copine VIII, a novel member of the copine family, in an aggressive acute myelogenous leukemia with t(12;21) translocation. Leukemia : official journal of the Leukemia Society of America, Leukemia Research Fund, U.K *17*, 1665-1666.

Renner, M., Specht, C.G., and Triller, A. (2008). Molecular dynamics of postsynaptic receptors and scaffold proteins. Curr. Opin. Neurobiol. *18*, 532-540.

Rust, M.B., Gurniak, C.B., Renner, M., Vara, H., Morando, L., Gorlich, A., Sassoe-Pognetto, M., Banchaabouchi, M.A., Giustetto, M., Triller, A.*, et al.* (2010). Learning, AMPA receptor mobility and synaptic plasticity depend on n-cofilin-mediated actin dynamics. EMBO J. *29*, 1889-1902.

Savino, M., d'Apolito, M., Centra, M., van Beerendonk, H.M., Cleton-Jansen, A.M., Whitmore, S.A., Crawford, J., Callen, D.F., Zelante, L., and Savoia, A. (1999). Characterization of copine VII, a new member of the copine family, and its exclusion as a candidate in sporadic breast cancers with loss of heterozygosity at 16q24.3. Genomics *61*, 219-226.

Schlager, M.A., and Hoogenraad, C.C. (2009). Basic mechanisms for recognition and transport of synaptic cargos. Mol Brain *2*, 25.

Sheng, M., and Hoogenraad, C.C. (2007). The postsynaptic architecture of excitatory synapses: a more quantitative view. Annu. Rev. Biochem. *76*, 823-847.

Sutton, R.B., Davletov, B.A., Berghuis, A.M., Sudhof, T.C., and Sprang, S.R. (1995). Structure of the first C2 domain of synaptotagmin I: a novel Ca2+/phospholipid-binding fold. Cell *80*, 929-938.

Tada, T., and Sheng, M. (2006). Molecular mechanisms of dendritic spine morphogenesis. Curr. Opin. Neurobiol. *16*, 95-101.

Thomas, G., Jacobs, K.B., Yeager, M., Kraft, P., Wacholder, S., Orr, N., Yu, K., Chatterjee, N., Welch, R., Hutchinson, A.*, et al.* (2008). Multiple loci identified in a genome-wide association study of prostate cancer. Nat. Genet. *40*, 310-315.

Tomsig, J.L., and Creutz, C.E. (2002). Copines: a ubiquitous family of Ca(2+)-dependent phospholipid-binding proteins. Cellular and molecular life sciences : CMLS *59*, 1467-1477.

Tomsig, J.L., Snyder, S.L., and Creutz, C.E. (2003). Identification of targets for calcium signaling through the copine family of proteins. Characterization of a coiled-coil copine-binding motif. The Journal of biological chemistry *278*, 10048-10054.

Tomsig, J.L., Sohma, H., and Creutz, C.E. (2004). Calcium-dependent regulation of tumour necrosis factor-alpha receptor signalling by copine. Biochem. J. *378*, 1089-1094.

Varoqueaux, F., Sigler, A., Rhee, J.S., Brose, N., Enk, C., Reim, K., and Rosenmund, C. (2002). Total arrest of spontaneous and evoked synaptic transmission but normal synaptogenesis in the absence of Munc13-mediated vesicle priming. Proc. Natl. Acad. Sci. U. S. A. *99*, 9037-9042.

Verhage, M., Maia, A.S., Plomp, J.J., Brussaard, A.B., Heeroma, J.H., Vermeer, H., Toonen, R.F., Hammer, R.E., van den Berg, T.K., Missler, M.*, et al.* (2000). Synaptic assembly of the brain in the absence of neurotransmitter secretion. Science *287*, 864-869.

Wang, Z., Meng, P., Zhang, X., Ren, D., and Yang, S. (2011). BON1 interacts with the protein kinases BIR1 and BAK1 in modulation of temperature-dependent plant growth and cell death in Arabidopsis. The Plant journal : for cell and molecular biology *67*, 1081-1093.

Whittaker, C.A., and Hynes, R.O. (2002). Distribution and evolution of von Willebrand/integrin A domains: widely dispersed domains with roles in cell adhesion and elsewhere. Mol. Biol. Cell *13*, 3369-3387.

Zhou, Q., Xiao, M., and Nicoll, R.A. (2001). Contribution of cytoskeleton to the internalization of AMPA receptors. Proc. Natl. Acad. Sci. U. S. A. *98*, 1261-1266.

Ziv, N.E., and Smith, S.J. (1996). Evidence for a role of dendritic filopodia in synaptogenesis and spine formation. Neuron *17*, 91-102.

CHAPTER 2

In vitro characterization of Copine 6

Based on the following manuscript in preparation:

Copine 6 is a Novel Calcium Sensor that Translates Synaptic Activity into Spine Plasticity

Milos Galic[1,4,5], Alexander Kriz[1,5], Judith R. Reinhard[1], Martijn Dekkers[1], Réjan Vigot[2], Yan-Ping Zhang-Schärer[3], Gabriela Bezakova[1], Thomas G. Oertner[3], Bernhard Bettler[2], Kaspar Vogt[1], Markus A. Ruegg[1]

[1]Biozentrum, University of Basel, Klingelbergstrasse 70, 4056 Basel, Switzerland
[2]Department of Biomedicine, Institute of Physiology, Pharmazentrum, University of Basel, 4056 Basel, Switzerland
[3]Friedrich Miescher Institute, 4058 Basel, Switzerland
[4]Current address: Department of Chemical and Systems Biology, Stanford School of Medicine, USA
[5]These authors contributed equally

Abstract

Neuronal activity can trigger structural changes of synaptic connections via calcium influx. Such changes can be mediated by “activity sensors”, i.e. molecules responsive to calcium, which in turn activate actin-modulating signaling cascades. Malfunctioning of such activity sensors or their downstream pathways can affect the number and shape of synapses and thus synaptic plasticity. Such synaptic pathologies are the basis of certain forms of mental disorders, such as autism spectrum disorders, schizophrenia or early stages of Alzheimer’s disease. Here we provide evidence that Copine 6 can act as such an activity sensor. Expression of Copine 6 in vivo and in primary hippocampal neurons coincides with synaptogenesis. In organotypic hippocampal slices, Copine 6 is enriched in dendritic spines. Copine 6 is primarily found in the cytosol but becomes enriched at postsynaptic densities from rat brain in a calcium-dependent manner. This enrichment requires activation of NMDA receptors in cultured hippocampal neurons. Lipid raft-like plasma membranes of COS 7 cells and brain tissue show enhanced affinity for Copine 6. Knockdown of Copine 6 in cultured neurons induces the formation of more synapses. Those synapses that are formed in the absence of Copine 6 are unstable and are transformed into filopodia by blocking neuronal activity or inhibition of the Rho-like GTPase Rac1. Overexpression of a calcium-insensitive mutant of Copine 6, decreases synapse density and increases filopodia number. Copine 6 binds to Rac1 and is necessary for calcium-mediated association of Rac1 and its downstream effector Pak1 at lipid raft-like membranes. Moreover, co-expression of Copine 6 enhances the activation of Rac1. Together, these data provide strong evidence that Copine 6 is a bidirectional, calcium-dependent shuttle protein that translates activity-induced, transient calcium signals into sustained synaptic changes through translocation and promotion of Rac1 activity in single spines.

Introduction

Dendritic spines are the principal postsynaptic sites of excitatory synapses and may function as the basic unit of synaptic integration (Harris and Kater, 1994; Schubert et al., 2006). Activity-dependent changes in spine structure and number are thought to contribute to learning and memory (Chklovskii et al., 2004; Keck et al., 2008; Nagerl et al., 2004; Yuste and Bonhoeffer, 2001), and changes in spine structure have been implicated in mental retardation including autism, fragile X and Rett syndromes (Newey et al., 2005; Penzes et al., 2011).

Spines are formed in a stepwise process whereby dendritic filopodia are transformed into mature spines (Marrs et al., 2001; Ziv and Smith, 1996). After their establishment, spines remain motile and change their shape and size in response to a variety of stimuli (Dunaevsky et al., 1999; Korkotian and Segal, 2001; Lendvai et al., 2000). These stimuli include growth factors, cell adhesion molecules and neuronal activity, all of which contribute to the dynamics of spines (Tada and Sheng, 2006). At the molecular level, many of these stimuli control the localization and the amount of individual proteins within spines (Hering and Sheng, 2003; Sala et al., 2001) thereby ultimately regulating the polymerization dynamics of the actin cytoskeleton (Calabrese and Halpain, 2005; Matus, 2000).

Several lines of evidence indicate that the influence of neuronal activity on the actin cytoskeleton is mediated by the small Rho-like GTPases Rac1, Cdc42 and RhoA (Bonhoeffer and Yuste, 2002). In particular, Rac1 and its effectors were shown to be involved in the translation of neuronal activity into changes of the actin cytoskeleton (Saneyoshi et al., 2008; Xie et al., 2007). Additionally, synaptic calcium transients trigger activation of certain guanine nucleotide exchange factors (GEFs) via calcium-binding proteins, such as calcium/calmodulin-dependent kinase II (CaMKII) (Penzes et al., 2008). Actin polymerization and spine stabilization, following NMDA receptor-mediated calcium influx became a favorite model of dendritic spine regulation and structural plasticity (Ackermann and Matus, 2003; Matsuzaki et al., 2004). Recently it was shown that the activity pattern of Cdc42 and RhoA greatly differ in their spatial spreading upon local induction of neuronal activity (Murakoshi et al., 2011). It is still an open question as to how the activity of GTPases is spatially confined. Calcium gradients in spines remain steep due to their transient nature and the excess of buffers and extrusion mechanisms (Majewska et al., 2000; Volfovsky et al., 1999). However, cytosolic proteins within an individual spine diffuse within seconds into the dendritic shaft if not actively retained (Svoboda et al., 1996; Zhang et al., 2008). Thus, creation of domains that confine the activity of cytosolic proteins to spines requires either fast turnover or an active targeting/retention of those proteins.

Copines are scarcely described cytosolic proteins, characterized by two C2-domains at the amino-terminus and an A domain at the carboxy-terminus (Fig. S1A). C2-domains are calcium and phospholipid-binding domains (Lemmon, 2008). The A-domain is capable of interacting with a wide variety of proteins that themselves are components of intracellular signaling pathways (Tomsig and Creutz, 2000). Nine Copines are predicted in mammals based on sequence identity and structural homology. We cloned and sequenced eight of those from rat tissue (Fig. S1A and B). Copines are evolutionary conserved and are expressed from Dictyostelium to humans. Several lines of evidence suggest that Copines translocate to plasma membranes upon calcium influx (Creutz et al., 1998; Damer et al., 2005; Perestenko et al., 2010). Moreover, they have been implicated in the surface targeting and stabilization of neurotransmitter receptors at the plasma membrane (Gottschalk et al.,

2005). Most of the Copine family members are expressed ubiquitously. However, Copine 6 expression is restricted to the brain and is particularly high in hippocampus (http://mouse.brain-map.org). Copine 6 expression in hippocampal neurons is upregulated upon kainate injection induced episodes of brief seizures and after induction of long-term potentiation (LTP) (Nakayama et al., 1998). A recent proteomic analysis of postsynaptic densities (PSDs) has shown that Copine 6 is present in these fractions (Schrimpf et al., 2005).

Here, we investigated the expression and function of Copine 6. We found that Copine 6 expression is upregulated during synapse formation in cultured hippocampal neurons and in the brain. NMDA receptor-mediated calcium influx promotes translocation of Copine 6 from the dendritic shaft into spines. Knockdown of Copine 6 by shRNA increases the density of filopodia in young cultured hippocampal neurons. In older cultures, loss of Copine 6 results in more spines but renders them sensitive to inhibition of neuronal activity or Rac1. Interestingly, overexpression of a calcium-insensitive Copine 6 mutant causes the formation of more filopodia but reduces spine number. As Copine 6 co-immunoprecipitates with Rac1 and increases Rac1 activation, these effects are probably caused by Copine 6-dependent translocation of Rac1 into spines and the enhanced activation of Rac1.

Results

Expression of Copine 6 correlates with synapse formation

To investigate whether expression of Copine 6 is upregulated in neurons during synaptogenesis, we first evaluated the precise time course of synapse formation and maturation in low density rat primary hippocampal cultures. To this end, cultures were stained for the postsynaptic scaffold protein PSD-95 and SynGAP, and the presynaptic marker Bassoon (Fig. S2). PSD-95 puncta were detected at day in vitro (DIV) 7 and their number and size increased between DIV 11 and DIV 15 (Fig. S2A and A'). Co-localization of SynGAP with Bassoon indicated that functional synapses were formed between DIV 7 and DIV 11 and that their number strongly increased from DIV 11 to DIV 15 (Fig. S2B and B'). Synapse maturation, indicated by the increased number of puncta positive for the AMPA receptor subunit GluR2 and SynGAP, was most prominent between DIV 11 and DIV 15 (Fig. S2C and C').

We next monitored expression of Copine 6 during this time window by qRT-PCR. Expression levels for each gene were normalized to the housekeeping gene 5-glyceraldehyde-3-phosphate dehydrogenase (GAPDH) and expressed in relative units. Expression of a gene of interest was arbitrarily set to 1 when above detection level. As a positive control, we measured transcript levels of the postsynaptic protein SynGAP. As shown in Figure 1A, Copine 6 expression increased during synapse formation. In contrast, transcript levels of the housekeeping gene phosphoglycerolkinase 1 (PGK1) were not altered. Upregulation of Copine 6 was also detected at the protein level in high density rat hippocampal cultures (Fig. 1B, left panel) and in lysates of rat cerebral cortex (Fig. 1B, right panel) during the peak of synaptogenesis. In the adult rat brain, Copine 6 was detected in all regions examined with highest levels in olfactory bulb and hippocampus (Fig 1C, lane 1 and 4), known to be regions of ongoing neurogenesis and synapse formation throughout adulthood (Zhao et al., 2008). In mouse hippocampus, Copine 6 immunoreactivity was high in the dentate gyrus and the CA3, CA2 and CA1 areas (Fig. 1D, top panel). Immunoreactivity in regions occupied by dendrites, like the stratum oriens (SO) was higher than in regions that predominantly contain axons, such as the corpus callosum (CC) (Fig. 1D, bottom panel). To determine the subcellular localization of Copine 6, we next stained cultured hippocampal neurons for Copine 6 and found that it indeed localized to dendrites but not to axons (Fig. 1E). Co-transfection of expression constructs encoding Copine 6-GFP and a cytosolic tandem-dimer red fluorescent protein (tdRFP) into organotypic slice cultures, revealed that Copine 6-GFP was enriched in dendritic spines by approximately 1.6-fold compared to the dendritic shaft (Fig. 1F). Thus, the high levels of Copine 6 in brain regions of high plasticity, the increase in its expression during synapse formation and its localization to synapses suggest a role of Copine 6 in synapse function.

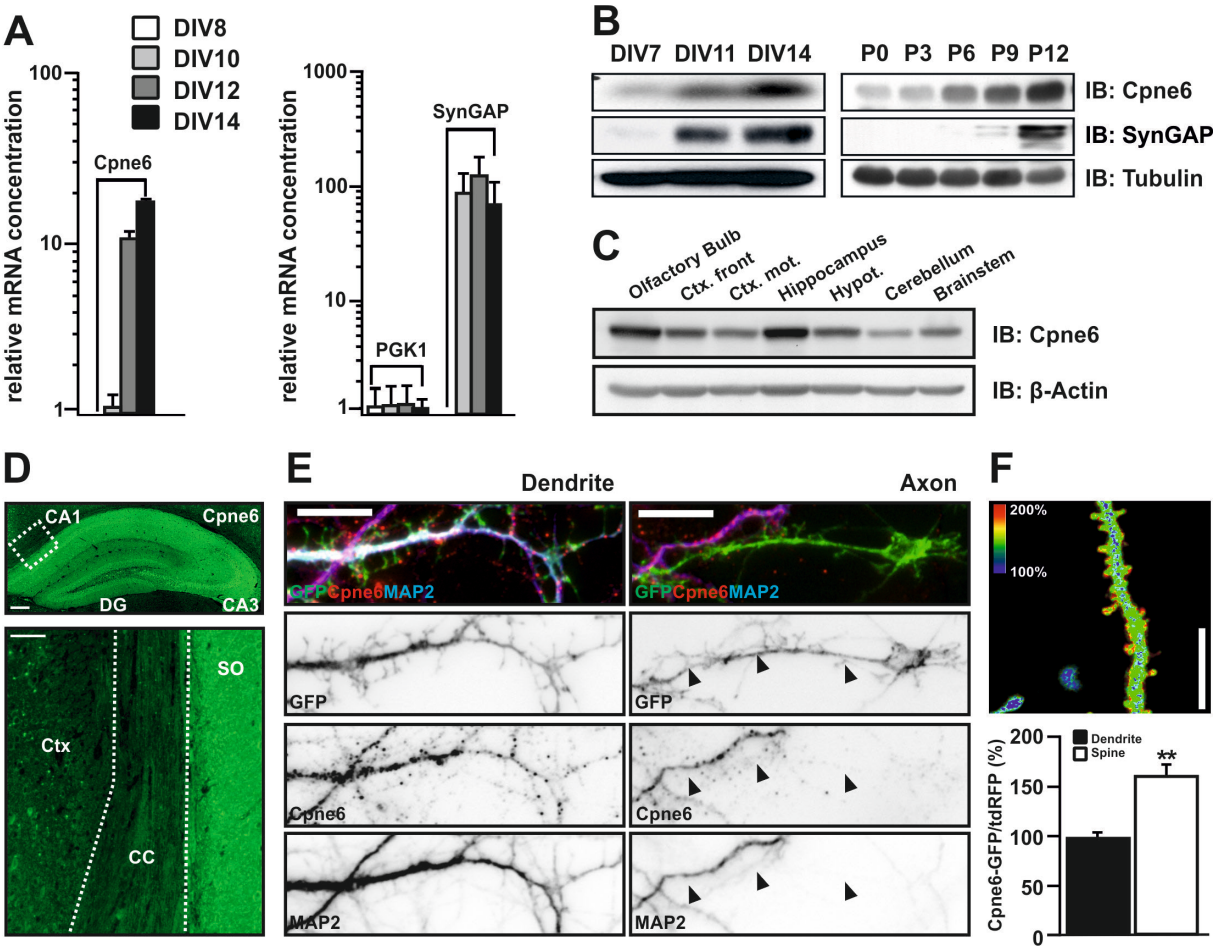

Figure 1. Expression pattern of Copine 6 in the CNS. (A) Expression levels of Copine 6 during synapse formation in low-density, primary hippocampal cultures as determined by quantitative real-time PCR. Values are plotted in a semi-logarithmic scale, relative to mRNA concentration of GAPDH. Expression of the housekeeping gene, phosphoglycerolkinase 1 (PGK1), did not change during synapse formation, while expression of the synaptic protein SynGAP was upregulated. Note that SynGAP was normalized to GAPDH but not set arbitrarily to 1 at first appearance since expression at DIV 10 was already 100-fold above detection level. Data represent mean ± SEM from three independent experiments, each time point was analyzed in triplicates. (B) Left panel: Western blot analysis of Copine 6 (top) and SynGAP (middle) in primary hippocampal cultures at DIV 7, DIV 11 and DIV 14. Tubulin was used as loading control (bottom). Right panel: Western blot analysis of rat cortex isolated at postnatal day 0, 3, 6, 9 and 12. Copine 6 is upregulated during the peak of synaptogenesis in vitro and in vivo. (C) Western blot analysis of different brain regions from adult rat. Samples were adjusted to the housekeeping gene β-actin. (D) Coronal mouse brain sections were stained with an anti-Copine 6 antibody. Copine 6 immunoreactivity is high in hippocampal areas (top). Especially high immunoreactivity was observed in the dendrite-dense stratum oriens (SO) whereas cortical areas (Ctx) and axon dense areas (corpus callosum, CC) were weakly stained (bottom). Scale bars are 200 µm (top) and 50 µm (bottom). (E) Primary hippocampal neurons were transfected at DIV 7 with a synapsin-driven GFP expression construct, fixed at DIV 12, and immunostained with Copine 6 and MAP2 antibodies. Copine 6 is expressed in dendrites (left), which are MAP2- and GFP-positive, while axons (right; marked by black arrowheads), which are MAP2-negative but GFP-positive, do not stain for Copine 6. Scale bars = 10 µm. (F) Pyramidal cell dendrite in organotypic culture from rat hippocampus co-transfected with GFP-tagged Copine 6 and freely diffusible tdRFP. The ratio of green (Copine 6-GFP) to red (tdRFP) fluorescence is displayed in rainbow colors with red indicating maximum concentration of Copine 6. Quantification of Copine 6-GFP concentration in spines after normalization to the values in dendrites is shown below. Data are mean ± SEM (N = 40 spines in 5 cells). ** $p < 0.01$. Scale bar = 10 µm.

Reversible, calcium-dependent association of Copine 6 with lipid raft-like membranes

C2-domain containing proteins, such as protein kinase C (PKC) or synaptotagmin, increase their affinity to certain phospholipids in plasma membranes upon calcium binding (Arac et al., 2006; Brose et al., 1992). To examine whether Copine 6 has similar properties, we measured how changes in the cytosolic calcium concentration affected its localization in transfected COS7 cells. One day after transfection, cells were homogenized (H) and fractionated into cytosol (C) and membrane (M). In the presence of EDTA, Copine 6-GFP was found in the cytosol whereas addition of calcium led to its enrichment in the membrane fraction (Fig. 2A). Treatment of COS7 cells with the calcium ionophore ionomycin induced a shift of the majority of Copine 6-GFP signal from a homogenous cytoplasmic to a spotted, membrane-bound appearance (Fig. 2A', middle panel). Removing extracellular calcium by the addition of EDTA prior to ionomycin treatment abolished this transition (Fig. 2A', right panel). To get an estimate of the calcium concentration needed to induce membrane enrichment of Copine 6, we next incubated homogenates with increasing concentrations of calcium and subsequently isolated cytoplasmic and membrane fractions. As shown in Figure 2B, calcium significantly increased the amount of Copine 6 bound to the membrane. Quantification of 3 independent experiments revealed an EC50 for calcium of approximately 4 µM for the membrane association of Copine 6 (Fig. 2B'). Importantly, the binding of Copine 6 to membranes was reversible as subsequent depletion of calcium by increasing concentrations of EGTA, released Copine 6 into the cytosol (Fig. 2B, right panel and Fig 2B', bottom panel).

The punctate pattern of Copine 6-GFP in COS7 cells treated with ionomycin suggested that Copine 6 may bind to specific subdomains in plasma membranes. Indeed, staining for cholesterol-rich domains showed that Copine 6-GFP co-localized with lipid raft markers such as choleratoxin B1 in ionomycin-treated but not in untreated COS7 cells (Fig. 2C). Additionally, Copine 6 from rat brain homogenates fractionated in high density sucrose gradients with the lipid raft marker Flotillin-1 in the presence of calcium (Fig. 2C', top panel). In the presence of EDTA Copine 6 was not detected in those detergent-resistant floating fractions (Fig. 2C', bottom panel). In contrast, calcium depletion by EDTA did not change the fractionation of the NMDA receptor subunit NR1, which has previously been shown to be enriched in lipid rafts (Hering et al., 2003) (Fig. 2C'). Lipid rafts or detergent-resistant membranes are characterized by elevated cholesterol content. To investigate the effect of cholesterol depletion for the binding of Copine 6 to membranes, we treated COS7 cells with 10 mM methyl-β-cyclodextrin for 1 h before fractionation. Such treatment significantly inhibited the calcium-induced association of Copine 6 with membranes (Fig. 2D). Together, these results show that the partitioning of Copine 6 to the cytosol and to lipid-raft-like membranes depends on the intracellular calcium concentration and that it is reversible (Fig. 2D'). These data in conjunction with the fact that synapses are sites of high calcium dynamics (Sabatini et al., 2002) and show a high content of lipid rafts (Hering et al., 2003), suggest that Copine 6 is a calcium sensor at synapses.

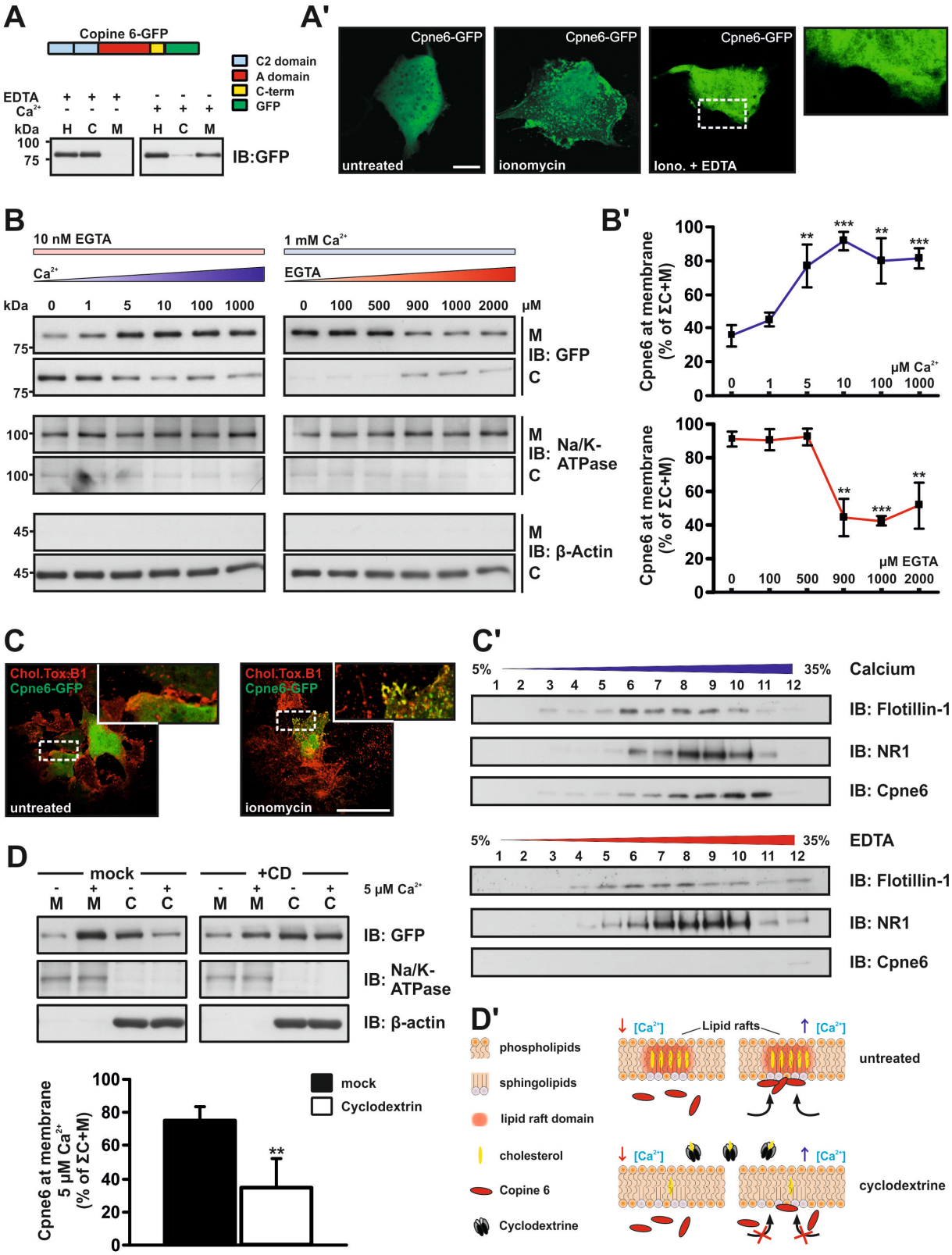
A
Copine 6-GFP
C2 domain
A domain
C-term
GFP
EDTA
Ca2+
kDa H C M H C M
100
75
IB:GFP
A'
Cpne6-GFP
untreated
ionomycin
Iono. + EDTA
B
10 nM EGTA
1 mM Ca2+
Ca2+
EGTA
kDa 0 1 5 10 100 1000
0 100 500 900 1000 2000 µM
M
IB: GFP
C
IB: Na/K-ATPase
IB: β-Actin
B'
Cpne6 at membrane (% of ΣC+M)
µM Ca2+
µM EGTA
C
Chol.Tox.B1
Cpne6-GFP
untreated
ionomycin
C'
5%
35%
Calcium
IB: Flotillin-1
IB: NR1
IB: Cpne6
EDTA
D
mock
+CD
5 µM Ca2+
IB: GFP
IB: Na/K-ATPase
IB: β-actin
Cpne6 at membrane 5 µM Ca2+ (% of ΣC+M)
mock
Cyclodextrin
D'
phospholipids
sphingolipids
lipid raft domain
cholesterol
Copine 6
Cyclodextrine
[Ca2+]
Lipid rafts
untreated
cyclodextrine

Figure 2. Calcium-dependent bidirectional binding of Copine 6 to cell membranes.(A) Homogenate (H) derived from COS7 cells expressing Copine 6-GFP were fractionated into cytoplasm (C) and membranes (M) in the absence (EDTA) or presence of calcium (Ca2+). (A') Fluorescence of untreated COS7 cells transfected with Copine 6-GFP (left) or after treatment with ionomycin (middle) or ionomycin in the presence of EDTA (right). Ionomycin induces association of Copine 6-GFP at cell membranes. Scale bar = 20 µm. Inset shows cell membrane at high magnification. (B) Concentration dependence and reversibility of calcium-dependent Copine 6-GFP localization to membranes (M) or cytoplasm (C), monitored by Western blot analysis. Efficacy in the fractionation procedure was tested with antibodies against the membrane protein Na/K-ATPase and the cytosolic marker β-actin. (B') Quantification of the results shown in (B). The sum of the Copine 6 signal in cytoplasmic and membrane fraction was defined as 100% and the relative Copine 6 signal in the membrane fraction is plotted. N = 3. (C) Cholera toxin B1-stained lipid rafts of COS7 cells transfected with Copine 6-GFP in the absence (left) and presence (right) of ionomycin. Only in ionomycin-treated cells, Cholera toxin B1 and Copine 6-GFP co-localize (yellow). Scale bar = 50 µm. (C') Fractionation of adult rat brain homogenates and Western blot analysis for Flotillin-1, NMDA receptor subunit 1 (NR1) and Copine 6 (Cpne6) in presence (top) or absence (bottom) of calcium. Co-fractionation of Cpne6 with Flotillin-1 and NR1 requires calcium. (D) COS7 cells expressing Copine 6-GFP were mock-treated or incubated with 10 mM cyclodextrin (CD) for 1 hour and membranes were isolated in the presence or absence of calcium. Quantification of the Copine 6-GFP signal detected by Western blot analysis (bottom). Cyclodextrin lowers the amount of Cpne6 bound to membranes in the presence of calcium, N = 3. (D') Model for the enrichment of Copine 6 at plasma membranes and its dependence on lipid rafts. Data are mean ± SEM; * $p < 0.05$, ** $p < 0.01$, *** $p < 0.001$

NMDA receptor-mediated calcium influx enriches Copine 6 in the PSD

As calcium changes the subcellular localization of Copine 6, the protein may be enriched in postsynaptic densities (PSDs) in a calcium-dependent manner. To test this, we homogenized brains of adult rats in 2 mM calcium. Subsequent fractionation by sucrose gradients were then carried out in the same buffer or by chelating calcium with 2 mM EDTA. As a reference, we used the postsynaptic marker PSD95 and the presynaptic marker synaptophysin (Syn). In the presence of 2 mM calcium, Copine 6 and PSD 95 were both highly enriched in PSDs (Fig. 3A) whereas the addition of 2 mM EDTA resulted in the loss of Copine 6 from microsomal and plasma membranes (P3) and its release into the cytoplasmic fraction S3 (Fig. 3A'). Flotillin-1 was also highly enriched in the PSD fraction (Fig. 3A and A'), confirming that synaptic membranes have a particularly high content of lipid rafts as shown previously (Hering et al., 2003). Our results therefore support that Copine 6 is strongly associated with PSDs at high calcium concentrations but remains in the cytoplasm in low calcium.

Calcium influx at excitatory synapses is triggered by neuronal activity. To test whether Copine 6 responds to this activity we transfected primary hippocampal neurons with Copine 6-GFP expression constructs at DIV 7. One week later, we added 50 µM glutamate for 10 minutes and fixed the cells. Like in COS7 cells, Copine 6-GFP in untreated neurons was homogenously distributed (Fig. 3B, top left). Treatment with glutamate resulted in a spotted, peripheral localization of Copine 6-GFP (Fig. 3B, top middle). The calcium influx was specifically mediated by NMDA receptors as pre-incubation with the NMDA receptor antagonist APV abolished the Copine 6 response to glutamate (Fig. 3B, top right) while the NMDA receptor agonist trans-ACBD triggered its translocation (Fig. 3B, bottom left). Moreover, blocking of voltage-gated calcium channels (VGCCs) by cadmium did not interfere with the glutamate-triggered Copine 6 response (Fig. 3B, bottom middle).

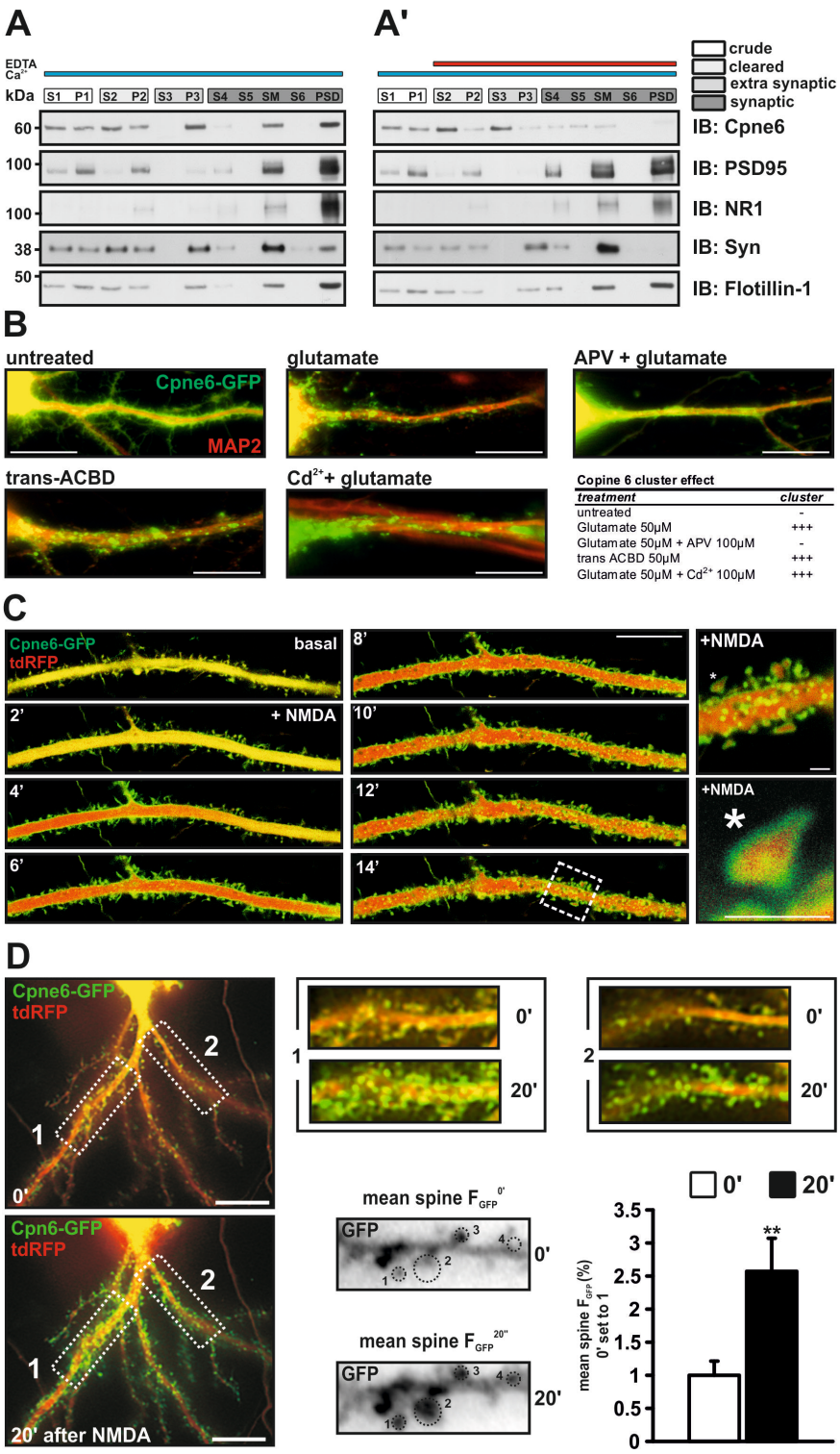

Figure 3. NMDA receptor-mediated calcium influx enriches Copine 6 at PSDs. Subcellular fractionation of adult rat brain in the presence of calcium (A) and with EDTA added after the first centrifugation (A'). Isolated fractions are: post nuclear supernatant (S1); nuclear pellet (P1); crude cytoplasm (S2); synaptosomal-mitochondrial pellet (P2); cytoplasmic proteins (S3); microsomal and plasma membranes (P3); post synaptosomal supernatant (S4); synaptosomal cytoplasm (S5); synaptic membranes (SM); post postsynaptic density supernatant (S6); postsynaptic densities (PSD). An equal amount of protein (3 µg) (A) and (2 µg) (A') was subjected to immunoblotting for Copine 6 (Cpne6), PSD95, NR1, synaptophysin (Syn) and the lipid raft marker Fotillin-1. Copine 6 is detected in the PSD fraction in a calcium-dependent manner. (B) DIV 12 hippocampal neurons expressing Copine 6-GFP (Cpne6-GFP; green) under the control of the synapsin promoter were treated with the indicated pharmacological agents and stained with antibodies to MAP-2 (red). Copine 6-GFP clustered after application of glutamate or trans-ACBD. Addition of APV blocked Copine 6-GFP translocation upon glutamate application whereas cadmium (Cd2+) did not affect it. Clustering effect of the different treatments is summarized in the Table. (C) Time lapse, confocal scan of DIV 14 hippocampal neurons expressing Copine 6-GFP and cytosolic tdRFP (red). Time points after NMDA application are indicated. Insets to the right represent are high magnification pictures from the region indicated by a dotted line and the asterisk. (D) Quantification of Copine 6-GFP enrichment at spines upon NMDA application. Representative dendritic stretches (regions 1 and 2) were magnified for better visualization of Copine 6 enrichment (top right). For quantification, the GFP signal was converted into grey values and pixel intensities at individual spines were measured at time zero and after 20 minutes (numbers indicate selected spines). The graph shows the quantification of the normalized mean signal intensity of Copine 6-GFP at time zero (open bar) and after 20 minutes (black) of NMDA application. N = 49 spines from 2 dendritic stretches of 2 cells. Values are mean ± SEM; ** $p < 0.01$. Scale bar = 20 µm.

Next, the spatio-temporal dynamics of Copine 6 distribution was examined in hippocampal neurons transfected with cytosolic tdRFP and Copine 6-GFP or freely diffusible GFP as control. At DIV 14, neurons were treatedwith 10 µM NMDA to trigger the opening of synaptic NMDA receptors (Soriano et al., 2006). Neurons were examined using time-lapse microscopy. In control neurons, tdRFP and GFP fluorescence overlapped perfectly (yellow color) and no change was observed upon NMDA application (Movie S1). In contrast, Copine 6-GFP (green) showed a highly dynamic movement into dendritic protrusions after addition of NMDA (Movie S2; Fig 3C). Note that Copine 6-GFP was already slightly enriched in those protrusions at time zero, consistent with its enrichment in spines at basal synaptic activity (see also Fig. 1F). The movement of Copine 6-GFP into dendritic protrusions and its depletion from the dendritic shaft (increase in the red signal) was visible after 4 minutes (Fig. 3C). Moreover, high magnification microscopy showed that the movement of Copine 6-GFP was directed to spines (Fig. 3C inset). To get an estimate for the extent of accumulation of Copine 6-GFP in spines, we measured the GFP fluorescence at individual spines at time zero and twenty minutes after NMDA application (Fig. 3D). Quantification of the signals at those two time points showed that the GFP signal increased in spines about 2.7 times upon NMDA application (Fig. 3D, bottom right). Together, these data identify the NMDA receptor as the site of calcium entry responsible for Copine 6 translocation into spines. The translocation is calcium-dependent, completed within minutes and targets Copine 6 to the postsynaptic compartment.

Copine 6 regulates synapse number

To probe for a functional role of Copine 6 in synapse formation we decided to perform RNA interference experiments. The shRNA constructs were first tested in COS7 cells for their capability of suppressing expression of Copine 6-GFP fusion protein (Fig. S3A). In primary hippocampal cultures, all experiments were performed with two shRNA constructs, but quantified for the more potent one. Cultured neurons were transfected at DIV 7 with a GFP expression vector in combination with a plasmid encoding shRNA to Copine 6 (shRNA Cpne6) or to CD4 (shRNA CD4). Staining of the cultures with antibodies to PSD95 showed that knockdown of Copine 6 caused a significant increase in the density of PSD95-positive puncta compared to control neurons transfected with shRNA to CD4 (Fig. 4A and A'). To exclude off-target effects we created a shRNA-resistant version of Copine 6 (Fig. 4B). Expression of shRNA directed against Copine 6 in conjunction with this construct reversed the increase in PSD95 puncta to control levels (Fig. 4B'). This clearly shows that the observed effect in neurons expressing shRNA Cpne6 is due to the loss of Copine 6 and not caused by off-target effects. To test whether the observed increase in postsynaptic structures was accompanied by an increase in the number of presynaptic terminals, neurons were stained for SynGAP and the presynaptic marker Bassoon. Like for PSD95-positive puncta, the density of synapses (i.e. SynGAP and Bassoon-positive structures) was increased upon loss of Copine 6 (Fig. 4C and C' left panel). Moreover, the diameter of the synapses was unchanged (Fig. 4C', right panel). To investigate whether these synapses were functional, we measured miniature excitatory postsynaptic currents (mEPSCs) using whole-cell patch-clamp recording. As shown in Figure 4D and D', the frequency was significantly increased in neurons expressing shRNA to Copine 6 compared to control neurons, whereas the amplitude of the mEPSCs remained unchanged. To further support the electrophysiological data, we quantified the postsynaptic localization of AMPA receptors, which are crucial for synaptic activity.

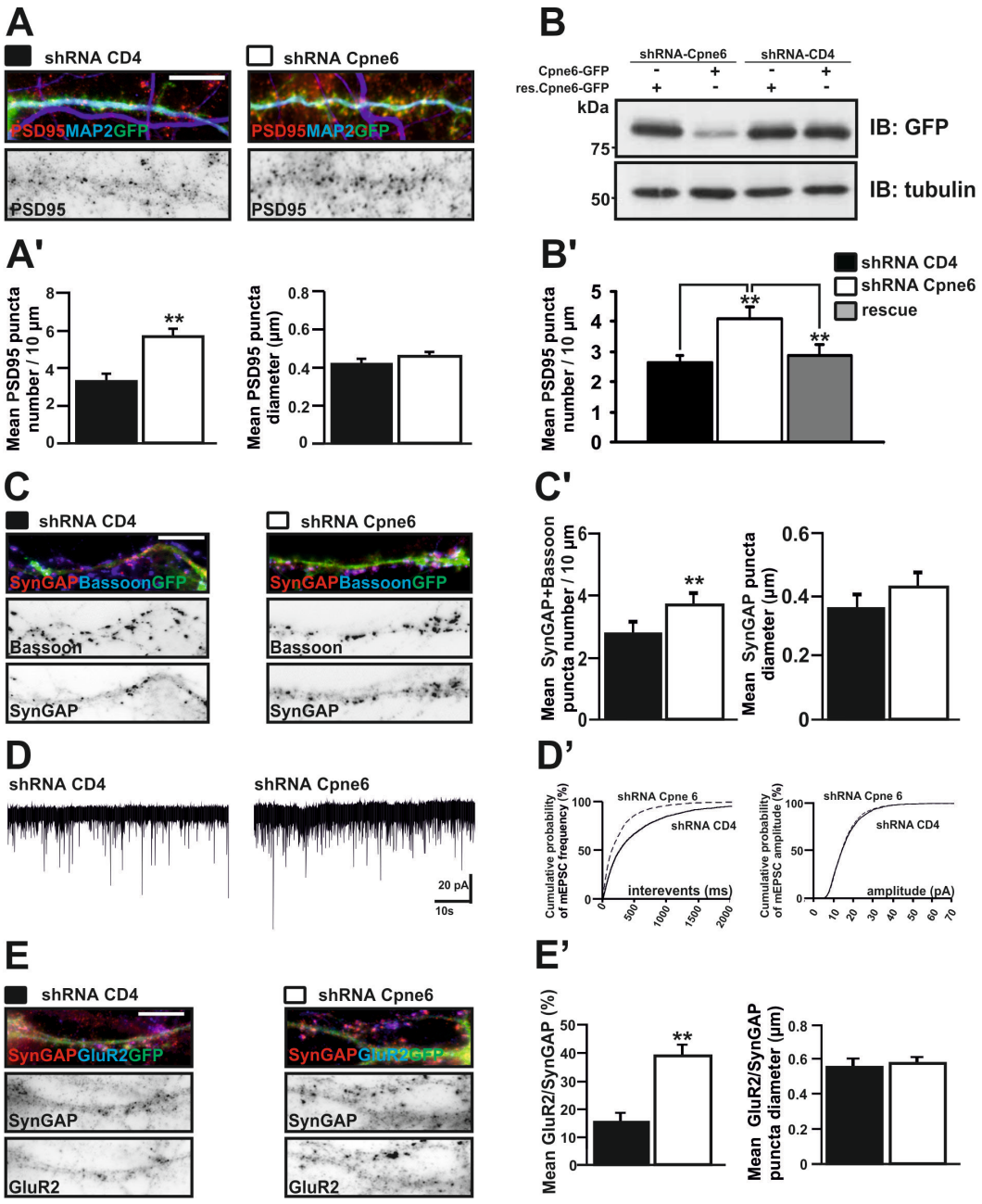

Figure 4. Knockdown of Copine 6 increases the number of glutamatergic synapses. Analysis of cultured high-density, primary hippocampal neurons at DIV 12, 5 days after transfection with plasmids encoding GFP (green) and shRNA to CD4 (shRNA CD4) or Copine 6 (shRNA Cpne6). (A) Postsynaptic structures on dendrites (MAP2-positive, blue) were visualized with antibodies against PSD95 (red). (A') Quantification of the effect of shRNA to Copine 6 on the number of PSD95-positive structures in a segment of 10 µm (i.e. density) and their diameter. (B) Test of shRNA resistance of a Copine 6-GFP mutant (res.Cpne6-GFP) in COS7 cells. Western blot analysis of cells that were transfected with the constructs indicated. (B') Expression of res.Cpne6-GFP together with shRNA Cpne6 (rescue) does not alter the density of PSD95 puncta in cultured hippocampal neurons (mean ± SEM; N = 12 neurons; 2 independent experiments). (C) Neurons stained for SynGAP (red) and Bassoon (blue). (C') Knockdown of Copine 6 results in an increase in the density of synapses stained for both Bassoon and SynGAP. (D) Analysis of miniature excitatory postsynaptic currents (mEPSCs). Characteristic traces of transfected neurons are shown to the left. (D') Knockdown of Copine 6 significantly increases the frequency but not the amplitude of mEPSCs ($p < 0.01$, Kolmogorov-Smirnov test, N = 6 neurons per condition, 600 events measured per neuron). (E) Expression of SynGAP (red) and GluR2 (blue). (E') Neurons expressing shRNA to Copine 6 have significantly more but not bigger synapses containing both SynGAP and GluR2. Data represent mean ± SEM from two experiments, N = 20-25 neurons per group, ≥1000 clusters per group. * $p < 0.05$, ** $p < 0.01$. Scale bar = 10 µm.

In neurons expressing shRNA to Copine 6, 40% of all SynGAP-positive puncta stained for the AMPA receptor subunit GluR2. In contrast, only 20% of all SynGAP-positive puncta co-localized with GluR2 in control neurons (Fig. 4E', left panel). The diameter of GluR2/SynGAP-positive synapses did not differ between neurons expressing shRNA to Copine 6 or CD4 (Fig. 4E', right panel). Thus, the overall increase in the density of SynGAP-positive structures (Fig. 4E', left panel) is accompanied by an increase in the percentage of active, GluR2-containing synapses.

Co-expression with tdRFP-tagged β-actin showed that the increase in synapses in shRNA Copine 6-expressing neurons was accompanied by a discontinuous outgrowth of actin-positive protrusions along the entire dendritic shaft (Fig. S3B). Moreover, the density of spines, defined by their globular shape and the accumulation of actin (Fischer et al., 1998) was increased; whereas the density of filopodia was unchanged (Fig. S3C). In conclusion, knockdown of Copine 6 results in more functional synapses in DIV 12 or DIV 14 cultures.

To test whether Copine 6 acts directly as an inhibitor of synapse formation, we also overexpressed Copine 6-GFP in hippocampal neurons from DIV 7 to DIV 14 using a synapsin promoter-driven construct. To better visualize spine structures we co-transfected β-actin-tdRFP. No changes in the overall morphology of Copine 6-GFP-expressing neurons were detected compared to GFP-expressing control neurons (Fig. S4A). Moreover, neither spine nor filopodia density were significantly changed (Fig. S4A'). Finally, no significant change in the frequency or amplitude of mEPSCs was detected (Fig. S4B and B'). The observation that overexpression of Copine 6 does not affect overall morphology, protrusion density or basic synaptic properties in cultured neurons, indicates that it does not act as a direct inhibitor of synapse formation.

A calcium-insensitive Copine 6 mutant causes spine loss and increases the number of filopodia

To investigate the significance of the calcium-mediated shuttling of Copine 6 into spines, we next generated a mutant that does not respond to calcium. To this end, we substituted the aspartate residue at position 167 in the C2B-domain with an asparagine (Fig. 5A). This amino acid residue resides in a region that is highly similar to the calcium-binding motifs of PKC and synaptotagmin (Corbalan-Garcia et al., 1999; Sutton et al., 1995). The Copine 6D167N mutant was not enriched at cell membranes upon calcium influx in COS7 cells but remained in the cytoplasm (Fig. 5A'). Similarly, unlike wild-type Copine 6-GFP (Fig. 2A'), Cpne6D167N-GFP did not accumulate at cell membranes after ionomycin treatment (Fig. 5A''). These results clearly indicate that mutation of aspartate167 to asparagine renders Copine 6 insensitive to changes in calcium concentrations. To test the consequence of this mutation on synapses, we overexpressed Copine 6D167N-GFP for 7 days in hippocampal neurons (DIV 7 to DIV 14). We observed an increase in the number of filopodia and a concomitant loss of spines (Fig. 5B and B'). These changes were accompanied by a decrease in mEPSC frequency (Fig. 5C). In contrast, the mEPSC amplitude was not changed (Fig. 5C'). These data indicate that calcium-mediated shuttling of Copine 6 into postsynaptic structures is involved in the generation and/or maintenance of spines. Thus, Copine 6 may retain a spine-inducing factor in the dendritic shaft. Hence, knockdown of Copine 6 would release this factor (which results in more spines) and overexpression of a calcium-insensitive mutant would confine the factor in the dendritic shaft (which results in fewer spines).

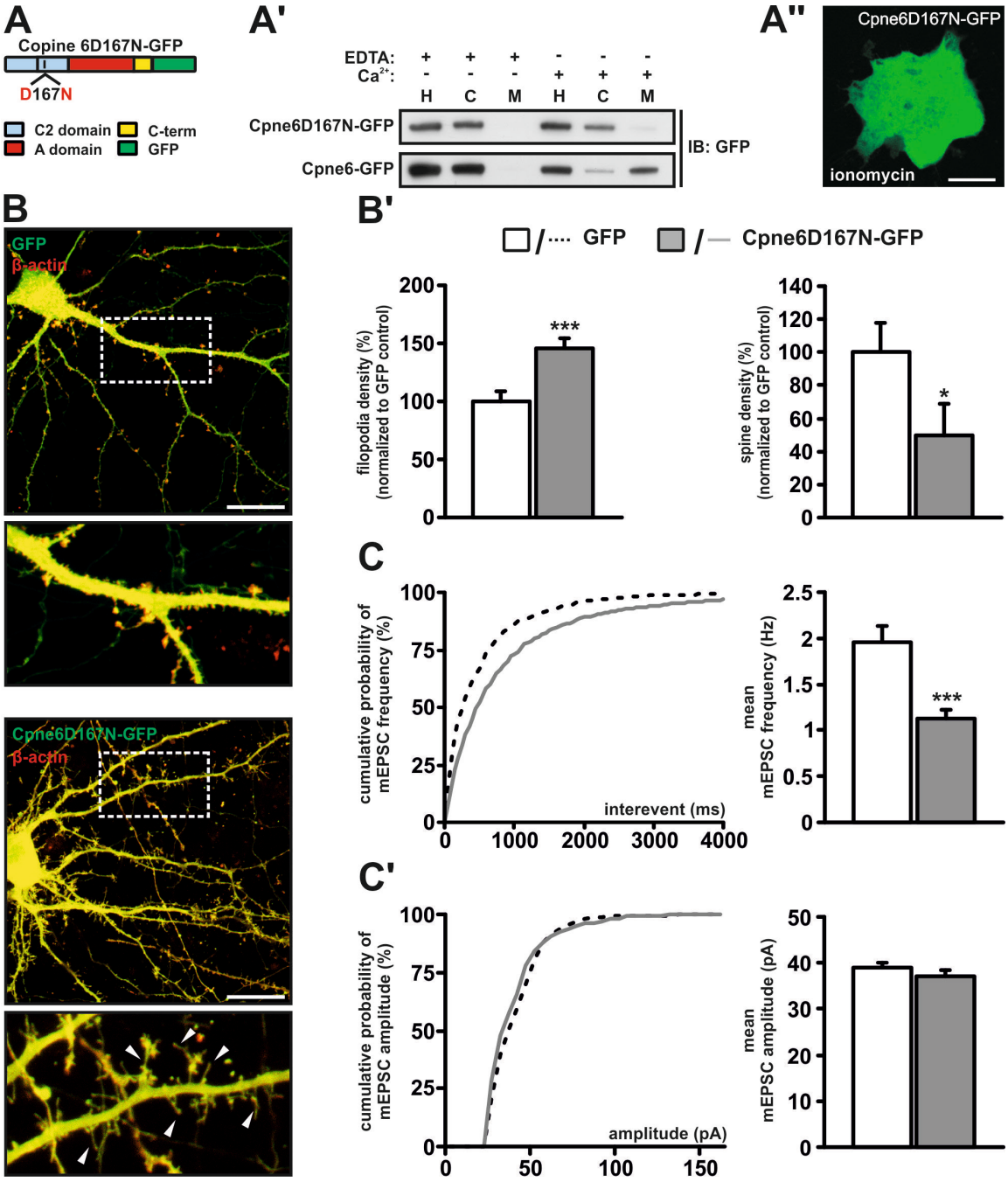

Figure 5. Neurons expressing a calcium-insensitive Copine 6 mutant have more filopodia and fewer spines. Mutation of D167 to N (A) renders Copine 6 non-responsive to calcium. (A') Fractionation of COS7 cells expressing Copine 6D167N-GFP (Cpne6D167N-GFP) or Copine 6-GFP (Cpne-GFP) in the presence of EDTA or calcium. Irrespective of the calcium levels, the mutant remains in the cytosol (C) whereas the wild-type version is enriched in membrane fractions (M). (A'') Cpne6D167N-GFP expressed in COS7 cells does not change its localization by ionomycin treatment. (B) DIV 14 hippocampal neurons expressing a synapsin-driven GFP (top) or Cpne6D167N-GFP (bottom) together with a β-actin-tdRFP. Neurons expressing Cpne6D167N-GFP contain more filopodia (arrowheads) and fewer spines than GFP-expressing controls. (B') Quantification of spine and filopodia number at 10 µm stretches of dendrite. Mean values ± SEM are shown, N = 3 with at least 12 neurons for each condition. (C and C') Analysis of miniature excitatory postsynaptic currents (mEPSCs). (C) Cumulative mEPSCs interevent interval is increased (left) while mean frequency is decreased in neurons expressing Cpne6D167N-GFP (right). (C') Cumulative and mean amplitude are unchanged. Kolmogorov-Smirnov test, N = 9 neurons per condition, more than 800 events measured per neuron; * $p < 0.05$, *** $p < 0.001$. Data represent mean ± SEM. Note that expression of wild-type Cpne6-GFP does not affect filopodia or spine number (Fig. S4).Knockdown of Copine 6 increases the number of glutamatergic synapses.

Copine 6 interacts with the small Rho like GTPase Rac1 and catalyzes its activation

Rho-like GTPases are known to be the main constituents that rearrange the actin cytoskeleton at synapses and affect the transition of filopodia to spines (Bonhoeffer and Yuste, 2002; Tashiro and Yuste, 2004). Moreover, changes in synaptic structure induced by neuronal activity have recently been linked to changes in GTP-Rac1 levels at individual spines (Ball et al., 2010; Cahill et al., 2009; Jourdain et al., 2003; Tolias et al., 2007). To test whether Copine 6 interacts with Rac1, we co-transfected COS7 cells with GFP-tagged Rac1 (GFP-Rac1) and wild-type or the Cpne6D167N mutant. As shown in Figure 6A, Copine 6 and the Cpne6D167N mutant were co-immunoprecipitated with GFP-Rac1. This interaction was also observed with GFP-tagged versions of the constitutive active, GTP-bound form of Rac1 (GFP-Rac1V12) or the dominant-negative, GDP-locked form (GFP-Rac1N17) (Fig. 6A’ and 6A''). These results show that Copine 6 interacts with Rac1 independent of its calcium-binding and the activation state of Rac1.

To investigate whether Copine 6 affects Rac1 activity, wild-type or the Copine 6 mutant were expressed together with GFP-Rac1 in COS7 cells. Activated Rac1 was purified on agarose beads loaded with a GST-tagged version of the binding domain of p21-activated kinase (GST-PBD) as a substrate. In the presence of Copine 6, the amount of active GTP-bound Rac1 was significantly higher than in the control (Fig. 6B and Fig. 6B'). Moreover, the Cpne6D167N mutant showed a similar enhancement of Rac1 activation (Fig. 6B and Fig. 6B'). To get a quantitative measure of Copine 6-mediated Rac1 activation, we also performed dose-response experiments in which we treated serum-starved COS7 cells with increasing concentrations of EGF. Cells were stimulated by EGF for 1 minute, which is the time needed for maximal Rac1 activation (Yasui et al., 2001). Intriguingly, the concentration of EGF required for half maximal activation of Rac1 was significantly lower in cells expressing Copine 6- compared to mock-transfected cells (Fig. 6C). Together, these results show that Copine 6 associates with Rac1 and catalyzes its activation independent of its capability to bind calcium.

Copine 6 recruits Rac1 to the membrane in a calcium-dependent manner

As the localization of Copine 6 to membranes is calcium dependent, we next asked whether calcium influx would also alter the cellular localization of Rac1 in a Copine 6-dependent manner. To test this, Copine 6-RFP and GFP-Rac1 were transfected separately (Fig. 7A) or in combination (Fig. 7A’) into COS7 cells. When expressed alone, GFP-Rac1 localization was cytosolic and remained unchanged upon treatment with ionomycin, in contrast to the localization of Copine 6-RFP (Fig. 7A). When Copine 6 and Rac1 were present in the same cell, we observed Rac1 recruitment at the membrane in an ionomycin-dependent manner (Fig. 7A’). Importantly, the co-localization was not observed in cells that co-expressed Copine 6 together with Cdc42 or RhoA (Fig. 7A’’). Finally, when we triple transfected GFP-Rac1, Copine 6-RFP and a myc-tagged version of p21-activated kinase (PAK1-myc), all three proteins co-aggregated at the plasma membrane when cells were treated with ionomycin (Fig. S5A). GFP-Rac1 and Pak1-myc did not aggregate when RFP instead of Copine 6-RFP was transfected (Fig. S5B). Staining for phospho-Pak1 showed that Rac1 was active in the clusters induced by Copine 6 (Fig. S5A).

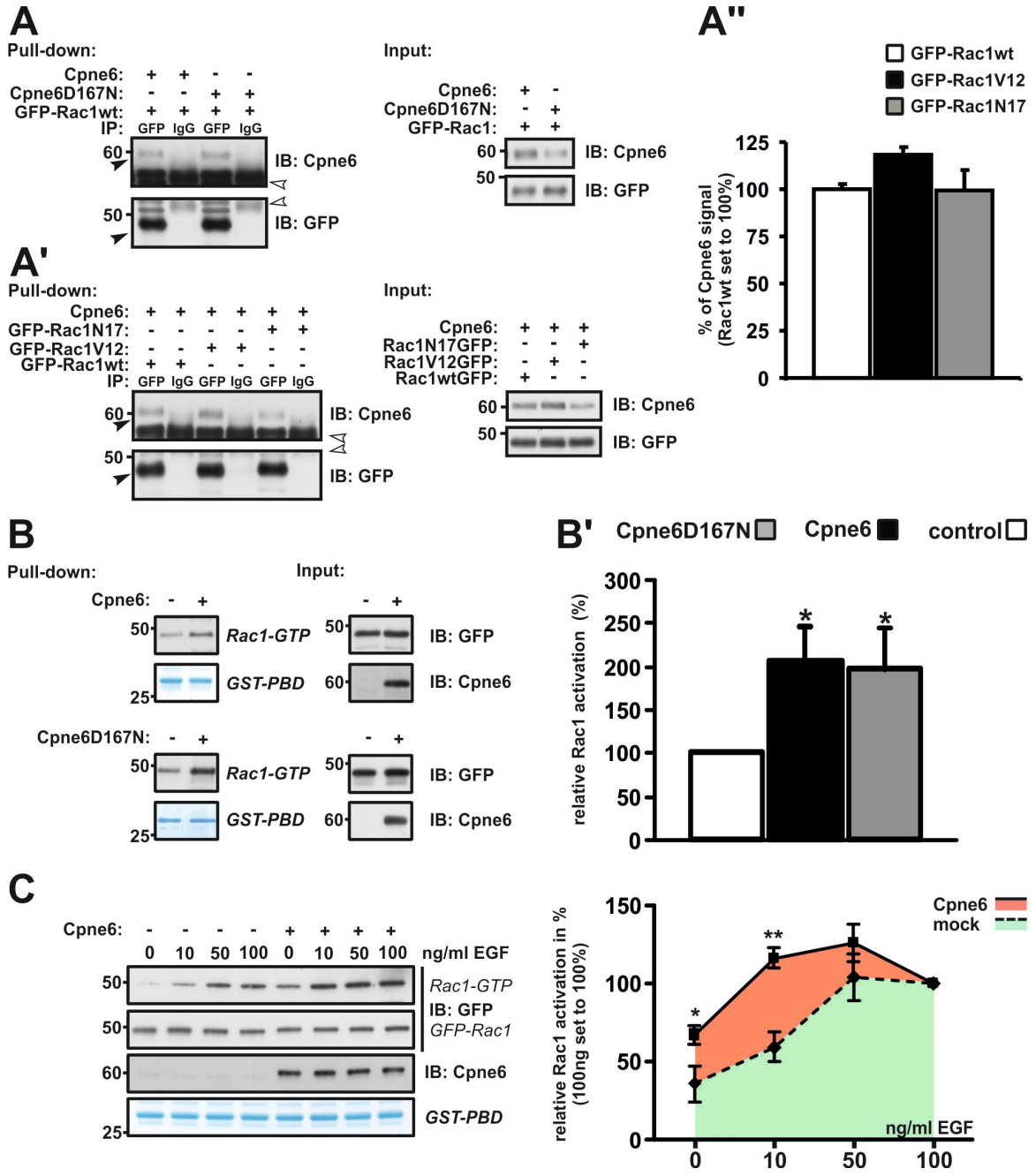

Figure 6. Copine 6 interacts with the small Rho-like GTPase Rac1 and promotes its activation. (A) COS7 cells were transfected with expression constructs encoding Copine 6 (Cpne6) or the calcium insensitive mutant (Cpne6D167N) together with GFP-Rac1. After crosslinking with Dithiobis-succinimidyl propionate (DSP), Rac1 complexes were subjected to pull-down using anti-GFP antibodies or non-immune IgG (control). Immunoprecipitates were analyzed with anti-Copine 6 and anti-GFP antibodies. Both Cpne6 and Cpne6D167N co-immunoprecipitated with anti-GFP but not with non-immune IgG. (A') Copine 6 interacts with a dominant-negative (GFP-Rac1N17) and a constitutively active form (GFP-Rac1V12) of Rac1. Input controls are always shown to the right. Black arrowheads indicate Copine 6 or GFP-Rac1; white arrowheads indicate antibody heavy chain. (A'') Quantification of (A'). (B) COS7 cells were transfected with GFP-Rac1 and either Cpne6, Cpne6D167N or empty plasmid (control). Activated GFP-Rac1 (Rac1-GTP) was isolated by GST-PBD mediated pull-down. Both, Cpne6 and Cpne6D167N, increase Rac1 activation compared to the control (B'). Values are normalized to the amount of GFP-Rac1 in the input control. The amount of activated Rac1 in control cells was set to 100%. (C) Dose-response of EGF-induced Rac1 activation in the presence of Cpne6. Copine 6 potentiates activation of Rac1 by EGF. Right panel: Quantification of the Cpne6-mediated potentiation of Rac1 activation. Data shown is mean value ± SEM; * $p < 0.05$; ** $p < 0.01$. Between 3 or 5 independent experiments were used for quantification.

Collectively, our data show that Copine 6 can form a complex with Rac1, mediates the accumulation of Rac1 at plasma membranes. Rac1 in this Copine 6 complex is active as indicated by the activity assay and the staining for phospho-Pak1.

Blocking Rac1 or neuronal activity in Copine 6 knockdown neurons increases filopodia number

If Rac1 were the principal target of Copine 6 and the increased number of synapses in Copine 6 knockdown neurons relied on a deregulation of Rac1, selective inhibition of the GTPase should affect this phenotype. To test this hypothesis, we applied NSC 23766, a Rac1-specific inhibitor that does not affect the activity of Cdc42 and RhoA (Gao et al., 2004; Kim et al., 2009). As shown in Figure 7B, blocking Rac1 activity had no effect on spine density in neurons expressing shRNA CD4 but abolished the increase of spine density in neurons expressing shRNA Cpne6. Interestingly, this loss of spines was accompanied by a highly significant increase in the number of filopodia (Fig. 7B'), reminiscent of the phenotype obtained by overexpressing the calcium-insensitive Copine 6 mutant (see Fig. 5B'). The fact that Rac1 inhibition did not affect spine number in control neurons suggests that the spines induced by the knockdown of Copine 6 may represent unstable, supernumerary spines.

Activation of excitatory synapses causes unstable, dynamic spines to become stable and non-motile in culture (Ackermann and Matus, 2003; Star et al., 2002). To test whether the spines induced by the knockdown of Copine 6 were indeed unstable, we compared synapse formation in cultured hippocampal neurons expressing shRNA Cpne6 and shRNA CD4. The increase in synapses was highly depending on the maturation state of the examined neuronal culture. During early stages, at DIV 9, loss of Copine 6 increased filopodia density (Fig. 7C, left and 7C', right). At DIV 10, neurons expressing shRNA Cpne6 had more spines than control neurons (Fig. 7C, left). This difference became even more pronounced at DIV 12. The high density of spines was lost by treating neurons for 8 hours with 1 µM TTX (Fig. 7C and 7C', left). Instead, the filopodia density was increased (Fig. 7C', right). We thus conclude that the increase in spine number in Copine 6 knockdown neurons is dependent on both neuronal activity and Rac1 GTPase activity. Consistent with this notion, the calcium-insensitive mutant would simulate a low calcium, low activity state of synapses, which has been shown to cause the breakdown of spines into filopodia (Nagerl et al., 2004).

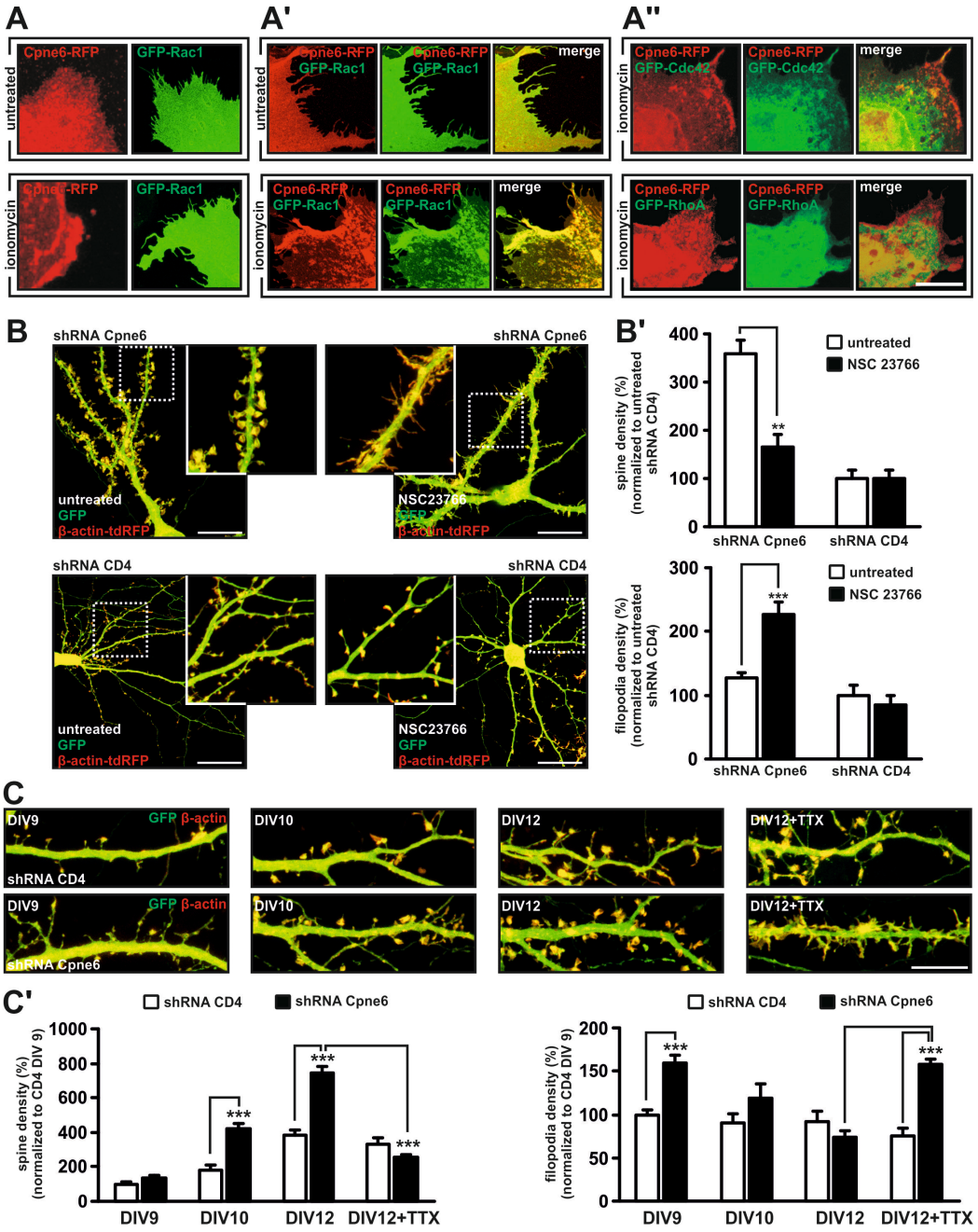

Figure 7. Copine 6 influences Rac1 localization and function. COS7 cells transfected with Copine 6-RFP (Cpne6-RFP) or GFP-Rac1 (A) or both constructs (A') were incubated with ionomycin or DMSO (untreated). In contrast to Cpne6-RFP, the localization of GFP-Rac1 does not change upon ionomycin application (A). GFP-Rac1, however, co-localizes together with Copine 6 in cotransfected cells (A'). This co-localization is not seen with GFP-Cdc42 or GFP-RhoA (A''); scale bar = 20 µm. (B) DIV 14 hippocampal neurons transfected with the constructs indicated were either treated with the Rac1 inhibitor NSC 23766 or DMSO (untreated). The number of spines in shRNA Cpne6 expressing neurons is highly sensitive to NSC 23766 (B, top) whereas spines of control neurons expressing shRNA CD4 are not (B, bottom). (B') Quantification of the effect on spine number (top) and filopodia number (bottom). Data shown are mean value ± SEM from N = 3 experiments with >12 neurons. At least two dendrites per neuron were counted; scale bar = 20 µm. (C) Knockdown of Copine 6 affects filopodia and spine number and is sensitive to TTX. Primary hippocampal neurons express control (shRNA CD4) or shRNA to Copine 6 together with GFP and β-actin-tdRFP. The number of spines (C', left) and filopodia (C', right) was counted at different time points (DIV 9, 10 or 12) and in the absence of neuronal activity (DIV 12+TTX). Neurons expressing shRNA Cpne6 had initially a higher density of filopodia and later of spines than controls. While spine density in control cultures was not sensitive to blockade of action potential by TTX, the supernumerary spines formed in shRNA Cpne6-expressing neurons were transformed to filopodia. N = 2 independent experiments and > 10 neurons were analyzed.

Discussion

Our study identifies the calcium-binding protein Copine 6 as a new player involved in the translation of neuronal activity into changes of synaptic structure. Moreover, our data indicate that Copine 6 has both a stabilizing and de-stabilizing function for synapses. This duality depends on calcium levels as Copine 6 is recruited into cholesterol-rich plasma membranes and into spines upon calcium influx while it remains mainly in the cytosol at calcium levels below 1 µM. Importantly, Copine 6 binds to Rac1 in a calcium-independent manner but recruits Rac1 and its downstream effector Pak1 to plasma membranes upon elevation of intracellular calcium. Finally, we also show that Copine 6 catalyzes the activation of Rac1. Thus, our data are in agreement with a model, whereby the dynamic shuttling of a Copine 6-Rac1 complex contributes to spine maturation and stabilization (Fig. 8A).

Spatial and temporal expression pattern of Copine 6 indicates a function in synapses

Consistent with a role in synapse formation, we show that Copine 6 expression is particularly high in regions and time points of ongoing synaptogenesis. We show that expression of Copine 6 is upregulated at the mRNA and the protein level during the formation of excitatory synapses in primary hippocampal neurons (Fig. 1A, B; Fig. S2). Moreover, Copine 6 expression increases during the time of synaptogenesis in vivo (Fig. 1B) and remains high in regions of high synaptic plasticity, such as hippocampus and olfactory bulb (Fig. 1C). In support of our expression data, Copine 6 expression has been shown to increase upon synaptic stimulation by kainate injection in vivo or after induction of LTP in CA1 regions of acute hippocampal slices (Nakayama et al., 1998).

In hippocampal slices, Copine 6 is enriched in spines (Fig. 1F), suggesting that Copine 6 might be involved in an activity-induced postsynaptic process. High neuronal activity leads to the opening of NMDA receptors, which in turn can cause changes in synaptic structure due to calcium influx, a process important for learning and memory (Matsuzaki et al., 2004; Shimizu et al., 2000). Opening of NMDA receptors has been shown to cause a transient, local increase in calcium to ~ 12 µM (Sabatini et al., 2002). Biochemical analysis of the membrane-binding properties of Copine 6 demonstrates half-maximal binding to membranes at ~ 4 µM of calcium (Fig. 2B), thus well below the calcium concentration observed in active postsynaptic spines. Our analysis also shows that Copine 6 is localized to the cytoplasm at calcium concentrations lower than 1 µM, which represents that of resting cells (Carafoli, 1987).

Several lines of evidence indicate that Copine 6 localizes to lipid raft-like membranes. First, if triggered to bind to membranes in COS7 cells by an increase in cytosolic calcium concentrations, Copine 6 accumulates at the plasma membrane in puncta positive for cholera toxin subunit B1, indicative of lipid rafts (Fig. 2C). Second, perturbation of lipid raft stability by depletion of cholesterol by methyl-β-cyclodextrin inhibits the membrane enrichment of Copine 6 (Fig. 2D and D'). Third, Copine 6 protein from adult rat brain extracts co-fractionates with the lipid raft marker Flotillin-1 and with the NMDA receptor subunit NR1 in the presence of calcium (Fig. 2C'). Lipid raft-like membranes are highly enriched in dendritic spines (Hering et al., 2003) and Copine 6 is enriched in postsynaptic densities (Fig. 3A). This argues that Copine 6 might associate with lipid-raft-like membranes of dendritic spines upon an increase in calcium. Indeed, Copine 6 expressed in hippocampal neurons

translocates into spines within minutes when NMDA receptors open (Fig. 3B-D). Importantly, the calcium-dependent membrane localization of Copine 6 was reversible (Fig. 2B, Fig. 3A'), indicating that Copine 6 switches between a postsynaptic, membrane-bound and a cytosolic form.

Perturbation of Copine 6 alters synapse stability

Examination of neuronal cultures where Copine 6 is removed by shRNA knockdown show an increase in the number of functional spines compared to control neurons (Fig. 4A-E). However, those spines were sensitive to blockade of neuronal activity since TTX application decreased their number while the density of filopodia increased. In contrast, spine and filopodia numbers were not changed in control neurons using the same paradigm (Fig. 7C). These experiments argue that the spines that are formed in Copine 6 knockdown cultures are not stable. Neuronal activity induces postsynaptic calcium transients, which affect synapse structure (Fischer et al., 2000; McKinney et al., 1999). Our results therefore indicate that postsynaptic calcium transients are critical to stabilize spines formed in Copine 6 knockdown cells. The observed shift of protrusion density from spine-rich to filopodia-rich upon TTX application is reminiscent of neurons overexpressing the calcium-insensitive mutant of Copine 6 (Fig. 5). The convergence of these two phenotypes is likely based on the failure of the Copine 6 mutant to translocate into spines and to facilitate a process that leads to the stabilization of spines. In analogy, the removal of Copine 6 from spines at low calcium levels might contribute to a destabilizing mechanism.

Copines do not contain any signaling domains but have been shown to interact with a wide range of target proteins, including MEK1 and the Cdc-42-binding kinase (Tomsig et al., 2003). Thus, the phenotype observed in the Copine 6 knockdown and overexpression experiments is probably based on Copine 6 modulating the localization and function of interacting proteins. In the absence of neuronal activity Copine 6 sequesters these interactors in the cytosol, while removal of Copine 6 releases them to the membrane causing the formation of filopodia and of unstable spines. In the presence of neuronal activity Copine 6 shuttles them to spines and stabilizes those. The calcium-insensitive Copine 6 mutant sequesters the interactors in the cytosol and thereby prevents their enrichment in spines.

Copine 6 modulates Rac1 distribution and activity

We identify Rac1 as the interactor of Copine 6 responsible for the observed changes in synaptic structures. First, Rac1 binds to Copine 6 (Fig. 6A). Second, Copine 6 changes the distribution of Rac1 in a calcium-dependent manner (Fig. 7A). Third, Copine 6 potentiates the activation of Rac1 (Fig. 6B and C). Finally, the supernumerary spines in the Copine 6 knockdown neurons are sensitive to NSC 23766, a Rac1-specific inhibitor (Fig. 7B). Based on our data we propose a model of Copine 6 function (Fig. 8A). In this model knockdown of Copine 6 prevents the retention of Rac1 in the cytosol and causes Rac1 to initially induce more filopodia (Fig. 8B, left). As neuronal activity increases those filopodia mature to spines (Fig. 8B, middle). Blocking neuronal activity or inhibition of Rac1 activation reverses the supernumerary spines to filopodia, indicating that the spines induced by the Copine 6 knockdown are unstable (Fig. 8B, right). In consequence, stabilization of spines is based on the

localization of Copine 6 to the PSD and the sustained local activation of Rac1 (Fig. 8A, right). Overexpression of the calcium-insensitive mutant of Copine 6 sequesters Rac1 in the cytosol. As a result, neuronal activity and the remaining Rac1 activity are not sufficient to transform filopodia into spines (Fig. 8C).

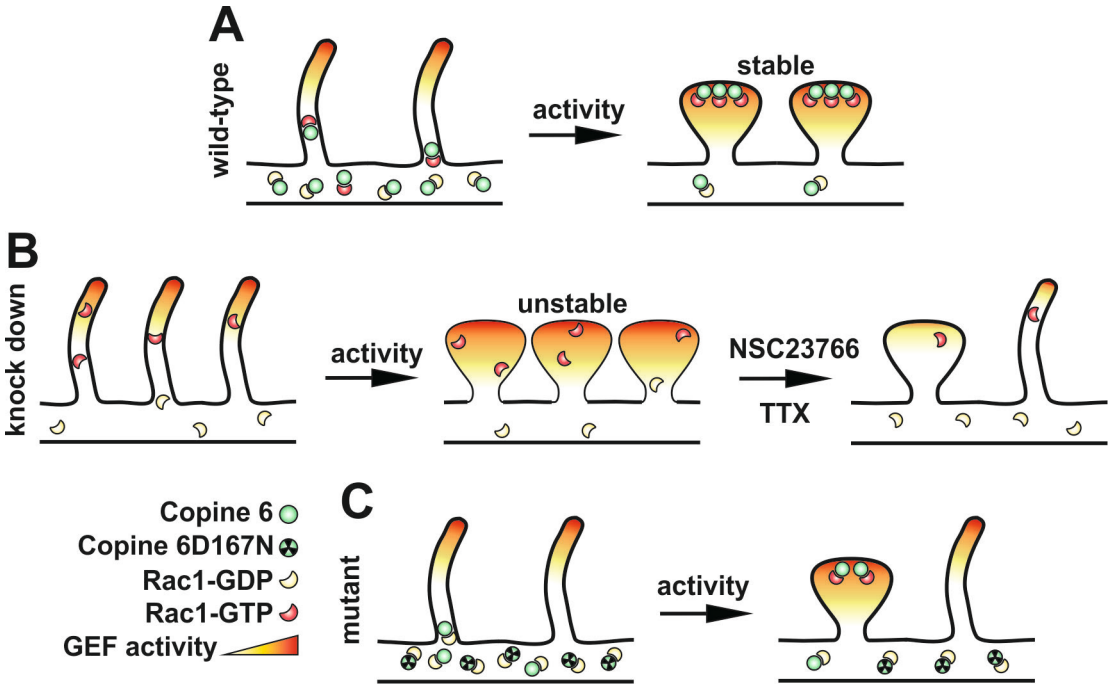

Figure 8. Model of Copine 6 function in neurons. (A) Function of Copine 6 in wild-type neurons. During low calcium states, Copine 6 retains Rac1 in the cytoplasm. Neuronal activity (activity) by increasing calcium concentrations at postsynapses induces the shuttling of the Copine 6 – Rac1 complex into the PSD. Intrinsic GEF activity is further enhanced by Copine 6, increases Rac1 activity and stabilizes the spine. (B) Response of neurons to the knock down of Copine 6. Without Copine 6-mediated retention of Rac1 in the dendritic shaft, Rac1 can reach the synaptic membrane and induce the formation of filopodia and of supernumerary, unstable spines, which are sensitive to the Rac1 inhibitor NSC23766 and TTX. (C) Response of neurons to expression of the calcium-insensitive mutant of Copine 6. As Copine 6D167N does not translocate to spines at high calcium, Rac1 is retained in the cytoplasm and prevents the formation of spines by neuronal activity.

Our observation that Copine 6 modulates Rac1 activity and localization and thereby influences spine formation and maintenance is in agreement with previous findings that have implicated Rac1 function in synapse formation. For example, both Rac1-GTP and its effector Pak1 are enriched in spines and their precursors (Zhang et al., 2005). Mice, in which Rac1 is deleted from neurons, show a decrease in spine number and an increase in filopodia density (Corbetta et al., 2009; Haditsch et al., 2009). Moreover, changes in Rac1 activity have been implicated in several forms of mental retardation that are characterized by subtle changes in spine morphology (Penzes et al., 2011). Similarly, overexpression of dominant-negative mutants of Rac1 or its downstream effectors Pak1 or Pak3, results in more filopodia and fewer spines (Tashiro and Yuste, 2004; Zhang et al., 2005).

Activation of Rac1 requires guanine nucleotide exchange factors (GEFs). Our findings on NSC 23766 (Fig. 7B), which specifically inhibits the binding site of Tiam1 and TrioN on Rac1 (Gao et al., 2004), indicate the involvement of those two GEFs in Copine 6-dependent regulation of Rac1 activity. Besides Tiam1 and TrioN several additional Rac1 GEFs including Kalirin-7, PIX and GIT1, have been shown to localize to spines and to be responsive to neuronal activity. Importantly, changes of their activity have been reported to affect spine morphology (Lambert et al., 2002; Penzes et al., 2001; Tolias et al., 2005). This study introduces dynamic, Copine 6-mediated translocation of Rac1 in response to changes in cytosolic calcium levels as a novel molecular mechanism.

Homology of function between Copine 6 and CaMKII in the CNS

Here we introduce Copine 6 as a novel factor that stabilizes spines and modulates their response to neuronal activity and their transition to filopodia. The functional properties of Copine 6 are very reminiscent of calcium/calmodulin dependent kinase II (CaMKII). It translocates into spines in an activity-dependent manner (Otmakhov et al., 2004; Zhang et al., 2008), its activation requires calcium influx via the NMDA receptor (Lee et al., 2009), and it is enriched in lipid rafts (Suzuki et al., 2008). In addition, CaMKII was shown to activate Tiam1 and Kalirin-7, which in turn, activate Rac1 and therefore stabilize synapses (Fleming et al., 1999; Xie et al., 2007). Due to its switch-like properties, CaMKII is considered a ‘memory molecule’, and manipulation of CaMKII activity in vivo strongly affects learning and recall of specific memories (Cao et al., 2008; Glazewski et al., 2000). Our work shows that Copine 6 has similar functional properties, acts in similar pathways and therefore may be of comparable importance for synaptic stability, learning and memory.

Experimental procedures

Animals

All animal procedures complied with Swiss animal experimental regulations (ethical application approval no 1693).

DNA constructs and antibodies

All shRNA constructs were designed according to (Elbashir et al., 2001) and cloned under a U6 promotor into a SK(-)-vector. All shRNAs target the open reading frame. Sequences for the sense strand of the central 21-nt double-stranded region are the following: for shRNA to CD4: 5'-CTCTAACCCCTTGACAGAGT-3'; the two used to target Copine 6 were: shRNA to Copine 6-1: 5'-GGAGATCTATAAGACCAATGG-3'; shRNA to Copine 6-2: 5'-GCAAGTCCACTATCACGATCG-3'. A shRNA Copine 6-1 resistent Copine 6 construct was generated by replacing the shRNA recognition sequence with a synthetic nucleotide stretch of silent mutations to: GGAAATATACAAAACAAACGG. Overexpression constructs were cloned into pEGFP(N3), pEGFP(C1), pIRES2-EGFP (BD Bioscience, Clontech), pcDNA3-1(+) and pcDNA3.1(-) (Invitrogen), pMH4 (gift from Thomas Oertner, FMI). Primers used for cloning were: Copine 6: ss HindIII 5'-CCCAAGCTTAGTGCCATGTCGGACCCAGAGATGGGATGGGTGCCTGAGC-3' and as BamHI 5'-CGCGGATCCTGGGCTGGGGCTGGG-3' for fusion to GFP and for IRES plus STOP as BamHI 5'-CGCGGATCCTCATGGGCTGGGGCTGGG-3', β-actin: ss EcoRI 5'-CCGGAATTCTTCGCCATGGATGAC-3' and as BamHI 5'-CGCGGATCCGAAGCATTTGCGGTGCAC -3'. Rac1V12GFP was generated from a wt template by single primer mutagenesis using: 5'-AGACGTAAGCTGTTGGTAAAACCT-3'. Rac1N17GFP was generated from a wt template by single primer mutagenesis using: 5'-AGACGGAGCTGTTGGTAAAAACT-3'. Following antibodies were used: PSD95 (ABR, #MA1-045), SynGAP (ABR, #PA1-046), N-Copine (BD Bioscience, #CG8695), Tubulin (BD Bioscience, #556321), MAP2 (Chemicon, #AB5622), GFP (Chemicon, #AB16901), Bassoon (Stressgen, #VAM-PS003), GluR2 (BD Bioscience, #556341), Flotillin-1 (BD Bioscience, #610820), Synaptophysin (Dako, #A0010), pPAK1 (cell signaling, #2601).

Quantitative real-time PCR

The real-time PCR was carried out on an ABI 7000 and 7700 Sequence Detection system (Applied Biosystems). Primer sequences were designed using Primer Express software (PE; Applied Biosystems). We selected primers close to the 3' end of the target genes with primers localized on different exons. Amplicons were 150 bp (± 10%) in size. Primers were: Copine 6s: (5'-CCCCAAGTACCGAGACAAGAAGA-3'); Copine 6as: (5'-GGAGGCTGTGAAGTCGATAGC-3'); GAPDHs: (5'-CATCGTGGAAGGGCTCATGAC-3'); GAPDHas: (5'- CTTGGCAGCACCAGTGGATG-3'); PGK 1s: (5'-GCCCATGCCCGACAAGTAC-3'); PGK 1as: (5'- GAGGTTCTCCAGGAGGATGAC-3'); SynGAPs: (5'-

GCCAGAAATACCTCAAGGATGCC-3'); SynGAPas: (5'- GCACAGGGCCAACTCACAG-3'). The reactions were all performed using the SYBR Green PCR Core Reagents (Applied Biosystems).

Pharmacological agents and inhibitors

Glutamic acid (Sigma Aldrich, Prod.No.: G-2128) 10 mM stock solution, set to 8-50 µM as reaction concentration; NMDA (Tocris, Prod.No.: 0114) 100 mM stock solution, set to 10 µM reaction concentration; D-APV (Tocris, Prod.No.: 0106) 10 mM stock solution, set to 50 µM reaction concentration; trans ACBD (Tocris, Prod.No.: 0270) 100 mM stock solution, set to 50 µM reaction concentration; CdCl2 (Sigma Aldrich, Prod.No.: 655198) 100 mM, set to 50 µM reaction concentration; NSC 23766 (Tocris, Prod.No.: 2161) 50 mM, set to 100 µM reaction concentration.

Primary hippocampal cultures

Low density cultures (~150 cells mm−2) were used for co-localization studies and expression profile experiments. Hippocampal cultures were established from 18 day old fetal Wistar rat hippocampi and primary astrocytes, used as feeder layer, were obtained from newborn rat cortical hemisphere. For functional and morphological studies, high density hippocampal primary neuronal cultures were used. The hippocampi were dissected from embryonic day (E) 18–19 rat embryos and washed in ice cold HBSS buffer followed by 15 min incubation in trypsin at 37°C. After a second wash with HBSS hippocampi were additionally washed in prewarmed DMEM complete plating medium containing 0.6% glucose. Dissociation was performed in prewarmed plating medium and plated at high density (750 cells mm^{-2}) on glass slides (pre coated with poly-l-lysine o/n followed by extensive washing with PBS). After 3 h plating medium was exchanged with culture medium containing: Neurobasal medium (Gibco), 0.5 mM glutamine, antibiotics and B27 supplement (Gibco). Experiments were performed in accordance with the Federal Ordinance on the Protection of Animals.

Transfection, Immunocytochemistry

Transfection of hippocampal culture was performed in 24-well-plates using Lipofectamine2000 following the manufacturer's instructions at DIV 7 with a total of 500 ng DNA per well (shRNA:GFP 4:1; shRNA:GFP:β-actin 4:0.5:0.5; CpneX-GFP:β-actin 4:1). Neuronal cells were fixed between DIV 12 and DIV 14 with 4% paraformaldehyde in PBS with 120 mM sucrose, permeabilized with 0.25% Triton X-100 in PBS and, subsequently incubated with primary antibody overnight at 4°C in PBS with 3% BSA. Finally, cells were treated with appropriate secondary antibody for 1 h at RT and the immunolabeled cells were mounted with Cervol.

Ionomycin treatment

Ionomycin (Sigma Aldrich; I9657) was dissolved in DMSO and diluted to 2 µM in empty DMEM. 24 h post transfected COS7 cells were washed twice with prewarmed PBS and incubated for 5 min in 2 µM ionomycin at 37°C. After washing in PBS cells were fixed with 4% PFA in PBS for 30 min.

Lipid raft staining

COS7 cells were fixed and subsequently stained for lipid rafts with 1 µg/ml Choleratoxin subunit B1 (Molecular probes; C-34778 conjugated with Alexa 647) for 1 h at RT. After washing with PBS glass slides were mounted and analyzed.

Imaging

Pictures were made on Leica DM5000 and analyzed using the "analySIS" software or in case of picture stacks with the Leica SPE or Leica SP5 system.

Cholesterol depletion

COS7 cells expressing Copine 6-GFP for 24 h were washed twice with prewarmed PBS followed by an incubation with 10 mM Cyclodextrin (Sigma Alrich; Prod.Nr.: C4555) in plain DMEM for 1 h at 37°C. After washing twice with ice cold PBS cells were scraped in lysisbuffer and subjected for further analysis.

Lipid raft isolation

According to (Hering et al., 2003) 1 adult rat brain was split into left and right hemisphere. Each hemisphere was homogenized in 2 ml of either TNXC + 5 mM $CaCl_2$ or TNXE + 5 mM EDTA; TNX buffer: 25 mM Tris pH 7.5; 320 mM Sucrose; 150 mM NaCl; 1% TX-100; Roche proteinase inhibitors by a motorized glass/teflon homogenizer 15 strokes, 1000 rpm. Debris was removed by 800 x g for 10 min at 4°C. The supernatant was further spun with 10.200 x g for 15 min at 4°C and the pellet resuspended in either TNE + 5 mM EDTA or TNC + 5 mM $CaCl_2$; TN buffer 50 mM Tris pH 7.5; 150 mM NaCl; Roche complete protease inhibitors. The resuspended pellet was sonicated for 5 sec at 4°C (MSE sonicator; amplitude stage 4; intensity low) and 0.1 vol of 10 x TNX(C/E) was added and mixed. After rotating for 20 min at 4°C the sample was adjusted to 45% sucrose by adding half of the total volume of 90%. Overlay the 45% sucrose sample with 12 ml of a linear sucrose gradient (35%-5% in TNE/C; cast by using stirrer columns). Centrifuge with 100.000 x g for 20 h at 4°C to cause floating of lipidraft fractions.

Subcellular fractionation of COS7 cells

According to (Guillemin et al., 2005) a 10 cm (56 cm^2) dish COS7 cells was transfected as a 40-50% confluent culture with 2.5 µg of DNA. After 24 h cells were washed 2x with ice cold PBS and scraped in 500 µl ice cold CLB buffer: 10 mM Hepes, 10 mM NaCl, 1 mM KH_2PO4, 5 mM $NaHCO_3$, 0.5 mM $MgCl_2$ and Roche complete protease inhibitors in presence or absence of either 1 mM $CaCl_2$, 10 nM EGTA or 2 mM EDTA. After homogenization in a motorized teflon/glas homogenizer (300 rpm, 10 strokes) 50 µl of 2.5 M sucrose was added and carefully mixed by pipetting up and down. Nuclei and cell debris were removed by an initial centrifugation (6300 x g, 4°C, 5 min) and the supernatant was distributed in 200 µl aliquots. Each aliquot was set to the appropriate $CaCl_2$, EGTA or EDTA concentration and incubated in head over head shaker for 15 min at 4°C. Membrane (M) and cytoplasmic (C) fractions were separated by spinning the aliquots with 100.000 x g, 4°C, 30 min in a TST 41.14 rotor. The 200 µl supernatant was removed and the pellet resuspended in 200 µl CLB (or aliquot volume) buffer followed by cooking in Laemmlibuffer for 10 min at 95°C.

PSD fractionation and isolation of rat brains

Following method was modified from (Lynn et al., 2001). 1 adult rat brain (2 g) was homogenized in 10 volumes of ice-cold buffer A (0.32 M sucrose, 1 mM $NaHCO_3$, 1 mM $MgCl_2$, 0.5 mM $CaCl_2$) with 12 strokes of a motor-driven (800 rpm) Teflon-glass homogenizer. The homogenate was centrifuged at 1.400 × g for 10 min (SS34, 10.500 rpm 4°C), the nuclear pellet was resuspended (+/- 2 mM EDTA) and centrifuged. The post-nuclear supernatants were combined and centrifuged at 13.800 × g 10 min 4°C to yield a synaptosomal-mitochondrial pellet (P2). The supernatant of P2 was centrifuged at 100.000 × g for 2 h to obtain a pellet consisting of microsomal and plasma membranes (P3 fraction). P2 was resuspended in buffer A (+/- 2 mM EDTA), layered onto a discontinuous 0.85 M, 1.0 M and 1.2 M sucrose density gradient containing 1 mM $NaHCO_3$, centrifuged at 82.500 × g for 2 h using a TST 41.14 rotor, and the subfraction located at the 1.0 M - 1.2 M sucrose density interface was collected. This crude synaptosome fraction was diluted in 4x vol. buffer B: 0.32 M sucrose, 1 mM $NaHCO_3$, 0.5 mM $CaCl_2$, (+/- 2 mM EDTA) and after resuspending was then centrifuged at 13.800 × g for 10 min at 4°C, the pellet, containing Triton-insoluble material (Pre-PSD), was resuspended in buffer C: 10 mM Hepes, (+/- 0.5 mM $CaCl_2$ and +/- 2 mM EDTA) + Roche complete Protease Inhibitors. After 15 min at 4°C hypotonic lysis occurred and synaptic membranes (SM) were pelleted by spinning the sample with 13.800 x g for 10 min at 4°C in an eppendorf table top centrifuge. The supernatant (S5) was stored as synaptosomal cytoplasm whereas the SM fraction was further incubated in 10 mM Hepes, 150 mM NaCl, 2%TX-100 for 15 min rotating at 4°C followed by a 100.000 x g centrifugation for 30 min at 4°C resulting in postsynaptic densities (PSD) and S6. Protein concentration was measured and equal amounts of protein subjected for immunoblotting.

Life imaging

18 mm glass slides covered with DIV 14 neurons transfected with Copine 6-GFP and tdRFP were transferred from a 12 well plate into a life imaging chamber (Ludin) into a low $MgCl_2$ prewarmed ringer solution: 135 mM NaCl, 3 mM KCl, 2 mM $CaCl_2$, 10 mM Hepes, 0.2 mM $MgSO_4$, 25 mM

Glucose, 20 µM Glycine (pH 7,3 - 7,4, 320 mOsm). After 20 min at 37°C the chamber was placed in a prewarmed Zeiss, Axiovert 135M Microscope. The ringersolution in the chamber was replaced to the 10 µM NMDA condition by two syringes followed by taking pictures every 30 sec for total time of 20 min.

Electrophysiology

High density cultures (DIV 12) were perfused with an ACSF solution containing (in mM): 119 NaCl, 2.5 KCl, 1.3 $MgCl_2$, 2.5 $CaCl_2$, 1 NaH_2PO_4, 26.2 $NaHCO_3$, 11 glucose, equilibrated with 95% O_2/5% CO_2 at room temperature (25°C) and delivered at 1.5 ml per min. Whole-cell patch-clamp recordings were performed from the somata of visually identified neurons. The recording electrode (3-5MΩ) was filled with a solution containing (in mM): 135 $CsMeSO_4$, 8 NaCl, 10 HEPES, 0.5 EGTA, 5 QX-314, 4 Mg-ATP, 0.3 Na-GTP (pH 7.25, 285 mOsm). Miniature EPSC (mEPSCs) were recorded at -70 mV in the presence of 0.5 µM TTX (Latoxan, Valence, France) and 100 µM picrotoxin (Fluka/Sigma, Buchs, Switzerland). Detection and analysis of mEPSCs were done using the MiniAnalysis software (Synaptosoft, Decatur, GA, USA). 600 consecutive events from each cell were used for the cumulative probability graph and the Kolmogorov-Smirnov tests. Data were obtained with an Axopatch 200B (Axon Instruments, Union City, CA, USA), filtered at 2 kHz and digitized at 10 kHz, acquired and analyzed with pClamp9 (Axon Instruments, Union City, CA, USA).

Two-photon laser imaging

Organotypic slice cultures were prepared from Wistar rats at postnatal day 5. Slices were transfected between day in vitro (DIV) 5 to 7 using a Helios gene gun (BioRad). Expression of Copine-GFP and RFP was analyzed between DIV 21-28. We used a custom-built 2-photon laser scanning microscope (2PLSM) based on a Olympus BX51WI microscope with LUMPlan 60x/0.90 objective, and a Ti:sapphire laser tuned to λ = 910 nm for excitation. Epi- and transfluorescence was detected using photomultiplier tubes (Hamamatsu). Image acquisition was controlled by custom software (ScanImage, HHMI Janelia Farm).

Immunoprecipitation and Western blotting

10 cm dish COS7 cells were transfected as a 40-50% confluent culture and harvested 24 h post-transfection. Cells were lysed in 1 ml lysis buffer: 50 mM Tris pH7.5, 150 mM NaCl, 1% NP-40, 0.5% deoxycholate and Roche complete mini protease inhibitors for 20 min on ice and insoluble materials were removed by centrifugation at 10.000 x g for 10 min at 4°C before antibody was applied to the supernatant for immunoprecipitation (2 µg of antibody for each IP was used). Brain lysates were prepared from adult rat brains. Olfactory bulb, frontal cortex, motoric cortex, hippocampus, cerebellum and brainstem were dissected and lysed in a weight:vol 1:10 ratio in RIPA buffer + Roche complete mini protease inhibitors. Tissues were passed 10 times through a 25G syringe and incubated for 20 min on ice. Insoluble materials were removed by centrifugation at 10.000 x g for 10

min at 4°C. Equal amounts of protein were separated by 10% SDS-PAGE, transferred to nitrocellulose membrane, and immuno-stained using antibodies previously described. After estimating the proper β-actin ratios samples were adjusted to the housekeeping gene and reloaded.

Crosslinking

24 h after transfection cells were washed twice with prewarmed PBS. After washing cells were incubated with 2 mM Dithiobis succinimidyl propionate (DSP; Pierce; Prod.Nr.: 22585) in PBS (derived from diluting a 25 mM DSP DMSO stock solution (freshly prepared) with PBS. After incubation on ice for 2 h, the reaction was stopped by adding 1 M Tris pH 7.5 to a final concentration of 20 mM followed by a further incubation of 15 min on ice.

Rac1 activation assay

COS7 cells were cultured on poly l-lysine coated 10 cm dishes. At 40% confluency cells were transfected with Copine 6-Ires or empty Ires and GFP-Rac1 in a ratio of 1.5 µg and 3.5 µg respectively. After 24 hours cells were starved for 4 h with plain DMEM (and treated with different concentrations of EGF for EGF race) washed twice with ice-cold PBS and lysed in 1 ml of ice cold 1x Mg2+ lysis/wash buffer (Millipore; 20-168). After 10 min incubation and rocking with 50 µl 50% slurry of Glutathion beads lysates were clean spun with 14.000 x g for 1 min. Cleared lysates were incubated with 5 µg GST-PBD substrate (Millipore; 14-325) for 1 h at 4°C followed by 3 wash steps with 700 µl washing buffer for 10 min and 14.000 x g for 1 min bead sedimentation. Finally GST-PBD beads were cooked in 100 µl Laemmli buffer.

Accession numbers

#AM747279 Rattus norvegicus mRNA for copine 1 protein (Cpne1 gene); #AM747280 Rattus norvegicus mRNA for copine 2 protein (Cpne2 gene); #AM746508 Rattus norvegicus mRNA for copine 3 protein (Cpne3 gene); #AM747281 Rattus norvegicus mRNA for copine 4 protein (Cpne4 gene); #AM747282 Rattus norvegicus mRNA for copine 5 protein (Cpne5 gene); #AM746509 Rattus norvegicus mRNA for copine 6 protein (Cpne6 gene); #AM747283 Rattus norvegicus mRNA for copine 7 protein (Cpne7 gene); #AM747284 Rattus norvegicus mRNA for copine 8 protein (Cpne8 gene)

References

Ackermann, M., and Matus, A. (2003). Activity-induced targeting of profilin and stabilization of dendritic spine morphology. Nat. Neurosci. *6*, 1194-1200.

Arac, D., Chen, X., Khant, H.A., Ubach, J., Ludtke, S.J., Kikkawa, M., Johnson, A.E., Chiu, W., Sudhof, T.C., and Rizo, J. (2006). Close membrane-membrane proximity induced by Ca(2+)-dependent multivalent binding of synaptotagmin-1 to phospholipids. Nat. Struct. Mol. Biol. *13*, 209-217.

Ball, R.W., Warren-Paquin, M., Tsurudome, K., Liao, E.H., Elazzouzi, F., Cavanagh, C., An, B.S., Wang, T.T., White, J.H., and Haghighi, A.P. (2010). Retrograde BMP signaling controls synaptic growth at the NMJ by regulating trio expression in motor neurons. Neuron *66*, 536-549.

Bonhoeffer, T., and Yuste, R. (2002). Spine motility. Phenomenology, mechanisms, and function. Neuron *35*, 1019-1027.

Brose, N., Petrenko, A.G., Sudhof, T.C., and Jahn, R. (1992). Synaptotagmin: a calcium sensor on the synaptic vesicle surface. Science *256*, 1021-1025.

Cahill, M.E., Xie, Z., Day, M., Barbolina, M.V., Miller, C.A., Weiss, C., Radulovic, J., Sweatt, J.D., Disterhoft, J.F., Surmeier, D.J.*, et al.* (2009). Kalirin regulates cortical spine morphogenesis and disease-related behavioral phenotypes. Proc. Natl. Acad. Sci. U. S. A. *106*, 13058-13063.

Calabrese, B., and Halpain, S. (2005). Essential role for the PKC target MARCKS in maintaining dendritic spine morphology. Neuron *48*, 77-90.

Cao, X., Wang, H., Mei, B., An, S., Yin, L., Wang, L.P., and Tsien, J.Z. (2008). Inducible and selective erasure of memories in the mouse brain via chemical-genetic manipulation. Neuron *60*, 353-366.

Carafoli, E. (1987). Intracellular calcium homeostasis. Annu. Rev. Biochem. *56*, 395-433.

Chklovskii, D.B., Mel, B.W., and Svoboda, K. (2004). Cortical rewiring and information storage. Nature *431*, 782-788.

Corbalan-Garcia, S., Rodriguez-Alfaro, J.A., and Gomez-Fernandez, J.C. (1999). Determination of the calcium-binding sites of the C2 domain of protein kinase Calpha that are critical for its translocation to the plasma membrane. Biochem. J. *337 (Pt 3)*, 513-521.

Corbetta, S., Gualdoni, S., Ciceri, G., Monari, M., Zuccaro, E., Tybulewicz, V.L., and de Curtis, I. (2009). Essential role of Rac1 and Rac3 GTPases in neuronal development. FASEB J. *23*, 1347-1357.

Creutz, C.E., Tomsig, J.L., Snyder, S.L., Gautier, M.C., Skouri, F., Beisson, J., and Cohen, J. (1998). The copines, a novel class of C2 domain-containing, calcium-dependent, phospholipid-binding proteins conserved from Paramecium to humans. J. Biol. Chem. *273*, 1393-1402.

Damer, C.K., Bayeva, M., Hahn, E.S., Rivera, J., and Socec, C.I. (2005). Copine A, a calcium-dependent membrane-binding protein, transiently localizes to the plasma membrane and intracellular vacuoles in Dictyostelium. BMC cell biology *6*, 46.

Dunaevsky, A., Tashiro, A., Majewska, A., Mason, C., and Yuste, R. (1999). Developmental regulation of spine motility in the mammalian central nervous system. Proc. Natl. Acad. Sci. U. S. A. *96*, 13438-13443.

Elbashir, S.M., Harborth, J., Lendeckel, W., Yalcin, A., Weber, K., and Tuschl, T. (2001). Duplexes of 21-nucleotide RNAs mediate RNA interference in cultured mammalian cells. Nature *411*, 494-498.

Fischer, M., Kaech, S., Knutti, D., and Matus, A. (1998). Rapid actin-based plasticity in dendritic spines. Neuron *20*, 847-854.

Fischer, M., Kaech, S., Wagner, U., Brinkhaus, H., and Matus, A. (2000). Glutamate receptors regulate actin-based plasticity in dendritic spines. Nat. Neurosci. *3*, 887-894.

Fleming, I.N., Elliott, C.M., Buchanan, F.G., Downes, C.P., and Exton, J.H. (1999). Ca2+/calmodulin-dependent protein kinase II regulates Tiam1 by reversible protein phosphorylation. J. Biol. Chem. *274*, 12753-12758.

Gao, Y., Dickerson, J.B., Guo, F., Zheng, J., and Zheng, Y. (2004). Rational design and characterization of a Rac GTPase-specific small molecule inhibitor. Proc. Natl. Acad. Sci. U. S. A. *101*, 7618-7623.

Glazewski, S., Giese, K.P., Silva, A., and Fox, K. (2000). The role of alpha-CaMKII autophosphorylation in neocortical experience-dependent plasticity. Nat. Neurosci. *3*, 911-918.

Gottschalk, A., Almedom, R.B., Schedletzky, T., Anderson, S.D., Yates, J.R., 3rd, and Schafer, W.R. (2005). Identification and characterization of novel nicotinic receptor-associated proteins in Caenorhabditis elegans. EMBO J. *24*, 2566-2578.

Guillemin, I., Becker, M., Ociepka, K., Friauf, E., and Nothwang, H.G. (2005). A subcellular prefractionation protocol for minute amounts of mammalian cell cultures and tissue. Proteomics *5*, 35-45.

Haditsch, U., Leone, D.P., Farinelli, M., Chrostek-Grashoff, A., Brakebusch, C., Mansuy, I.M., McConnell, S.K., and Palmer, T.D. (2009). A central role for the small GTPase Rac1 in hippocampal plasticity and spatial learning and memory. Mol. Cell. Neurosci. *41*, 409-419.

Harris, K.M., and Kater, S.B. (1994). Dendritic spines: cellular specializations imparting both stability and flexibility to synaptic function. Annu. Rev. Neurosci. *17*, 341-371.

Hering, H., Lin, C.C., and Sheng, M. (2003). Lipid rafts in the maintenance of synapses, dendritic spines, and surface AMPA receptor stability. J. Neurosci. *23*, 3262-3271.

Hering, H., and Sheng, M. (2003). Activity-dependent redistribution and essential role of cortactin in dendritic spine morphogenesis. J. Neurosci. *23*, 11759-11769.

Jourdain, P., Fukunaga, K., and Muller, D. (2003). Calcium/calmodulin-dependent protein kinase II contributes to activity-dependent filopodia growth and spine formation. J. Neurosci. *23*, 10645-10649.

Keck, T., Mrsic-Flogel, T.D., Vaz Afonso, M., Eysel, U.T., Bonhoeffer, T., and Hubener, M. (2008). Massive restructuring of neuronal circuits during functional reorganization of adult visual cortex. Nat. Neurosci. *11*, 1162-1167.

Kim, I.H., Park, S.K., Hong, S.T., Jo, Y.S., Kim, E.J., Park, E.H., Han, S.B., Shin, H.S., Sun, W., Kim, H.T.*, et al.* (2009). Inositol 1,4,5-trisphosphate 3-kinase a functions as a scaffold for synaptic Rac signaling. J. Neurosci. *29*, 14039-14049.

Korkotian, E., and Segal, M. (2001). Regulation of dendritic spine motility in cultured hippocampal neurons. J. Neurosci. *21*, 6115-6124.

Lambert, J.M., Lambert, Q.T., Reuther, G.W., Malliri, A., Siderovski, D.P., Sondek, J., Collard, J.G., and Der, C.J. (2002). Tiam1 mediates Ras activation of Rac by a PI(3)K-independent mechanism. Nat. Cell Biol. *4*, 621-625.

Lee, S.J., Escobedo-Lozoya, Y., Szatmari, E.M., and Yasuda, R. (2009). Activation of CaMKII in single dendritic spines during long-term potentiation. Nature *458*, 299-304.

Lemmon, M.A. (2008). Membrane recognition by phospholipid-binding domains. Nat. Rev. Mol. Cell Biol. *9*, 99-111.

Lendvai, B., Stern, E.A., Chen, B., and Svoboda, K. (2000). Experience-dependent plasticity of dendritic spines in the developing rat barrel cortex in vivo. Nature *404*, 876-881.

Lynn, B.D., Rempel, J.L., and Nagy, J.I. (2001). Enrichment of neuronal and glial connexins in the postsynaptic density subcellular fraction of rat brain. Brain Res. *898*, 1-8.

Majewska, A., Brown, E., Ross, J., and Yuste, R. (2000). Mechanisms of calcium decay kinetics in hippocampal spines: role of spine calcium pumps and calcium diffusion through the spine neck in biochemical compartmentalization. J. Neurosci. *20*, 1722-1734.

Marrs, G.S., Green, S.H., and Dailey, M.E. (2001). Rapid formation and remodeling of postsynaptic densities in developing dendrites. Nat. Neurosci. *4*, 1006-1013.

Matsuzaki, M., Honkura, N., Ellis-Davies, G.C., and Kasai, H. (2004). Structural basis of long-term potentiation in single dendritic spines. Nature *429*, 761-766.

Matus, A. (2000). Actin-based plasticity in dendritic spines. Science *290*, 754-758.

McKinney, R.A., Capogna, M., Durr, R., Gahwiler, B.H., and Thompson, S.M. (1999). Miniature synaptic events maintain dendritic spines via AMPA receptor activation. Nat. Neurosci. *2*, 44-49.

Murakoshi, H., Wang, H., and Yasuda, R. (2011). Local, persistent activation of Rho GTPases during plasticity of single dendritic spines. Nature *472*, 100-104.

Nagerl, U.V., Eberhorn, N., Cambridge, S.B., and Bonhoeffer, T. (2004). Bidirectional activity-dependent morphological plasticity in hippocampal neurons. Neuron *44*, 759-767.

Nakayama, T., Yaoi, T., Yasui, M., and Kuwajima, G. (1998). N-copine: a novel two C2-domain-containing protein with neuronal activity-regulated expression. FEBS letters *428*, 80-84.

Newey, S.E., Velamoor, V., Govek, E.E., and Van Aelst, L. (2005). Rho GTPases, dendritic structure, and mental retardation. J. Neurobiol. *64*, 58-74.

Otmakhov, N., Tao-Cheng, J.H., Carpenter, S., Asrican, B., Dosemeci, A., Reese, T.S., and Lisman, J. (2004). Persistent accumulation of calcium/calmodulin-dependent protein kinase II in dendritic spines after induction of NMDA receptor-dependent chemical long-term potentiation. J. Neurosci. *24*, 9324-9331.

Penzes, P., Cahill, M.E., Jones, K.A., and Srivastava, D.P. (2008). Convergent CaMK and RacGEF signals control dendritic structure and function. Trends Cell Biol. *18*, 405-413.

Penzes, P., Cahill, M.E., Jones, K.A., Vanleeuwen, J.E., and Woolfrey, K.M. (2011). Dendritic spine pathology in neuropsychiatric disorders. Nat. Neurosci. *14*, 285-293.

Penzes, P., Johnson, R.C., Sattler, R., Zhang, X., Huganir, R.L., Kambampati, V., Mains, R.E., and Eipper, B.A. (2001). The neuronal Rho-GEF Kalirin-7 interacts with PDZ domain-containing proteins and regulates dendritic morphogenesis. Neuron *29*, 229-242.

Perestenko, P.V., Pooler, A.M., Noorbakhshnia, M., Gray, A., Bauccio, C., and Jeffrey McIlhinney, R.A. (2010). Copines-1, -2, -3, -6 and -7 show different calcium-dependent intracellular membrane translocation and targeting. Febs J *277*, 5174-5189.

Sabatini, B.L., Oertner, T.G., and Svoboda, K. (2002). The life cycle of Ca(2+) ions in dendritic spines. Neuron *33*, 439-452.

Sala, C., Piech, V., Wilson, N.R., Passafaro, M., Liu, G., and Sheng, M. (2001). Regulation of dendritic spine morphology and synaptic function by Shank and Homer. Neuron *31*, 115-130.

Saneyoshi, T., Wayman, G., Fortin, D., Davare, M., Hoshi, N., Nozaki, N., Natsume, T., and Soderling, T.R. (2008). Activity-dependent synaptogenesis: regulation by a CaM-kinase kinase/CaM-kinase I/betaPIX signaling complex. Neuron *57*, 94-107.

Schrimpf, S.P., Meskenaite, V., Brunner, E., Rutishauser, D., Walther, P., Eng, J., Aebersold, R., and Sonderegger, P. (2005). Proteomic analysis of synaptosomes using isotope-coded affinity tags and mass spectrometry. Proteomics *5*, 2531-2541.

Schubert, V., Da Silva, J.S., and Dotti, C.G. (2006). Localized recruitment and activation of RhoA underlies dendritic spine morphology in a glutamate receptor-dependent manner. J. Cell Biol. *172*, 453-467.

Shimizu, E., Tang, Y.P., Rampon, C., and Tsien, J.Z. (2000). NMDA receptor-dependent synaptic reinforcement as a crucial process for memory consolidation. Science *290*, 1170-1174.

Soriano, F.X., Papadia, S., Hofmann, F., Hardingham, N.R., Bading, H., and Hardingham, G.E. (2006). Preconditioning doses of NMDA promote neuroprotection by enhancing neuronal excitability. J. Neurosci. *26*, 4509-4518.

Star, E.N., Kwiatkowski, D.J., and Murthy, V.N. (2002). Rapid turnover of actin in dendritic spines and its regulation by activity. Nat. Neurosci. *5*, 239-246.

Sutton, R.B., Davletov, B.A., Berghuis, A.M., Sudhof, T.C., and Sprang, S.R. (1995). Structure of the first C2 domain of synaptotagmin I: a novel Ca2+/phospholipid-binding fold. Cell *80*, 929-938.

Suzuki, T., Du, F., Tian, Q.B., Zhang, J., and Endo, S. (2008). Ca2+/calmodulin-dependent protein kinase IIalpha clusters are associated with stable lipid rafts and their formation traps PSD-95. J. Neurochem. *104*, 596-610.

Svoboda, K., Tank, D.W., and Denk, W. (1996). Direct measurement of coupling between dendritic spines and shafts. Science *272*, 716-719.

Tada, T., and Sheng, M. (2006). Molecular mechanisms of dendritic spine morphogenesis. Curr. Opin. Neurobiol. *16*, 95-101.

Tashiro, A., and Yuste, R. (2004). Regulation of dendritic spine motility and stability by Rac1 and Rho kinase: evidence for two forms of spine motility. Molecular and cellular neurosciences *26*, 429-440.

Tolias, K.F., Bikoff, J.B., Burette, A., Paradis, S., Harrar, D., Tavazoie, S., Weinberg, R.J., and Greenberg, M.E. (2005). The Rac1-GEF Tiam1 couples the NMDA receptor to the activity-dependent development of dendritic arbors and spines. Neuron *45*, 525-538.

Tolias, K.F., Bikoff, J.B., Kane, C.G., Tolias, C.S., Hu, L., and Greenberg, M.E. (2007). The Rac1 guanine nucleotide exchange factor Tiam1 mediates EphB receptor-dependent dendritic spine development. Proc. Natl. Acad. Sci. U. S. A. *104*, 7265-7270.

Tomsig, J.L., and Creutz, C.E. (2000). Biochemical characterization of copine: a ubiquitous Ca2+-dependent, phospholipid-binding protein. Biochemistry (Mosc). *39*, 16163-16175.

Tomsig, J.L., Snyder, S.L., and Creutz, C.E. (2003). Identification of targets for calcium signaling through the copine family of proteins. Characterization of a coiled-coil copine-binding motif. The Journal of biological chemistry *278*, 10048-10054.

Volfovsky, N., Parnas, H., Segal, M., and Korkotian, E. (1999). Geometry of dendritic spines affects calcium dynamics in hippocampal neurons: theory and experiments. J. Neurophysiol. *82*, 450-462.

Xie, Z., Srivastava, D.P., Photowala, H., Kai, L., Cahill, M.E., Woolfrey, K.M., Shum, C.Y., Surmeier, D.J., and Penzes, P. (2007). Kalirin-7 controls activity-dependent structural and functional plasticity of dendritic spines. Neuron *56*, 640-656.

Yasui, H., Katoh, H., Yamaguchi, Y., Aoki, J., Fujita, H., Mori, K., and Negishi, M. (2001). Differential responses to nerve growth factor and epidermal growth factor in neurite outgrowth of PC12 cells are determined by Rac1 activation systems. J. Biol. Chem. *276*, 15298-15305.

Yuste, R., and Bonhoeffer, T. (2001). Morphological changes in dendritic spines associated with long-term synaptic plasticity. Annu. Rev. Neurosci. *24*, 1071-1089.

Zhang, H., Webb, D.J., Asmussen, H., Niu, S., and Horwitz, A.F. (2005). A GIT1/PIX/Rac/PAK signaling module regulates spine morphogenesis and synapse formation through MLC. J. Neurosci. *25*, 3379-3388.

Zhang, Y.P., Holbro, N., and Oertner, T.G. (2008). Optical induction of plasticity at single synapses reveals input-specific accumulation of alphaCaMKII. Proc. Natl. Acad. Sci. U. S. A. *105*, 12039-12044.

Zhao, C., Deng, W., and Gage, F.H. (2008). Mechanisms and functional implications of adult neurogenesis. Cell *132*, 645-660.

Ziv, N.E., and Smith, S.J. (1996). Evidence for a role of dendritic filopodia in synaptogenesis and spine formation. Neuron *17*, 91-102.

Supplementary Figures

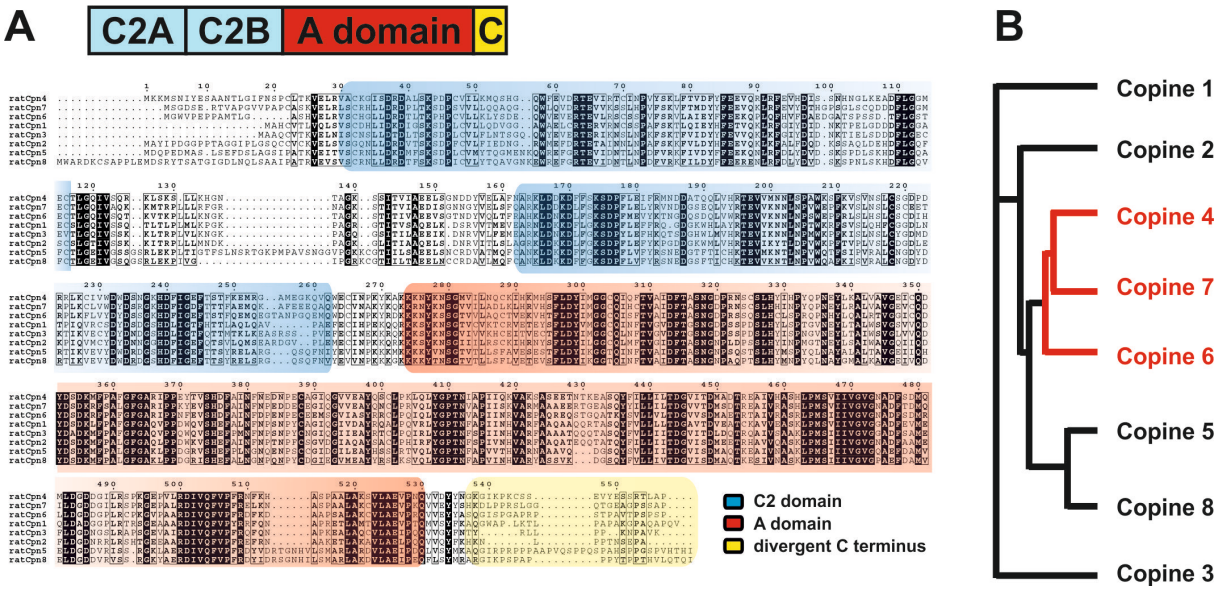

Figure S1. The Copine family, structure and similarity. (A) Overall structure of the Copine protein comprises two calcium binding C2 domains (blue) at the N-terminus followed by an A domain (red) and a highly divergent C-terminus (green). Sequences were aligned using ClustalW. Residues of high homology are highlighted in black boxes. (B) Cladogram showing the relative Copine homologies between the individual family members.

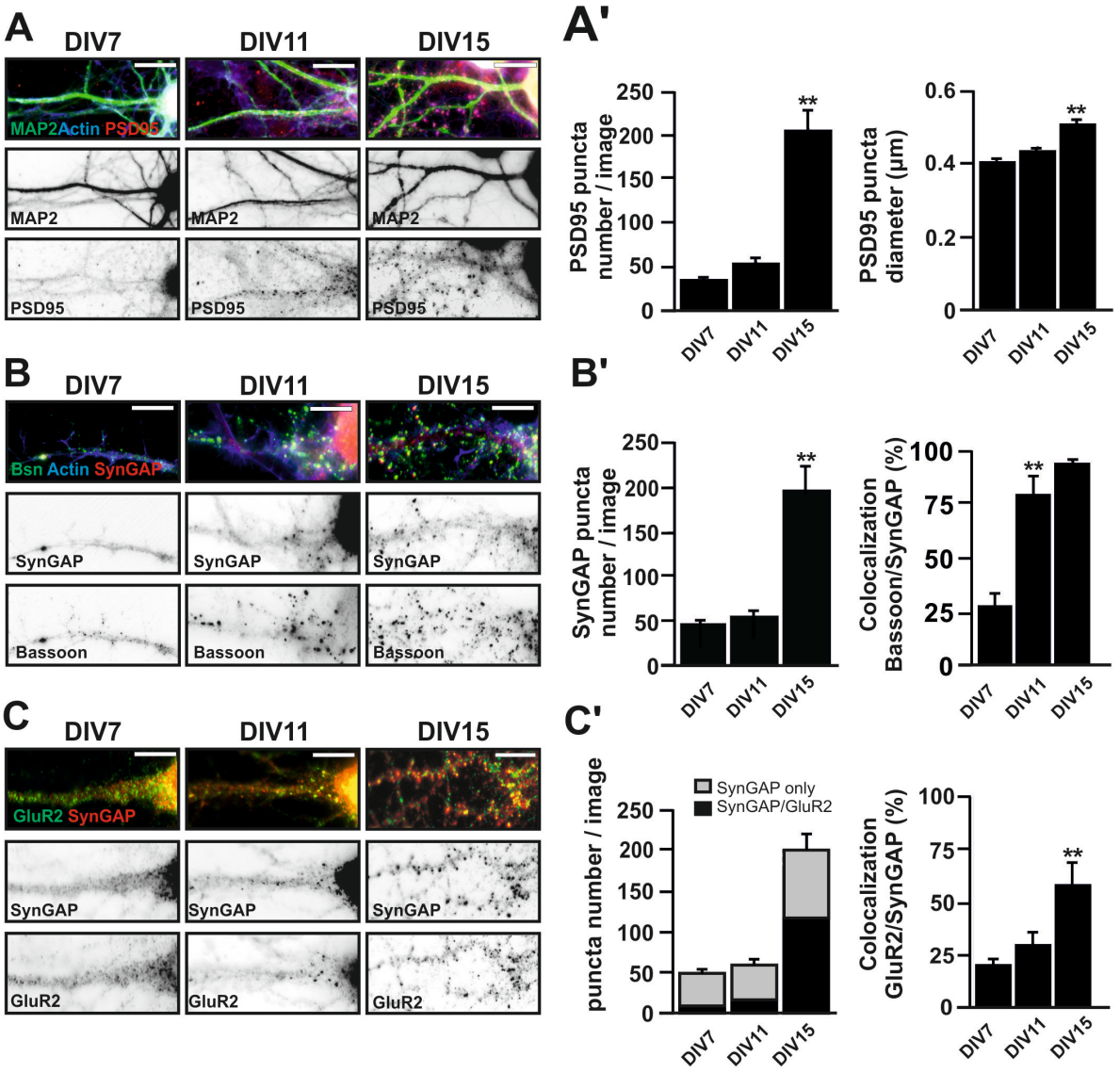

Figure S2. Time course of synapse formation in primary hippocampal neurons. (A) Primary hippocampal culture stained for actin (blue), the dendritic marker MAP2 (green) and the postsynaptic scaffolding protein PSD95 (red). Single channels depicting MAP2 and PSD95 staining are shown below. (A') Quantification of the number (left) and the diameter (right) of PSD95-positive puncta. A significant increase in the number and diameter of such puncta is observed between DIV 11 and DIV 15. (B) Neuron stained for actin (blue), the presynaptic marker Bassoon (Bsn, green) and the postsynaptic scaffolding protein SynGAP (red). Single channels depicting SynGAP and Bassoon staining are shown below. (B') Quantification of the number of SynGAP-positive puncta per picture (left) and the percentage of co-localization between Bassoon and SynGAP (right). Like PSD95-positive puncta (A', left), the number of SynGAP-positive puncta increases the most between DIV 11 and DIV 15. In contrast, co-localization of pre- and postsynaptic elements is essentially completed at DIV 11. (C) Neuron stained for the AMPA receptor subunit GluR2 (green) and SynGAP (red). Single channels depicting SynGAP and GluR2 staining are shown below. (C') Quantification of the relative percentage of GluR2/SynGAP co-localization (right) and the number of GluR2- and SynGAP-positive puncta (left). Note that the number of puncta given represent the number per image and not per neuron because of the strong dendrite arborization at DIV 15. For each image, regions were selected with similar neuron density and the puncta on the soma were not included. Data are derived from two independent experiments. For each parameter, 1520 pictures and more than 800 clusters were counted. Data represent mean ± SEM. ** $p < 0.01$ compared to the previous time point. Scale bar = 10 µm. Immunofluorescence in all the black and white pictures was inversed.

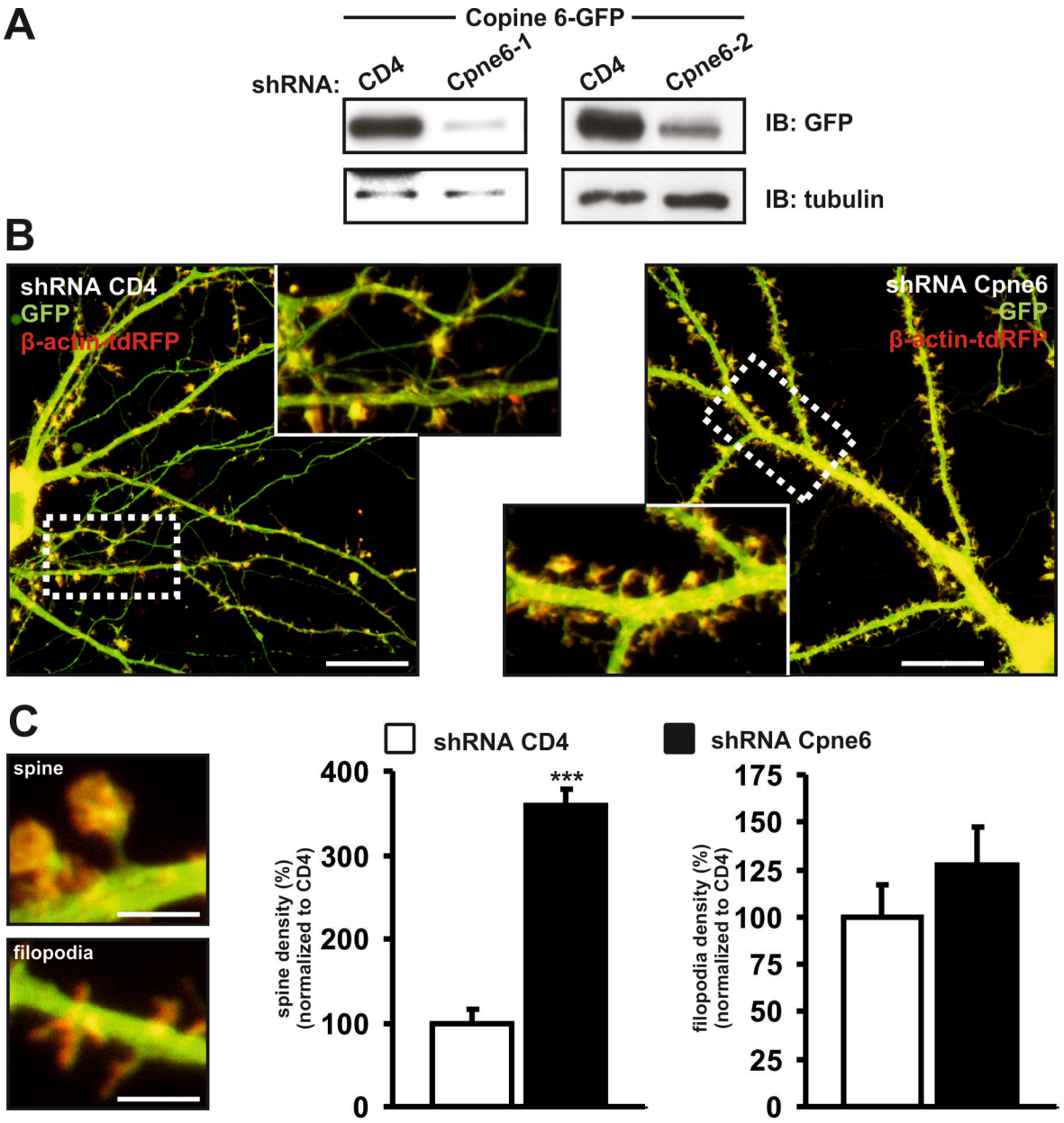

Figure S3. Copine 6 knock down induces the formation of actin rich protrusions. (A) Testing of both shRNA constructs to Copine 6 in COS7 cells overexpressing a Copine 6–GFP protein. Two independent shRNA Copine 6 constructs were used, shRNA CD4 control leaves Copine 6 expression levels unchanged (the left tubulin blot is a high exposed reblot, the signal above the tubulin band is Copine 6). (B) Representative pictures of DIV 14 primary hippocampal neurons co-transfected with either shRNA to CD4 or shRNA to Copine 6 together with β-actin-tdRFP. Scale bar = 20 µm. (C) Quantification of β-actin-tdRFP positive protrusions classified as either spines or filopodia depending on their morphology. Data is mean value ± SEM per 10 µm dendrite length N = 3 experiments with more than 12 neurons examined for each condition, ***$p < 0.001$. Scale bar = 4 µm.

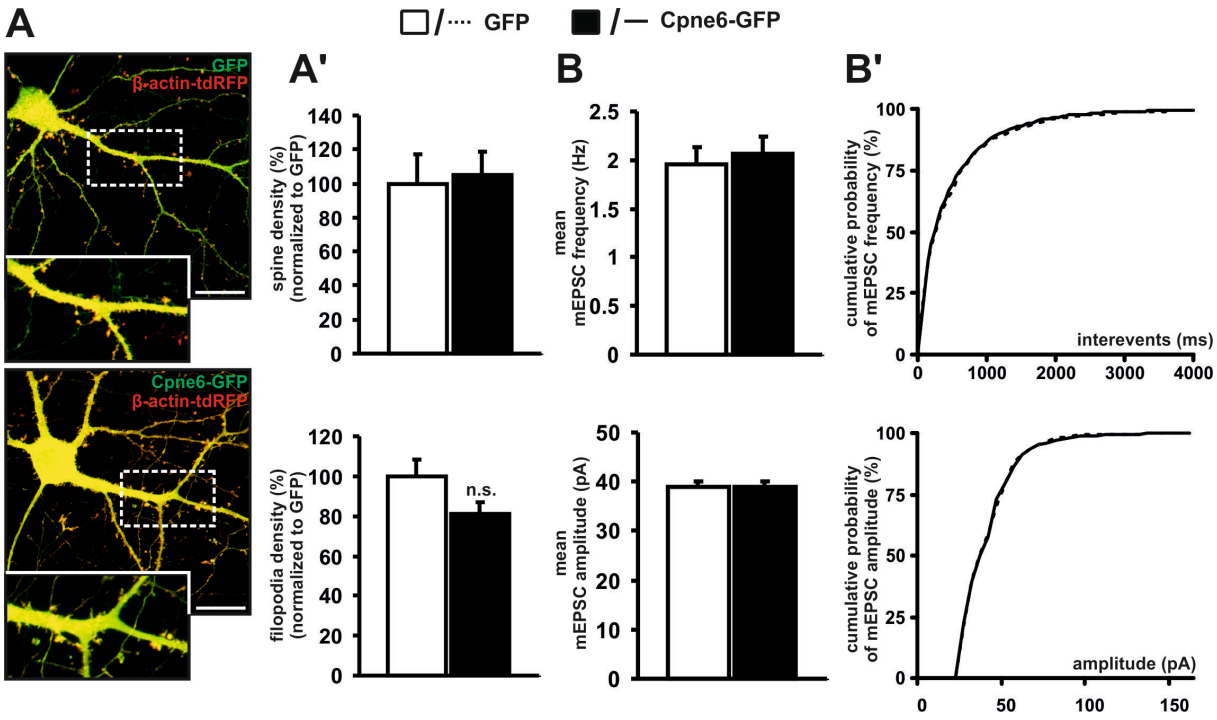

Figure S4. Overexpression of Copine 6 has no effect on neuronal morphology or synaptic transmission. (A) DIV 14 hippocampal neurons expressing β-actin-tdRFP together with synapsin driven GFP or Copine 6-GFP. (A') Quantification of spine (top) and filopodia (bottom) number of 10 µm dendrite stretches normalized to the control (GFP). (B) Analysis of miniature excitatory postsynaptic currents (mEPSCs) show no changes in frequency (top) and amplitude (bottom). (B') No significant changes are visible in the cumulative plot. Kolmogorov-Smirnov test, n= 9 neurons per condition, more than 800 events measured per neuron. Mean values are shown, n=3 more than 12 neurons for each condition ± SEM. Scale bar = 20 µm

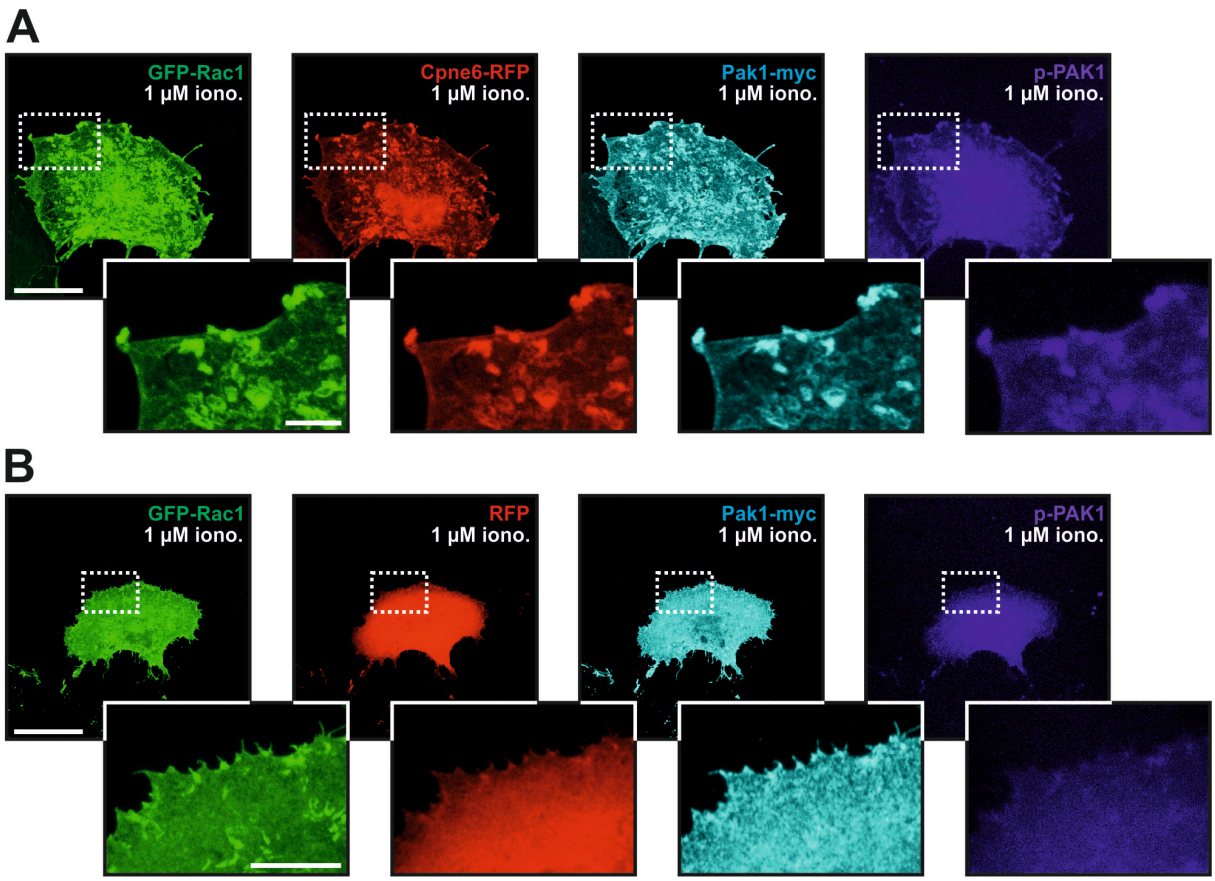

Figure S5. Copine 6 - Rac1 cluster colocalize with pPAK1. COS7 cells co-transfected with Copine 6-RFP and GFP-Rac1, Pak1-myc (A) or RFP and GFP-Rac1, Pak1-myc (B) were treated with 1 µM ionomycin for 4' and subsequently fixed. Copine 6 induces the formation of GFP-Rac1 clusters which are positive for Pak1-myc whereas RFP alone does not. Staining for phosphorylated Pak1 shows that Pak1 in the clusters is active (scale bar = 20 µm overview; 5 µm inset).Overexpression of Copine 6 has no effect on neuronal morphology or synaptic transmission.

CHAPTER 3

The role of Copine 6 in vivo

Abstract

In vitro, the postsynaptic calcium sensor Copine 6 controls spine number and stability by affecting the localization and activity-state of the small GTPase Rac1. By creating mice deficient for Copine 6, we here analyzed the role of Copine 6 *in vivo*. We found that Copine 6 expression starts postnatally during the peak of synaptogenesis, is strongest in the hippocampus and is restricted to excitatory neurons. Copine 6 is dispensable for development and health into adulthood, as Copine 6 knockout mice are born in a correct Mendelian ratio and are indistinguishable from their littermate controls. In contrast to Copine 6 deficient hippocampal cultures, *in vivo* loss of Copine 6 does not change the spine number but it decreases the density of long, thin filopodia. These data indicate that *in vivo*, Copine 6 plays a role in activity-dependent spine formation/remodeling in the adulthood rather than spine formation during development. Consistent with this idea, Copine 6-deficient mice lack hippocampal LTP. In Copine 6-deficient cultures of hippocampal neurons, we observed a reduced phosphorylation of the Rac1 downstream target, the actin filament modulator Cofilin. Suggesting that Copine 6 regulates the actin cytoskeleton via Rac1-Cofilin signaling hereby is necessary for its modulation/stabilization during LTP. Our studies define Copine 6 as a novel player critically involved in the regulation of synaptic plasticity *in vivo*.

Introduction

Activity-dependent modulations of the synaptic strength are thought to underlie learning and memory processes (Leuner et al., 2003). This synaptic plasticity is so far best described to occur at excitatory synapses whose postsynaptic sites are located on dendritic spines. Since the number and morphology of spines changes in an activity-dependent manner their plasticity may correlate with the plasticity of a synaptic connection (Engert and Bonhoeffer, 1999; Kasai et al., 2003; Lang et al., 2004; Maletic-Savatic et al., 1999). Several lines of evidence indicate that structural changes of spines are controlled by remodeling of the actin cytoskeleton (Cingolani and Goda, 2008; Dillon and Goda, 2005). The formation, organization and stabilization of actin filaments in spines have been shown to be regulated by the small Rho GTPases (Bonhoeffer and Yuste, 2002; Tashiro and Yuste, 2008). Its family members i.e. Rac1, RhoA and Cdc42 have been implicated in spine formation and maturation but also play a role in the remodeling of pre-existing spines during spine plasticity (Haditsch et al., 2009; Tashiro and Yuste, 2004, 2008).

We have recently identified the novel postsynaptic calcium sensor Copine 6 to be involved in the regulation of spines (Chapter 2). In vitro, a shRNA-mediated Copine 6 knockdown increases the number of spines and influences their stability in an activity-mediated manner (Chapter 2). Furthermore, the cytosolic Copine 6 translocates into postsynaptic sites upon calcium influx through NMDA-receptors and influences the localization and activation state of Rac1 in heterologous cells (Chapter 2). We therefore proposed that Copine 6 acts as a calcium-dependent shuttle-protein that translates changes in neuronal activity into structural changes of dendritic spines by influencing the localization and/or activation of Rac1 (Chapter 2).

In the last years several pathways and molecules have been identified to influence the number, morphology and plasticity of dendritic spines *in vitro*. Since culture systems are much more vulnerable to perturbations and do not reflect the complex neuronal networks *in vivo*, the physiological relevance of such pure *in vitro* evidence is disputable.

Here, we aimed to elucidate the function of Copine 6 *in vivo* and generated mice that are deficient for Copine 6 in all tissues. By a lacZ-knockin in the endogenous Copine 6 locus we identified Copine 6 expressing cells. We found that the expression of Copine 6 starts postnatally, is limited to certain brain regions and is strongest in the hippocampus. In the hippocampus, the expression of Copine 6 is restricted to excitatory neurons. We analyzed the spine density in the hippocampus from Copine 6 knockout mice and found that in contrast to *in vitro*, Copine 6 deficiency *in vivo* does not influence the number of spines. In line with this, no alteration in the Rac1 activity or localization was detected. We evaluated changes in synaptic plasticity by measuring long-term potentiation (LTP). Interestingly, loss of Copine 6 causes a deficiency in LTP consolidation during the first hour after initiation. This demonstrates that Copine 6 is critically involved in synaptic plasticity *in vivo*. It supports a model in which, Copine 6 influences the Rac1-Cofilin pathway under conditions of increased activity rather than basal and thereby specifically controls structural modifications underlying synaptic plasticity and not spine formation.

Results

Generation of Copine 6 knockout mice

In order to access the function of Copine 6 *in vivo,* we generated Copine 6-deficient mice. As all coding exons of Copine 6 are in the same reading frame, we replaced the complete Copine 6 coding region to avoid the generation of a hypomorph mutant. For further identification of Copine 6-expressing cells an nlsLacZ cassette was inserted under the control of the endogenous Copine 6 starting codon (Figure 1A). In addition, LoxP sites flanking the neomycin resistance cassette were inserted for the selection of targeted ES cells. This cassette was later excised by crossing the F1 generation with Cre deleter mice (Figure 1A).

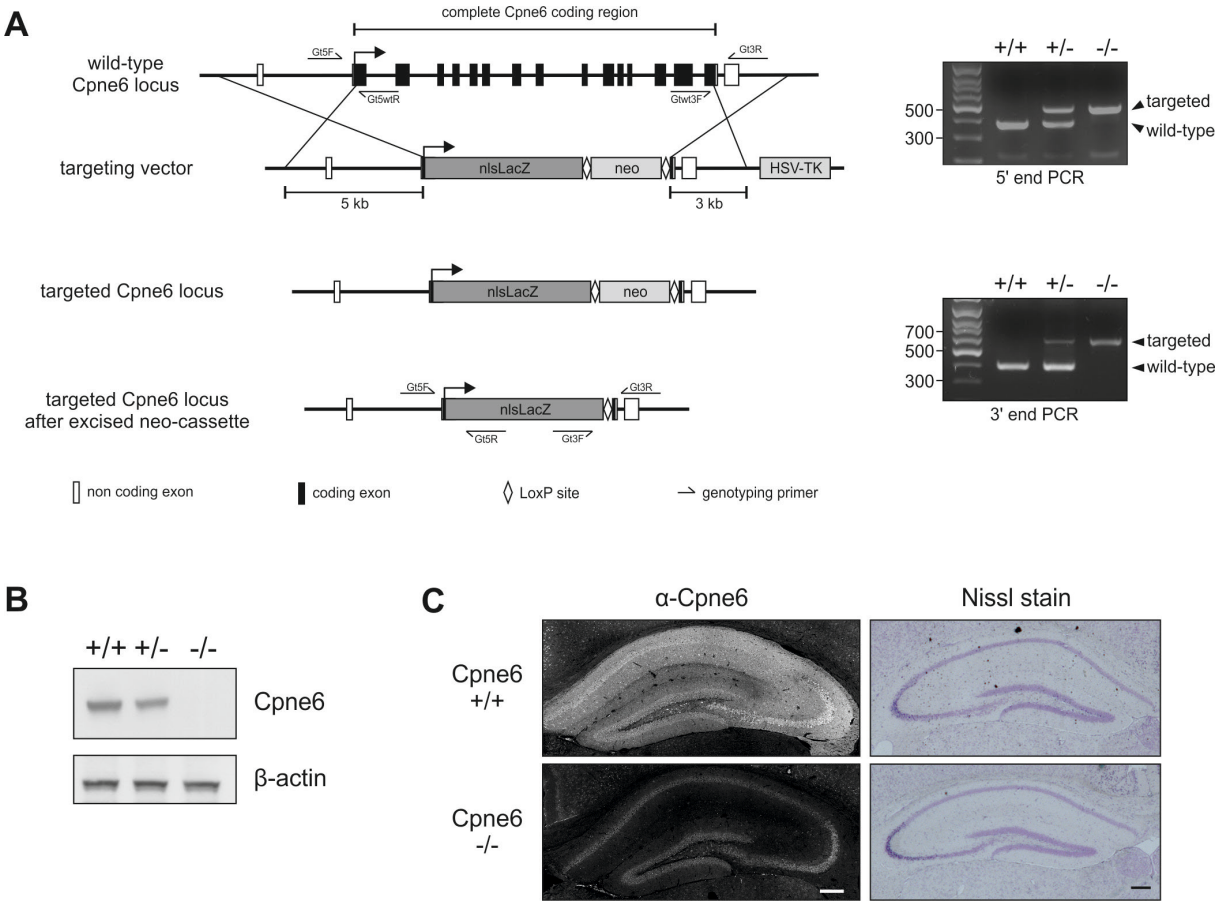

Figure 1. Targeting scheme of Cpne6 mice and confirmation of Cpne6 deficiency. (A) Targeting scheme of Copine 6 knockout/nls-LacZ knockin mice. Genotyping PCRs on tail lysate with primers indicated in scheme show presence of targeted allele. (B) Representative immunoblot on adult mouse brains with Copine 6-specific antibody. β-actin was used as loading control. Copine 6 is reduced in heterozygotes mice and absent in knockout mice. (C) Copine 6 immunostained hippocampi of wild-type and knockout (right). Nissl staining of adult Cpne 6 KO mice (left). Scale bars represent 200 µm.

The genotype of the mice was determined by PCR on tail lysate (Figure 1A). Copine 6-deficient mice were born in an expected Mendelian ratio and appeared healthy and of normal size during development and into adulthood, indistinguishable from their wild-type littermates. The absence of Copine 6 protein was confirmed by Western blot analysis on brain lysate. Heterozygous Copine 6 mice showed a reduction of Copine 6 whereas no Copine 6 was detectable in knockout mice (Figure 1B). Staining of Copine 6 in adult brain slices revealed that Copine 6 is present in the dendritic regions of the hippocampus. This staining is completely absent in Copine 6 knockout mice (Figure 1C). The general hippocampal morphology was not altered in knockout mice as shown by Nissl staining (Figure 1C).

Copine 6 expression starts postnatally and is restricted to excitatory neurons

We analyzed the temporal expression of Copine 6 in hippocampal extracts from mice of various age. These experiments revealed that Copine 6 is not detectable at birth, increases during the first two weeks postnatally and stays high into adulthood (Figure 2A).

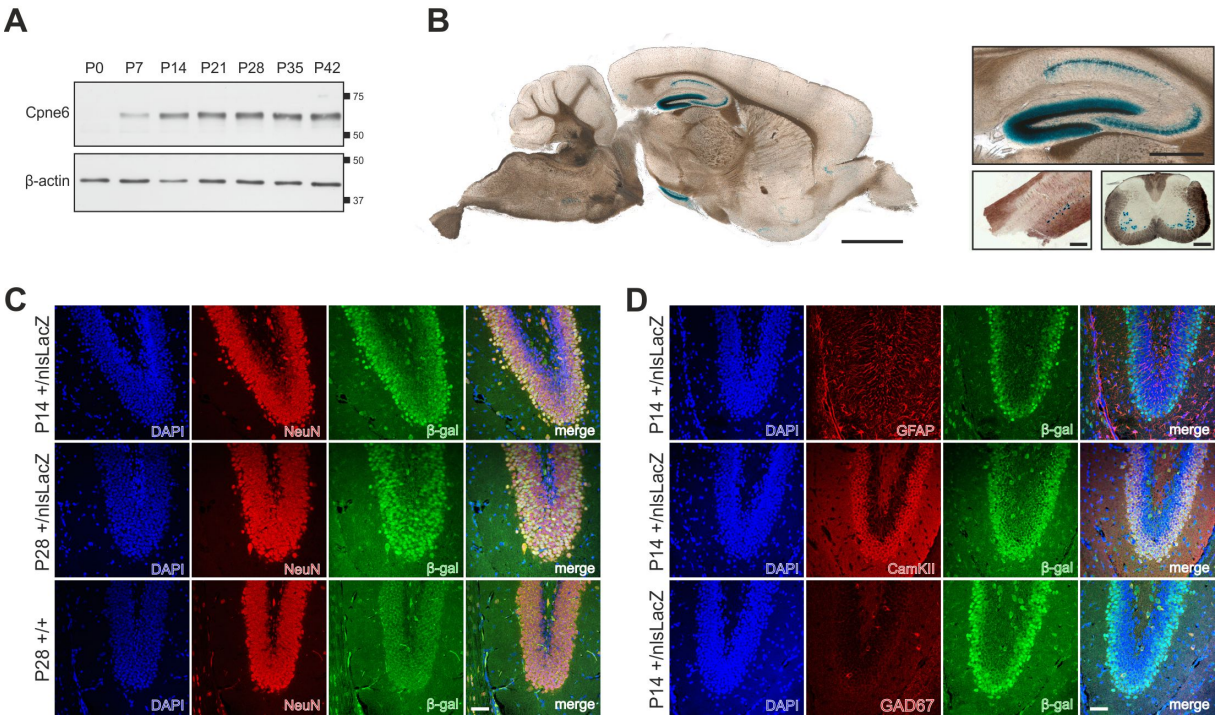

Figure 2. Temporal and spatial expression of Copine 6. (A) Temporal expression of Copine 6. Immunoblots on hippocampal extracts of mice at different age (P0-P42). β-actin was used as loading control. (B) Sagittal brain section from an adult Cpne6$^{+/nlsLacZ}$. Cpne6 expression is strongest in the hippocampus. β-gal positive cells are also detected in the spinal cord. Sagittal (left) and coronal (right) section of the spinal cord. Scale bar in whole brain sagittal section (left) represents 1.5 mm and in the pictures on the right 500 µm. (C) Co-staining of the dentate gyrus at different ages. The fraction of Copine 6-expressing cells is increasing. Staining on Cpne6$^{+/+}$ sections were used as β-gal staining control. (D) Co-staining of the dentate gyrus with different cell markers. β-gal expression does not overlap with GFAP (marker for astrocytes) and GAD67 (inhibitory neurons) but is expressed in CaMKII (excitatory neurons) positive cells. Scale bar in (C) and (D) represents 50 µm.

Previous data indicate that Copine 6 is expressed only in the central nervous system (Nakayama et al., 1998). Here, we evaluated its expression pattern in the CNS. The nls-LacZ knockin in the *Copine 6*-locus enabled us to identify Copine 6 expression cells by β-galactosidase staining. In adult *Cpne6*$^{+/nlsLacZ}$ mice, the Copine 6 expression is limited to certain brain areas (Figure 2B, left). Interestingly, no Copine 6 expression is detectable in the cerebellum, in other brain areas some Copine 6 expressing cells are found i.e. in the cortex (Figure 2B, left). But, the strongest Copine 6 expression is detected in the hippocampus (Figure 2B, left). LacZ reporter expression is present in all regions of the pyramidal layer (Figure 2B, right). It appears especially strong in the dentate gyrus (Figure 2B, right) but this might be due to the highest density of nuclei in this region. Furthermore, Copine 6 expressing cells were identified in the spinal cord (Figure 2B, right). Cross section of the spinal cord showed that the Copine 6 reporter is most likely present in the motoneuron pool (Figure 2B, right). To further access the cell type of Copine 6-expressing cells, we performed colocalization studies of immunostainings with different neuronal markers in the dentate gyrus (Figure 2C and 2D). Reporter expression was identified by staining with β-galactosidase antibody. We observed that all Copine 6 expression cells were positive for the neuronal marker NeuN, but not all NeuN cells were also β-gal positive (Figure 2C). Analysis at different ages showed that especially at P14, cells close to the subgranular zone do not express the *Cpne6*-driven reporter (Figure 2C). The thickness of the β-gal positive nuclei layer increases with age (P14 versus P28) (Figure 2C). These data indicate that Copine 6 is only expressed in mature neurons. As it has been shown that the expression level of Copine 6 is increased upon activity (Nakayama et al., 1998), the mosaic expression pattern of Copine 6 may represent cells that recently experienced neuronal activity. Furthermore, we excluded Copine 6 expression in astrocytes and inhibitory neurons as we observed no colocalization with the astrocyte marker GFAP or the inhibitory interneuron marker GAD67 (Figure 2D). Complete colocalization was detected with the excitatory neuron marker CamKII (Figure 2D). Taken together these data indicate that Copine 6 expression is strongest in mature excitatory neurons in the hippocampus.

Expression of postsynaptic proteins is not affected by Copine 6 deletion

We demonstrate that Copine 6 is most strongly expressed in the hippocampus (Figure 2) and therefore anticipate that absence of Copine 6 would primarily results in alteration in this brain region. As Copine 6 is present in postsynaptic regions and its knockdown changes the number of postsynapses, we evaluated the expression of members of the postsynaptic density in Copine 6 knockout mice. In hippocampal lysates of adult knockout mice, we observed neither change in the expression of subunits of excitatory receptors nor of postsynaptic scaffolds (Figure 3A). Next, we examined if removal of the calcium-binding protein Copine 6 resulted in changes in postsynaptic calcium signaling. We analyzed the phosphorylation state of CamKII and Creb and found no significant change between knockout and wild-type mice (Figure 3B). Copine 6 is responsive to activation of NMDA receptors and subsequent calcium influx (Chapter 2). The main downstream signaling event of this NMDAR-mediated calcium influx is the phosphorylation of CamKII (Lisman et al., 2012). We therefore analyzed if stimulation of NMDA receptors via induction of a chemical LTP resulted in alterations in CamKII activation in Copine 6 knockout mice. We found that the increase in p-CamKII upon LTP is not significantly changed in knockout mice (Figure 3C). These data demonstrate that loss of Copine 6 does not affect the calcium-mediated CamKII activation in a basal state and also

not upon increased activity. Furthermore, it indicates that the principal LTP induction pathway is intact in Copine 6 knockout mice.

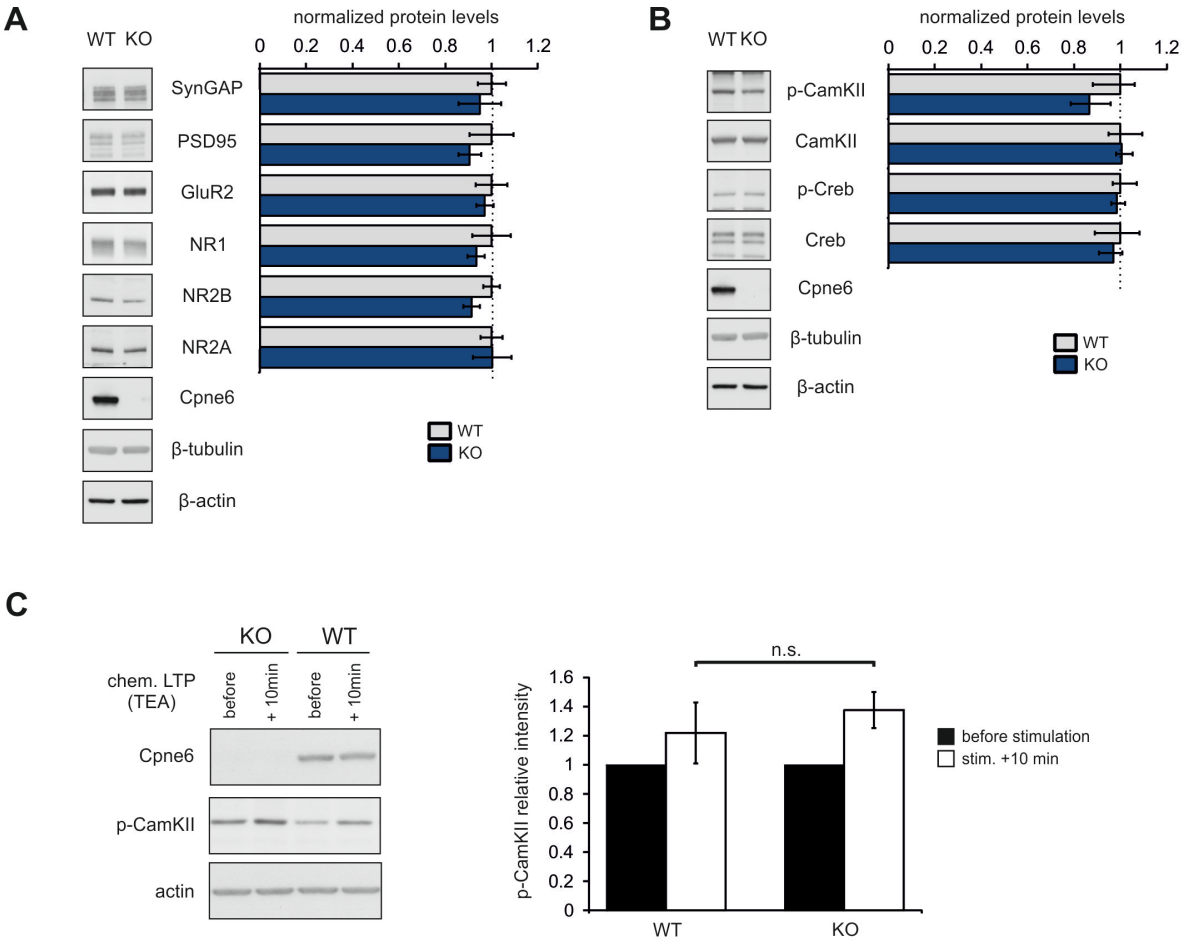

Figure 3. Loss of Copine 6 does not affect the expression of postsynaptic molecules or the activation of calcium signaling targets. (A-B) Representative immunoblots from total hippocampal lysates of mice at the age of 6 weeks. No significant change is observed in the expression of members of the postsynaptic density (A) or calcium signaling targets (B). WT: N=5-12; KO: N=5-9. (C) Acute hippocampal slices from 6-week old mice before and after chemical LTP induction. The increase in p-CamKII upon LTP induction is not significantly changed in KO mice. WT: N=6; KO: N=8. Standard error of the mean is indicated; $p > 0.05$.

Spine density and morphology in Copine 6 knockout mice

Knockdown of Copine 6 in primary hippocampal culture strongly affects spine density (Chapter 2). To access the spine density *in vivo* we intercrossed Copine 6 knockout mice with Thy1-mGFP expressing mice (De Paola et al., 2003). The Thy1-driven, membrane-tagged GFP expression in a subset of CA1 neurons (Figure 4A) enabled us to analyze spine density and morphology in three-dimensional reconstructions. We analyzed the spine density of secondary apical dendrites in CA1 neurons and found no significant change (Figure 4B). Next, we classified the spines into mushroom, stubby and thin spines and also there, detected no alteration in Copine 6-deficient neurons (Figure 4C). In

agreement with this observation the mean spine head diameter of all quantified spines was not significantly different (Figure 4D). In contrast, the mean spine length in knockout neurons was marginally but significantly reduced (Figure 4E, left).

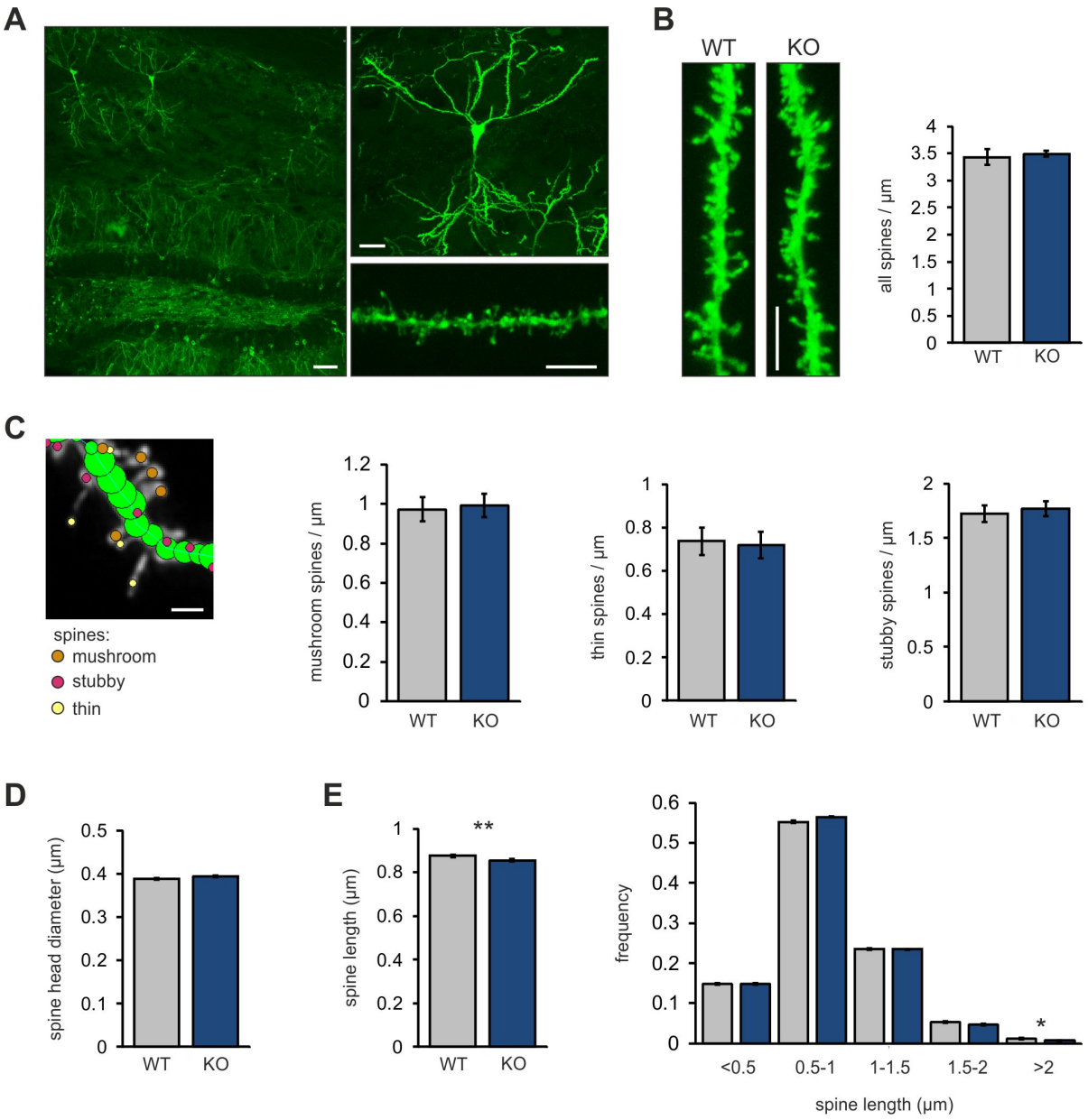

Figure 4. Spine density and morphology in Copine 6 knockout mice. (A) GFP expression in Thy1-mGFP mice. Scale bars represent (from left to right) 50 µm, 20 µm and 5 µm. (B) Confocal pictures of representative dendritic stretches and quantification of the spine density. Scale bar represents 5 µm. (C) Classification of spine types and quantification of their density. Scale bar represents 1 µm. (D) Mean spine head diameter. (E) Mean spine length and frequency distribution. (F) Mean filopodia density. N=4 male mice per genotype (four independent littermate pairs). Eight dendritic stretches from eight different neurons per mouse were quantified. N=4160 spines from WT and 4693 spines from KO. Standard error of the mean is indicated; statistical significance is indicated by * $p < 0.05$, ** $p < 0.01$.

To further access the origin of this change in the mean spine length, we analyzed the spine length distribution. In KO neurons a significant reduction in the frequency of spines longer than 2 µm was detected (Figure 4E, right). Very long, thin spines have been described as early forms of spines and are termed filopodia (Jontes and Smith, 2000; Yuste and Bonhoeffer, 2004). We therefore assessed the occurrence of this filopodia according to previously defined morphological criteria (Grutzendler et al., 2002) and found a significant decrease in filopodia density in Copine 6 knockout mice (Figure 4F). Since this filopodia are formed in an activity-dependent manner (Matsumoto-Miyai et al., 2009), these data indicate that Copine 6 is involved in activity-dependent processes. Next, we analyzed the functional properties of the synapses in knockout mice. No significant change in amplitude and frequency of mEPSCs (Figure 5A) or mIPSCs (Figure 5B) was detected. This finding is consistent with the lack of prominent changes in density and morphology of spines in CA1 neurons (Figure 4).

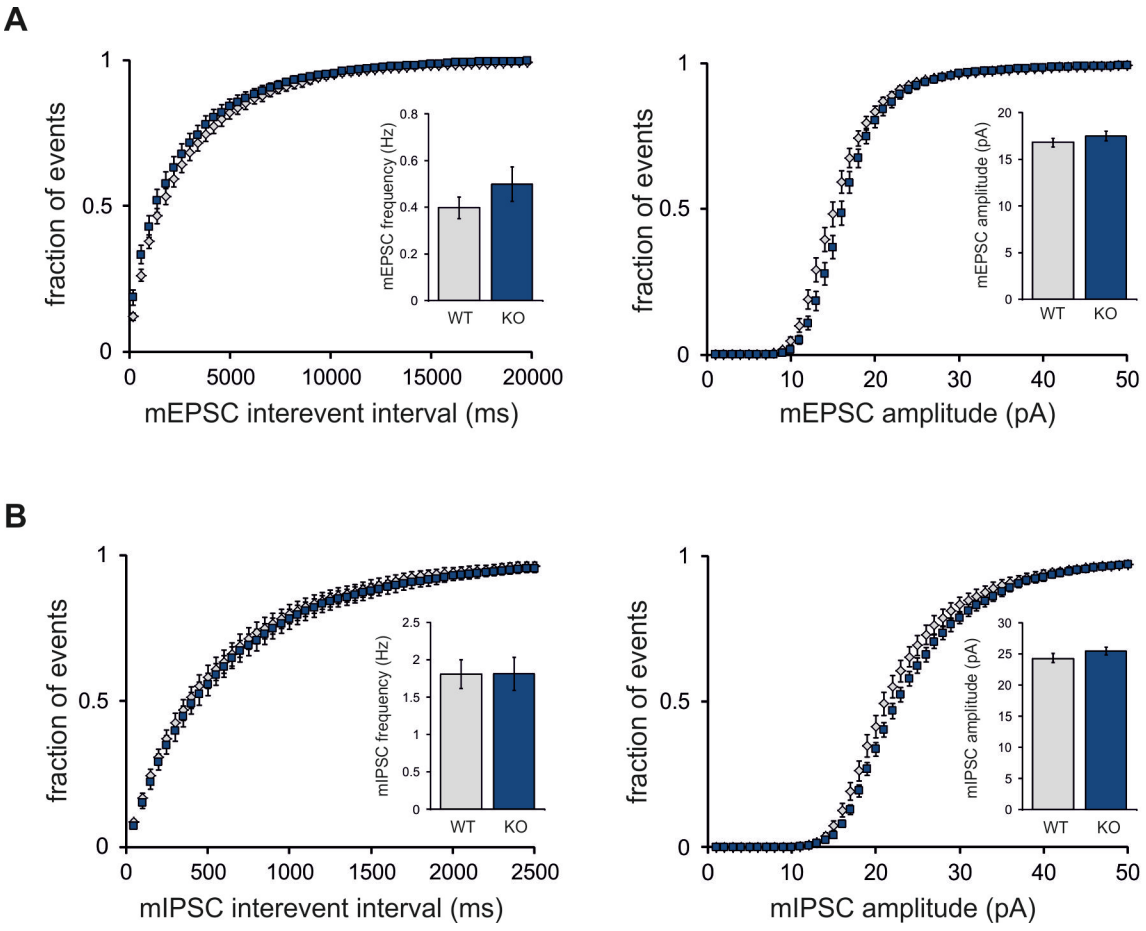

Figure 5. mEPSC and mIPSC in CA1 neurons of Copine 6-deficient mice. (A) mEPSC and (B) mIPSC. Cumulative distribution of interevent intervals and mean frequency (left). Cumulative distribution of amplitude and mean amplitude (right). N=18-19 cells per genotype (from 5 mice per genotype; 3-5 cells were recorded form one mouse). No significant change is observed in the means. $p > 0.05$ with Student's t-test and in the cumulative distribution $p > 0.05$ with KS test. Standard error of the mean is indicated.

Knockout of Copine 6 does not affect Rac1 activity or localization

In vitro, Copine 6 increases Rac1 activity (Chapter 2). We therefore also examined Rac1 signaling in Copine 6 knockout mice. To assess this, we first analyzed the Rac1 downstream targets in adult hippocampal extracts. We found that the phosphorylation of Pak1 or Cofilin is not significantly changed in knockout mice (Figure 6A). Furthermore Rac1 activation level as analyzed by a Rac1-GTP pulldown assay was not significantly changed (Figure 6B). In heterologous cells, Copine 6 influences the localization of Rac1 (Chapter 2). If Copine 6 were a regulator of Rac1 localization in neurons, its loss would cause localization changes. To determine the subcellular localization of Rac1 we performed subcellular fractionation of hippocampal extracts. However, lack of Copine 6 did not affect the amount of Rac1 in the cytosol or membrane of non-synaptic and in the synaptic fractions (PSD and non-PSD) (Figure 6C).

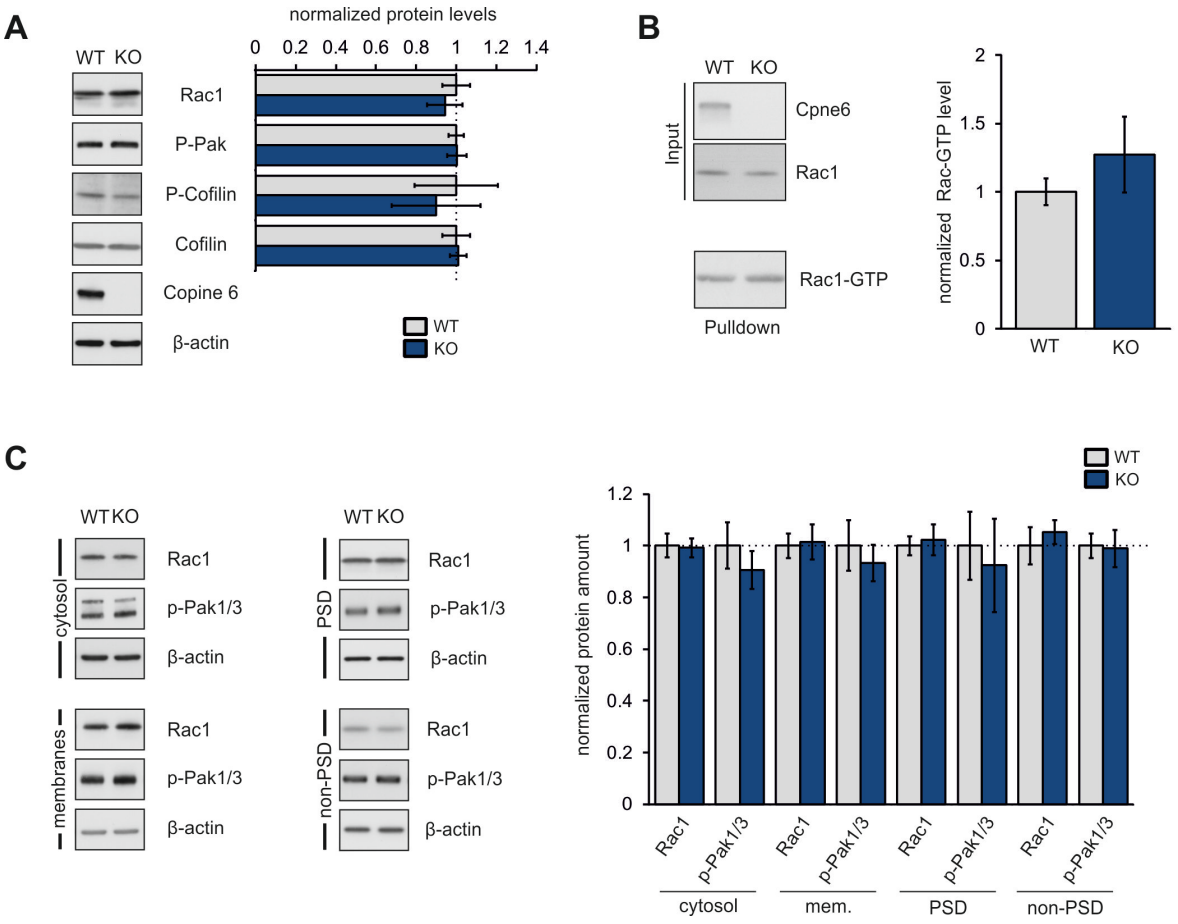

Figure 6. Loss of Copine 6 in vivo does not affect Rac1 activity and localization. (A) Representative immunoblots from hippocampal lysate of 6-week-old mice. Quantification shows no significant difference between wild-type and Cpne6 knockout mice. N=5 independent littermate pairs. (B) Assessment of Rac1 activity by Rac1-GTP pull-down on hippocampal lysate. No significant change was observed in KO mice. N=5 independent littermate pairs. (C) Subcellular fractionation of hippocampal extracts. Quantification revealed no significant difference in the subcellular localization of Rac1 or p-Pak1/3 in Cpne6 KO mice. N=5 independent littermate pairs. Standard error of the mean is indicated. $p > 0.05$.

We analyzed Rac1 activity in these fractions by comparing the phosphorylation level of Pak1/3. P-Pak1/3 was not significantly altered in Copine 6 knockout mice in the analyzed subcellular fractions (Figure 6C). These data indicate that *in vivo,* Copine 6 is dispensable for basal Rac1 signaling and that Copine 6 is also not responsible for its subcellular localization under basal conditions.

Spine density and Rac1 signaling is changed in cultured hippocampal neurons from Copine 6 knockout mice

Acute Copine 6 knockdown in primary rat hippocampal cultures drastically increases the spine density (Chapter 2). Here, we examined primary hippocampal cultures derived from Copine 6 knockout embryos. First, we analyzed the expression of Copine 6 in such mouse-derived cultures. We found that Copine 6 is weakly expressed at DIV8 and its expression increases when cultures mature and synapses are formed together with the expression of the postsynaptic scaffolding molecule PSD95 (Figure 7A). Due to this increase in Copine 6 expression when cultures mature we decided to analyze knockout cultures at DIV16. Since presence of Copine 6 increases Rac1 activity in heterologous cells (Chapter 2), we examined this pathway in Copine 6 KO cultures. The phosphorylation of the Rac1 downstream target Cofilin was significantly reduced in Copine 6 knockout cultures (Figure 7B).

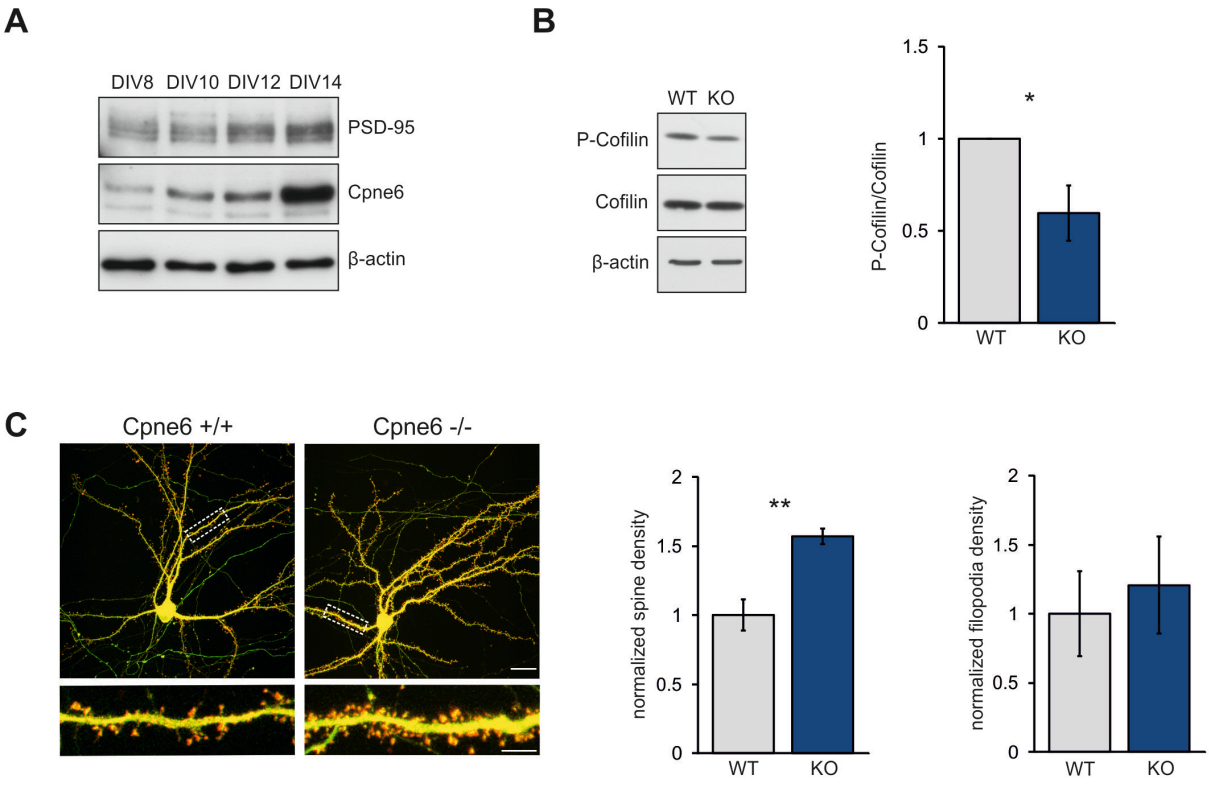

Figure 7. Phenotype of Copine 6-deficient neurons. (A) Westen blot analysis of PSD95 and Copine 6 expression in primary mouse hippocampal neurons at DIV8-14. β-actin was used as loading control. (B) Representative immunoblots on P-Cofilin and total Cofilin from extracts of DIV16 cultures. Quantification shows a decrease in p-Cofilin in Copine 6 KO cultures. N = 6 cultures per genotype from 6 littermate pairs. (C) DIV16 neurons expressing GFP (green) and β-actin-tdRFP (red). Quantification shows an increase in spine density but no change in filopodia density. N=4 cultures per genotype (10-12 neurons per culture. Scale bar represents 20 µm (top) and 5 µm (bellow). Standard error of the mean is indicated; statistical significance is indicated by * $p < 0.05$, ** $p < 0.01$.

This decrease in inactive – phosphorylated Cofilin - indicates an increase in actin remodeling. To address whether this change is reflected in alterations in spine density, we visualized neurons and spines by transfection at DIV7 with GFP (green) and β-actin-tdRFP. At DIV 16, we analyzed spine and filopodia density. In Copine 6 knockout cultures, the spine density was significantly increased whereas the filopodia density was not affected (Figure 7C). These data confirm our previous findings, that a shRNA-mediated knockdown of Copine 6 increases the spine density, but does not alter the filopodia density in mature cultures (Chapter 2).

Loss of Copine 6 affects long-term potentiation

In contrast to the *in vitro* data, we do not observe a change in phosphorylated Cofilin under basal condition *in vivo* (Figure 6). Cofilin has been shown to regulate actin remodeling during synaptic plasticity (Gu et al., 2010; Rex et al., 2009; Rust et al., 2010). To address whether *in vivo* Copine 6 plays a role in activity-dependent actin-remodeling, we measured long-term potentiation in the CA1 area of Copine 6 knockout mice. With three trains of high-frequency stimulation, we induced a robust LTP in control mice (Figure 8). In Copine 6 KO mice, the initially potentiated responses returned near to baseline within 60 minutes (Figure 8). This failure in LTP consolidation in Copine 6 KO mice strongly resembles the effect of perturbed actin remodeling during LTP (Meng et al., 2002; Rex et al., 2009). It indicates that Copine 6 plays a role in activity-dependent actin remodeling and subsequent spine remodeling/stabilization.

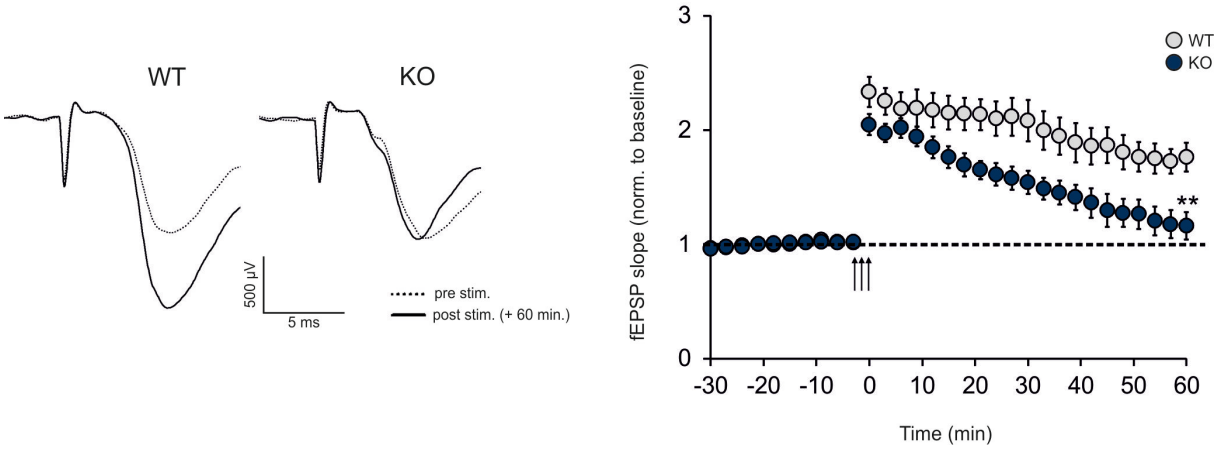

Figure 8. Copine 6 restricts long-term potentiation. Extracellular field potential (fEPSPs) were measured in 6-week old Copine 6 KO mice and their littermate controls. (Left) Representative traces before and 60 min. after high-frequency stimulation. 1-2 slices per mouse were recorded. N=6 mice per genotype (WT: 9 recordings; KO: 7 recordings). LTP is significantly reduced from 18-60 min. post stimulation. Standard error of the mean is indicated; statistical significance is indicated by ** $p < 0.01$.

Discussion

Our results revealed that *in vivo,* Copine 6 required for synaptic plasticity induced by electrical stimulation during adulthood. Consistent with its expression being strongest in mature excitatory neurons (Figure 2), loss of Copine 6 does not affect brain development and synapse formation (Figure 1 and 4), but it abolishes activity-mediated synaptic modulations, as Copine 6 KO mice lack hippocampal LTP (Figure 8).

Loss of Copine 6 affects spine number and morphology in an activity-dependent manner

Previously, we have demonstrated that shRNA-mediated knockdown of Copine 6 in primary rat hippocampal cultures increases the density of dendritic spines (Chapter 2). In these cultures, Copine 6 expression was acutely perturbed in very few neurons that remained surrounded and connected by unaffected neurons. Here, we observed that also cultures containing only Copine 6 knockout cells, a increase in spine number was found (Figure 7). Controversially, the spine density is not changed in the hippocampus of Copine 6 knockout mice (Figure 4). But we observe changes in the number of long-thin filopodia. It is widely accepted that such filopodia are formed in an activity-dependent manner and serve as precursors of new spines (Jontes and Smith, 2000; Knott and Holtmaat, 2008; Matsumoto-Miyai et al., 2009; Yuste and Bonhoeffer, 2004). Unaffected overall spine number but changes in filopodia density *in vivo* indicates that Copine 6 is not required for activity-independent spine formation, but plays a role in activity-dependent processes. The increase in spine number *in vitro* may represent spines that are formed in an activity-dependent manner caused by the high level of neuronal network activity common to high-density cultures (Canepari et al., 1997; Murphy et al., 1992; Wagenaar et al., 2005). In line with this hypothesis, this supernumerous spines disappear if the activity in cultures is reduced by TTX treatment (Chapter 2, Figure 7C). On the other hand, the chronic absence of Copine 6 *in vivo* may be compensated by other Copine family members, causing an attenuation of the *in vivo* phenotype. We checked the expression level of all Copines in whole brains or isolated hippocampi of Copine 6 knockout mice by real-time PCR and observed no significant difference (Erni, 2011). By in situ hybridization, we found that in adult wild-type mice, the expression of certain Copines, i.e Copine 4 and 7, is very restricted to distinct hippocampal regions (Erni, 2011). This distinct pattern is not perturbed in Copine 6 knockout mice (Erni, 2011). These data argue that absence of Copine 6 does not cause compensatory upregulation of other Copine family members, but it does not rule out the possibility that Copine 6 function is partially compensated by other Copines, especially under conditions of low neuronal activity.

Copine 6 modulates Rac1-Cofilin signaling in neurons

It is widely accepted that the formation of new dendritic spines and the re-shaping of pre-exiting spines upon changes in activity, are based on changes in their actin cytoskeleton (Cingolani and Goda, 2008; Fischer et al., 1998). The small GTPase Rac1, which acts upstream of the actin filament severing protein Cofilin, has been implicated in all these processes (Hayashi-Takagi et al., 2010; Tashiro and Yuste, 2004, 2008). Previously, we have demonstrated that Copine 6 modulates Rac1

localization and activation in heterologous cells (Chapter 2). Here we confirm that Copine 6 acts upstream of Rac1-Cofilin signaling in neurons, as the amount of phosphorylated Cofilin is decreased in primary hippocampal neurons derived from Copine 6-deficient mice (Figure 7). As these changes suggest an increase in actin remodeling, it may explain the increase in spine density observed in Copine 6 KO cultures. Interestingly, in hippocampal lysates from adult Copine 6 KO animals, we observe neither a difference in the amount of activated Rac1 or its downstream targets, nor its localization. Our previous *in vitro* data indicated that Copine 6 affects Rac1 in an activity-dependent manner (Chapter 2). The discrepancy between *in vitro* and *in vivo* may be explained by the higher level of basal neuronal activity in cultures. *In vivo*, a very strict time-dependent control of the activity of Cofilin has been shown to be essential for actin modulation during LTP (Chen et al., 2007; Gu et al., 2010; Rex et al., 2009). The LTP deficiency in Copine 6 KO mice, very strongly resembles the LTP consolidation deficiency caused by perturbation of Cofilin and actin polymerization (Rex et al., 2009; Rust et al., 2010). This indicates that *in vivo,* Copine 6 is involved in the regulation of actin remodeling via its signaling on Rac1-Cofilin upon increase in neuronal activity rather than under basal conditions.

Experimental procedures

Mice

Conventional Copine 6 knockout mice were generated by homologues recombination leading to a complete removal of the Copine 6 coding region (exon 2-16) and replacement by an nls-LacZ casette. Gene targeting was carried out in 129Sv derived ES cells. The targeting vector contained 5 kb of 5'arm composed of Cpne6 promoter, exon1, intron1 and a small portion of exon 2, followed by nlsLacZ-SV40 polyA signal-LoxP-PGKneo-LoxP and 3 kb of 3'arm composed of Cpne6 exon 16, intron 16, exon 17 and 3'downstream sequence, followed by MC1-HSV-TK (for negative selection). Chimeric mice were obtained by microinjection of correctly targeted clones into C57BL/6 blastocysts. Germline transmission was tested by crossing the chimeric mice with C57BL/6 mice. The LoxP flanked neo-cassette was removed by intercross with Hprt-cre (Cre-delete) mice. Genotypes were identified by PCR flanking the 5' end with following specific primers Gt5F (5'-TGCAGCACTGGCTCATAGAC-3') and Gt5R (5'-GGAAAGTCCTTGGGGTCTTC-3') Gt5wtR (5'-GCACCCATCCCATCTCTG-3') or at 3' end: Gt3R (5'-ATCTGAGGCATGACGGGTAG-3'), Gt3wtF (5'-CTATGACTCCCAGCCCTAGC-3') and Gt3F (5'-CACTGCATTCTAGTTGTGGTTTG-3'). The mouse line was maintained in a mixed C57BL6/129Sv background and homozygotes WT and KO mice from the same litter were compared to control for the same genetic background of the mice analyzed. If not otherwise indicated, mice were analyzed at the age of 6 weeks. All experiments including mice were performed according to the federal guidelines for animal experimentation and approved by the Swiss authorities.

Antibodies

For immunostaings and Western blot analysis the following antibodies were used: anti-Copine 6 (clone 42, Santa Cruz Cat. sc-136357), β-actin (Cell Signaling Cat. 4970), NeuN (Millipore Cat. MAB377), β-gal (Abcam Cat. ab9361), GFAP (Millipore Cat. MAB360), CamKII (Chemicon Cat. MAB8699), GAD67 (Chemicon Cat. MAB5406), SynGAP (Affinity Bioreagents Cat. PA1046), PSD95 (Affinity Bioreagents Cat. MA1045), GluR2 (BD-Pharmigen Cat. 556341), NR1 (BD-Pharmigen Cat. 556308), NR2A (Millipore Cat. 07-632), NR2B (Millipore Cat. 06-600), β-tubulin (BD-Pharmigen Cat. 556321), p-CaMKII (Cell Signaling Cat. 3361), p-Creb (Cell Signaling Cat. 9198), Creb (Cell Signaling Cat. 9197), Rac1 (Thermo Scientific Cat.89856D), p-Pak (Cell Signaling Cat. 2601), p-Cofilin (Abcam Cat. ab42824), Coflin (phospho S3, Abcam Cat. ab12866).

Stainings

Mice were transcardially perfused with 4% PFA /PBS and dissected tissue was postfixed overnight in 4% PFA /PBS. For β-galactosidase staining brains or spinal cords were dehydrated (30% sucrose, overnight) and embedded in O.C.T. 100 µm thick sections were cut on a cryostat. Free floating sections were washed in PBS and then incubated 3 times for 30 min. in rinse buffer (100 mM sodium phosphate buffer pH 7.3, 2 mM $MgCl_2$, 0.01% sodium deoxycholate and 0.02% NP-40). For staining,

sections were incubated overnight at 37°C in the dark in staining solution (5 mM potassium ferricyanide, 5 mM potassium ferrocyanide and 1 mg/ml X-gal). Stained sections were postfixed for 2 h at 4°C in 10% formalin and mounted on glass slides.

For immunostaings brains were embedded in paraffin and cut in 5 µm thick sections on a microtome. Sections were deparaffinized with Xylol and rehydrate by serial ethanol steps. Antigen retrieval was performed in boiling citrated buffer (10 mM sodium citrate pH 6, 0.05% Tween-20) after washing in PBS sections were incubated for 30 min. at RT in blocking solution (5% BSA, 0.2% Triton-X in PBS) subsequently sections were incubated in primary antibody in blocking solution overnight at 4°C. After extensive wash with PBS sections were incubated for 1 h at RT in appropriate secondary antibody (and DAPI). Coverslips were mounted with cervol.

Tissue preparation, Rac1 activity assay and western blot analysis

Hippocampi form 6-week-old mice were dissected on ice and homogenized in lysis buffer (50 mM Tris pH 7.5, 5 mM EDTA, 150 mM NaCl, 1% NP-40, 0.5% deoxycholic acid, proteases and phosphatase inhibitors) by glass-teflon homogenizer. Insoluble material was removed by centrifugation (16.000 g, 15 min, 4°C). For direct Western blot analysis the protein concentration was determined by BCA assay and samples were cooked in Laemmli buffer for 5 min at 95°C. Equal amounts of total protein were loaded on SDS-PAGE. For Rac1 activity assay two hippocampi were homogenized and lysed in Mg^{2+} lysis/wash buffer (Millipore; Cat. 20-168). Lysate was precleared with glutathion sepharose beads and Insoluble material was removed by centrifugation (16.000 g, 15 min, 4°C). Equal protein amount of cleared lysates was incubated with 5 µg GST-PBD substrate (Millipore; 14-325) for 1 h at 4°C followed by extensive wash with Mg^{2+} lysis/wash buffer. Proteins bound to beads were extracted by addition of sample buffer and boiling for 5 min at 95°C. After centrifugation supernatant was loaded on SDS-PAGE.

Chemical stimulation

Chemical stimulation of acute hippocampal slices was performed as described (Matsumoto-Miyai et al., 2009). In brief, hippocampi form 6-week-old mice were rapidly dissected and cut into 400 µm thick slices using a Mcllwain tissue chopper. The slices were transferred into artificial cerebrospinal fluid (ACSF) without calcium (120 mM NaCl, 3 mM KCl, 1.2 mM NaH_2PO_4, 23 mM $NaHCO_3$, 11 mM glucose, 2.4 mM $MgCl_2$) constantly oxygenated with 95% O_2/5% CO_2 and incubated for 1 h at RT to recover from slicing. Before stimulation, the slices were incubated for 20 min in ACSF with calcium (2.4 mM $CaCl_2$) and then stimulated for 10 min with TEA (30 mM TEA in ACSF containing 2.4 mM $CaCl_2$). After stimulation slices were transferred into complete ACSF and incubated for 10 min and then immediately frozen in liquid nitrogen and stored at -80°C for subsequent Western blot analysis.

Subcellular fractionation

Subcellular fractionation was performed on hippocampi from 6-week-old mice using an adapted protocol (Milnerwood et al., 2010). After dissection on ice the pooled hippocampi from one mouse were homogenized in ice-cold homogenization buffer (0.32 M sucrose, 10 mM HEPES pH 7.4, proteases and phosphatase inhibitors). Nuclei and insoluble material (P1) was removed by centrifugation (1.000 g, 10 min, 4°C). The obtained S1 fraction was further centrifuged (12.000 g, 20 min, 4°C) resulting in S2 fraction (microsomes and cytosol) and P2 (crude synaptosomes). The S2 fraction was centrifuged (100.000 g, 2 h, 4°C) to obtain cytosol (S3) and membrane- and organelles fraction (P3). The P2 fraction was resuspended in HEPES buffer (4 mM HEPES pH 7.4, 1 mM EDTA) and again centrifuged (12.000 g, 20 min, 4°C). Resuspension and centrifugation of the pellet was repeated. The obtained pellet was resuspended in buffer A (20 mM HEPES pH 7.4, 100 mM NaCl, 0.5% triton-X-100) and rotated slowly for 15 min at 4°C. The triton-insoluble fraction (pellet) was separated by centrifugation (12.000 g, 20 min, 4°C) and the triton-soluble fraction (non-PSD) was retained. The pellet was resuspended in buffer B (20 mM HEPES pH 7.4, 0.15 mM NaCl, 1% triton-X-100, 1% deoxycholic acid, 1% SDS, 1mM DTT) followed by gentle rotation (1 h, 4°C) the insoluble material was pellet by centrifugation (10.000 g, 15 min, 4°C) and discarded and the supernatant (triton-insoluble PSD fraction) retained.

Quantification of spine density and morphology

To analyzed the spine density in Copine 6 knockout mice, we intercrossed heterozygotes Copine 6 mice with the mouse line Thy1-mGFP (L15) expressing a membrane-targeted GFP in a subset of CA1 neurons (De Paola et al., 2003; Matsumoto-Miyai et al., 2009). 6-week-old male littermate pairs were transcardially perfused with 4% PFA/PBS, brains were postfix for 2 h in 4% PFA/PBS and dehydrated in 30% sucrose. Brains were embedded in O.C.T. and cut in 80 µm sections on a cryostat. Sections were mounted on glass slides and imaged with confocal microscopy (Leica SPE). Imaging, 3D reconstructions of dendritic stretches and automated spine quantification was performed as described (Dumitriu et al., 2011). The whole imaging and analysis procedure was done blinded to genotype. In brief, low resolution images of CA1 neurons with 1 µm intervals along z-axis were taken. On these stacks, healthy looking secondary apical dendritic stretches which were clearly traceable to the soma were selected and imaged with high resolution (0.08 µm z-axis intervals, 2.048 x 2.048 pixels). After deconvolution (Huygens Deconvolution software) images were analyzed with NeuronStudio software. Automated detection of dendrites and spines were performed and manually adjusted. For classification of spines default NeuronStudio classification scheme was used. Filopodia were identified according previously described criteria (Grutzendler et al., 2002; Matsumoto-Miyai et al., 2009).

Electrophysiology

Electrophysiological recordings were performed on sagittal hippocampal slices (400 µm for extracellular field recordings, 250 µm for whole cell patch clamp recordings) that were maintained in artificial cerebro-spinal fluid (ACSF: 119mM NaCl, 1mM NaH_2PO_4, 2.5 mM KCl, 2.5 mM $CaCl_2$, 1.3 mM

$MgCl_2$, 11 mM D-glucose, 26.2 mM $NaHCO_3$ constantly oxygenated with 95% O_2/5% CO_2). For whole cell patch clamp recordings slices were cut in low calcium ACSF (0.125 mM $CaCl_2$ and 3.3 mM $MgCl_2$). Miniature events were recorded using an Axonpatch Multiclamp 700B amplifier and borosilicate glass pipettes (3-4 mΩ) filled with intracellular solution (135 mM $CsMeSO_4$, 8 mM NaCl, 10 mM HEPES, 0.5 mM EGTA, 4 mM Mg-ATP, 0.3 mM Na-GTP, 5 mM Lidocaine-N-ethylbromid). For mEPSC recording, the holding potential was set to -70 mV. For mIPSC recording the holding potential was set to 0 mV. In both conditions, the postsynaptic current was recorded for 10 min. in the presence of 0.5 µM TTX. Traces were further analyzed with the Mini Analysis Program v6 (Synaptosoft).

For extracellular field recordings stimulation electrode was placed into to Schaffer collateral pathway and fEPSP were recorded in the CA1 stratum radiatum. Baseline responses were set as 40-50% of maximum fEPSP. LTP was induced by 3 trains of high frequency stimulation (100 Hz for 1 s, with 240 s interval between trains).

Primary hippocampal cultures

Primary mouse hippocampal neuronal cultures were prepared from E16.5 mouse hippocampi. After dissection in HBSS, hippocampi were washed in ice-cold HBSS. For dissociation, hippocampi were incubated for 15 min in trypsin at 37°C followed by suspension in plating medium (MEM with glutmax, 0.6% glucose, fetal calf serum and pen/strep). Neurons were plated at a density of 750 cells per mm^2 on poly-l-lysine coated glass slides. After 3 h plating medium was exchanged by culture medium (Neurobasal medium, 0.5 mM glutamine, B27 supplement and pen/step).

Transfection was performed at DIV7 with Lipofectamin 2000 (Invitrogen) according to manufacturer's instructions with a total of 500 ng DNA per well (24-well plate). Neurons were fixed at DIV 16 with 4% PFA in PBS with 120 mM sucrose.

References

Bonhoeffer, T., and Yuste, R. (2002). Spine motility. Phenomenology, mechanisms, and function. Neuron *35*, 1019-1027.

Canepari, M., Bove, M., Maeda, E., Cappello, M., and Kawana, A. (1997). Experimental analysis of neuronal dynamics in cultured cortical networks and transitions between different patterns of activity. Biol. Cybern. *77*, 153-162.

Chen, L.Y., Rex, C.S., Casale, M.S., Gall, C.M., and Lynch, G. (2007). Changes in synaptic morphology accompany actin signaling during LTP. J. Neurosci. *27*, 5363-5372.

Cingolani, L.A., and Goda, Y. (2008). Actin in action: the interplay between the actin cytoskeleton and synaptic efficacy. Nat. Rev. Neurosci. *9*, 344-356.

De Paola, V., Arber, S., and Caroni, P. (2003). AMPA receptors regulate dynamic equilibrium of presynaptic terminals in mature hippocampal networks. Nat. Neurosci. *6*, 491-500.

Dillon, C., and Goda, Y. (2005). The actin cytoskeleton: integrating form and function at the synapse. Annu. Rev. Neurosci. *28*, 25-55.

Dumitriu, D., Rodriguez, A., and Morrison, J.H. (2011). High-throughput, detailed, cell-specific neuroanatomy of dendritic spines using microinjection and confocal microscopy. Nat Protoc *6*, 1391-1411.

Engert, F., and Bonhoeffer, T. (1999). Dendritic spine changes associated with hippocampal long-term synaptic plasticity. Nature *399*, 66-70.

Erni, A. (2011). Analysis of mRNA Expression of Copine genes in Copine 6 knock-out mice. Master Thesis, Biozentrum, University of Basel.

Fischer, M., Kaech, S., Knutti, D., and Matus, A. (1998). Rapid actin-based plasticity in dendritic spines. Neuron *20*, 847-854.

Grutzendler, J., Kasthuri, N., and Gan, W.B. (2002). Long-term dendritic spine stability in the adult cortex. Nature *420*, 812-816.

Gu, J., Lee, C.W., Fan, Y., Komlos, D., Tang, X., Sun, C., Yu, K., Hartzell, H.C., Chen, G., Bamburg, J.R.*, et al.* (2010). ADF/cofilin-mediated actin dynamics regulate AMPA receptor trafficking during synaptic plasticity. Nat. Neurosci. *13*, 1208-1215.

Haditsch, U., Leone, D.P., Farinelli, M., Chrostek-Grashoff, A., Brakebusch, C., Mansuy, I.M., McConnell, S.K., and Palmer, T.D. (2009). A central role for the small GTPase Rac1 in hippocampal plasticity and spatial learning and memory. Mol. Cell. Neurosci. *41*, 409-419.

Hayashi-Takagi, A., Takaki, M., Graziane, N., Seshadri, S., Murdoch, H., Dunlop, A.J., Makino, Y., Seshadri, A.J., Ishizuka, K., Srivastava, D.P.*, et al.* (2010). Disrupted-in-Schizophrenia 1 (DISC1) regulates spines of the glutamate synapse via Rac1. Nat. Neurosci. *13*, 327-332.

Jontes, J.D., and Smith, S.J. (2000). Filopodia, spines, and the generation of synaptic diversity. Neuron *27*, 11-14.

Kasai, H., Matsuzaki, M., Noguchi, J., Yasumatsu, N., and Nakahara, H. (2003). Structure-stability-function relationships of dendritic spines. Trends Neurosci. *26*, 360-368.

Knott, G., and Holtmaat, A. (2008). Dendritic spine plasticity--current understanding from in vivo studies. Brain Res. Rev. *58*, 282-289.

Lang, C., Barco, A., Zablow, L., Kandel, E.R., Siegelbaum, S.A., and Zakharenko, S.S. (2004). Transient expansion of synaptically connected dendritic spines upon induction of hippocampal long-term potentiation. Proc. Natl. Acad. Sci. U. S. A. *101*, 16665-16670.

Leuner, B., Falduto, J., and Shors, T.J. (2003). Associative memory formation increases the observation of dendritic spines in the hippocampus. The Journal of neuroscience : the official journal of the Society for Neuroscience *23*, 659-665.

Lisman, J., Yasuda, R., and Raghavachari, S. (2012). Mechanisms of CaMKII action in long-term potentiation. Nat. Rev. Neurosci. *13*, 169-182.

Maletic-Savatic, M., Malinow, R., and Svoboda, K. (1999). Rapid dendritic morphogenesis in CA1 hippocampal dendrites induced by synaptic activity. Science *283*, 1923-1927.

Matsumoto-Miyai, K., Sokolowska, E., Zurlinden, A., Gee, C.E., Luscher, D., Hettwer, S., Wolfel, J., Ladner, A.P., Ster, J., Gerber, U.*, et al.* (2009). Coincident pre- and postsynaptic activation induces dendritic filopodia via neurotrypsin-dependent agrin cleavage. Cell *136*, 1161-1171.

Meng, Y., Zhang, Y., Tregoubov, V., Janus, C., Cruz, L., Jackson, M., Lu, W.Y., MacDonald, J.F., Wang, J.Y., Falls, D.L.*, et al.* (2002). Abnormal spine morphology and enhanced LTP in LIMK-1 knockout mice. Neuron *35*, 121-133.

Milnerwood, A.J., Gladding, C.M., Pouladi, M.A., Kaufman, A.M., Hines, R.M., Boyd, J.D., Ko, R.W., Vasuta, O.C., Graham, R.K., Hayden, M.R.*, et al.* (2010). Early increase in extrasynaptic NMDA receptor signaling and expression contributes to phenotype onset in Huntington's disease mice. Neuron *65*, 178-190.

Murphy, T.H., Blatter, L.A., Wier, W.G., and Baraban, J.M. (1992). Spontaneous synchronous synaptic calcium transients in cultured cortical neurons. J. Neurosci. *12*, 4834-4845.

Nakayama, T., Yaoi, T., Yasui, M., and Kuwajima, G. (1998). N-copine: a novel two C2-domain-containing protein with neuronal activity-regulated expression. FEBS Lett. *428*, 80-84.

Rex, C.S., Chen, L.Y., Sharma, A., Liu, J., Babayan, A.H., Gall, C.M., and Lynch, G. (2009). Different Rho GTPase-dependent signaling pathways initiate sequential steps in the consolidation of long-term potentiation. J. Cell Biol. *186*, 85-97.

Rust, M.B., Gurniak, C.B., Renner, M., Vara, H., Morando, L., Gorlich, A., Sassoe-Pognetto, M., Banchaabouchi, M.A., Giustetto, M., Triller, A.*, et al.* (2010). Learning, AMPA receptor mobility and synaptic plasticity depend on n-cofilin-mediated actin dynamics. EMBO J. *29*, 1889-1902.

Tashiro, A., and Yuste, R. (2004). Regulation of dendritic spine motility and stability by Rac1 and Rho kinase: evidence for two forms of spine motility. Mol. Cell. Neurosci. *26*, 429-440.

Tashiro, A., and Yuste, R. (2008). Role of Rho GTPases in the morphogenesis and motility of dendritic spines. Methods Enzymol. *439*, 285-302.

Wagenaar, D.A., Madhavan, R., Pine, J., and Potter, S.M. (2005). Controlling bursting in cortical cultures with closed-loop multi-electrode stimulation. J. Neurosci. *25*, 680-688.

Yuste, R., and Bonhoeffer, T. (2004). Genesis of dendritic spines: insights from ultrastructural and imaging studies. Nat. Rev. Neurosci. *5*, 24-34.

CHAPTER 4

Identification of a novel Copine 6 interaction partner

Neuronal NF-kappa B activity is regulated by Copine 6 via its new interacting partner SIMPL

Abstract

In neurons, long-lasting adaptions in response to neuronal activity demand a synapse-to-nucleus communication that finally induces changes in gene expression. NMDA-receptor activation and subsequent calcium influx recruits Copine 6 from the dendritic shaft into the postsynaptic density. Here, we identify SIMPL (IRAK1BP1), the co-activator of the transcription factor NF-kappa B, as a novel Copine 6 interacting partner. We demonstrate that Copine 6 binds to SIMPL via its unique C-terminal ending. In neurons, Copine 6 anchors SIMPL in the cytoplasm and prevents its translocation into the nucleus. In consequence, absence of Copine 6 increases the amount of nuclear SIMPL, which in turn promotes NF-kappa B activity. In summary, these data indicate that the Copine 6-SIMPL interaction may provide a novel pathway to translate synaptic activity into transcriptional changes.

Introduction

The key function of a postsynaptic neuron is to sense neuronal activity and translate it into short- and long-lasting alteration in neuronal structure and function. Long-lasting adaptive plasticity is based on transformation of synaptic signals into changes in gene expression. The NF-kappa B transcription factor is widely known to regulate immune response and inflammation but also for its ubiquitous role in the control of cell survival and apoptosis. In neurons, NF-kappa B signaling has been implicated in pathophysiological conditions but also in synaptic signaling and behavior (Lubin and Sweatt, 2007; Meberg et al., 1996; Meffert et al., 2003).

We recently described the novel postsynaptic calcium sensor Copine 6 with previously unknown function (Chapter 2). Copine 6 is a member of a family of cytoplasmic proteins, which are highly conserved from paramecium to human (Tomsig and Creutz, 2000). The nine mammalian Copines are characterized by two C2-domains at the N-terminus followed by an A-domain. The C2-domain is well described in synaptotagmins, where it mediates calcium-dependent phospholipid-binding (Brose et al., 1992). The A-domain is characterized to mediate protein-protein interactions in integrins (Whittaker and Hynes, 2002). The C2-domains and the A-domain are highly conserved among Copine family members, whereas the C-term is highly divergent (see supplementary Figure 2). In contrast to other Copines, Copine 6 is expressed only in the central nervous system (CNS) and its expression is restricted to glutamatergic neurons in brain regions known for synaptic plasticity as for example the hippocampus (Chapter 3). Copine 6 can sense neuronal activity via its calcium-binding C2-domain. Specifically, NMDA-receptor mediated calcium transients recruit the cytosolic Copine 6 from the dendritic shaft into postsynaptic densities (Chapter 2). In primary hippocampal neurons, knockdown of Copine 6 by shRNA increases spine number and influences their stability in an activity-dependent manner (Chapter 2). Furthermore, Copine 6 affects the activity and localization of the small GTPase Rac1, a key regulator of actin polymerization, which is the basis of morphological changes of spines. It was therefore proposed that Copine 6 acts as a calcium-dependent shuttle protein that translates local and transient synaptic signals into morphological changes trough translocation of on effector protein (i.e Rac1) into activated spines (Chapter 2).

To identify new Copine 6-interacting partners, we performed a yeast-two hybrid screen using Copine 6 as bait to screen at adult mouse brain library. This screen identified SIMPL as a novel Copine 6 binding partner. SIMPL (signaling molecule that interact with mouse Pelle-like kinase; or IRAK1BP1) is a small, poorly characterized protein that lacks any domains of described function. Originally, it was identified as a binding partner of IRAK/mPLK, which is linked to NF-kappa B-dependent gene expression (Vig et al., 2001). Ectopic expression of SIMPL increases the activation of NF-kappa B-dependent promoters, whereas its down-regulation reduces it (Vig et al., 2001). The cytosolic SIMPL can translocate into the nucleus via its nuclear localization signal (NLS), where it acts a as co-activator of the transcription factor NF-kappa B (Kwon et al., 2004). Functionally, SIMPL acts an inhibitor of inflammation by promoting the activity of the NF-kappa B subunit p50 (Conner et al., 2010) and in hematopoietic progenitor cells loss of SIMPL increases apoptosis (Benson et al., 2010).

Here, we provide evidence that SIMPL plays a role in the regulation of neuronal survival. We demonstrate that Copine 6 influences the localization of SIMPL, which in turn, affects NF-kappa B

transcriptional activity. We propose that the Copine 6-SIMPL interaction may provide a novel pathway to translate synaptic signals into changes in gene expression.

Results

Copine 6 interacts with SIMPL in a yeast-two hybrid system

In order to identify Copine 6 interacting partners we used the full-length Copine 6 as bait in a yeast-two hybrid system and screen 2.67 x 10^6 clones from a mouse brain cDNA library (Figure 1A). The expression of the full-length Copine 6 in yeast was verified by Western blot analysis with Copine 6 specific antibody (Figure 1B). After exclusion of autoactivation of reporters by the bait construct (supplementary Figure 1A) transformants were selected for growth on leucine-deficient media and expression of β-galactosidase activity. After retransformation of positive clones, two clones remained positive for LacZ expression and protrotroph for leucine. Both clones contained an identical cDNA fragment encoding the full-length version of a protein named SIMPL (or IRAK1BP1). To map the binding region of Copine 6 with SIMPL, deletion mutants were generated (according to scheme in Figure 1C). The expression of these constructs was verified by Western blot analysis (supplementary Figure 1B).

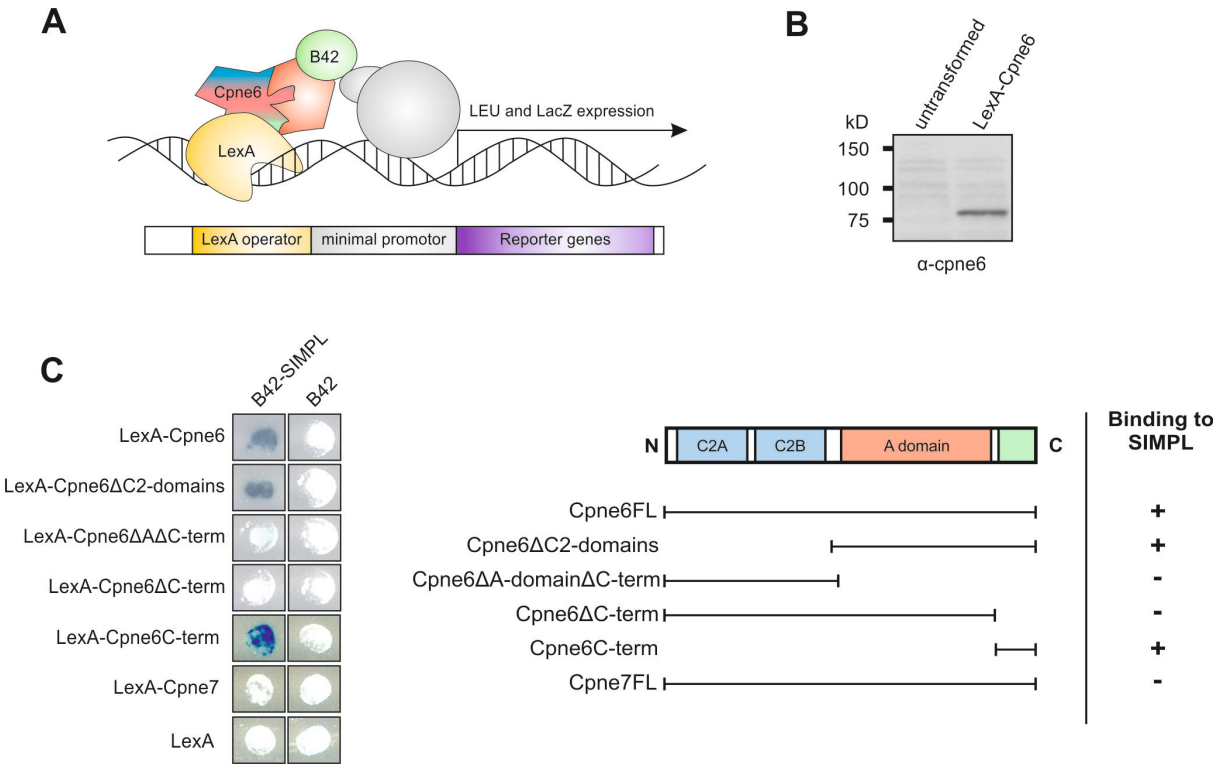

Figure 1. SIMPL is a new Copine 6 interacting partner. (A) Schematic illustration of the yeast two-hybrid system. Copine 6 was fused to the DNA binding domain LexA (bait) and transformed into yeast together with a cDNA library containing proteins fused to the activator domain B42 (prey). Binding of the bait and a prey protein results in the activation of the two reporter genes (LacZ and LEU). (B) Expression of the LexA-Copine 6 fusion protein in yeast was verified by Western blot analysis. (C) Binding domain of Copine 6 with SIMPL was identified. Deletion mutants according to scheme (right) were generated. Binding of the two proteins resulted in LacZ expression (blue color). Note that the C-terminal region of Copine 6 is essential and sufficient for the interaction with SIMPL and Copine 7 is not interacting with SIMPL.

Testing the ability of these deletion mutants to induce β-galactosidase activity together with the SIMPL prey construct, showed that the very C-terminal part of Copine 6 is both essential and sufficient to interact with SIMPL (Figure 1C). Since this C-terminal region is very specific for Copine 6 and not conserved among other Copine family members (supplementary Figure 2A), we predicted that SIMPL is a Copine 6 specific binding partner. This hypothesis was confirmed by co-expression of Copine 7 (the most related Copine family member (supplementary Figure 2B)) together with SIMPL, which did not cause reporter activation (Figure 1C).

SIMPL and Copine 6 bind each other *in vitro*

To validate the interaction between Copine 6 and SIMPL, we examined their binding when overexpressed in COS7 cells. We found that Copine 6 co-immunoprecipitates with SIMPL (Figure 2A). Direct binding between these two proteins was confirmed by the expression and purification of GST-tagged Copine 6 and HIS-tagged SIMPL out of E.coli and following pull-down experiments (Figure 2B).

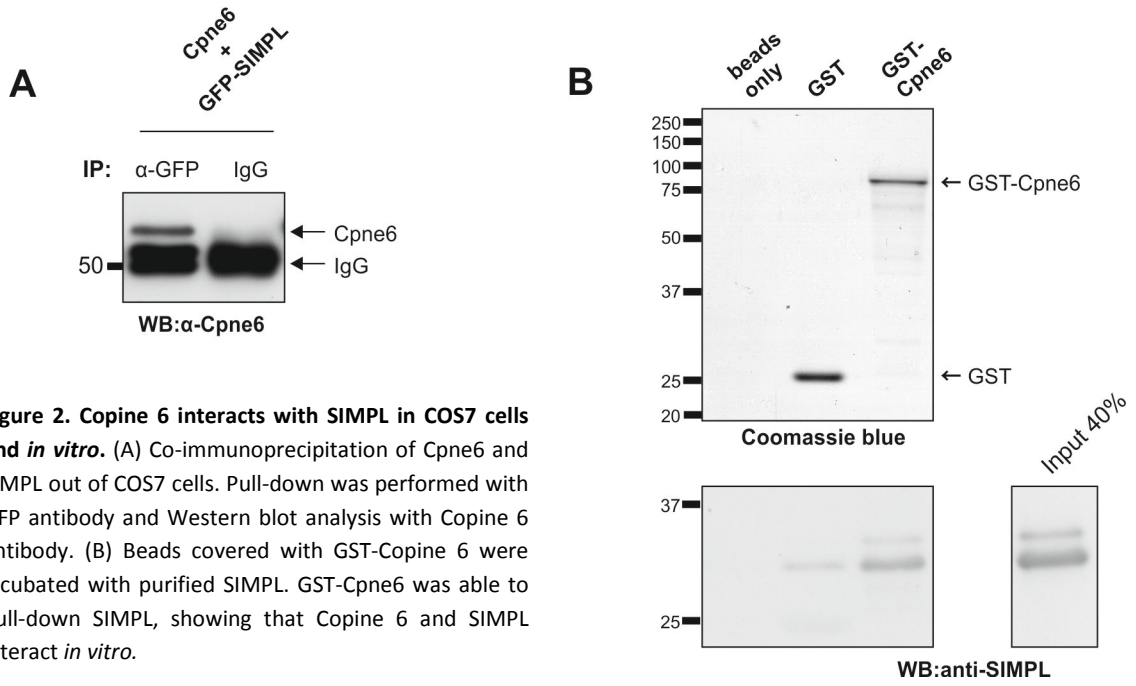

Figure 2. Copine 6 interacts with SIMPL in COS7 cells and *in vitro*. (A) Co-immunoprecipitation of Cpne6 and SIMPL out of COS7 cells. Pull-down was performed with GFP antibody and Western blot analysis with Copine 6 antibody. (B) Beads covered with GST-Copine 6 were incubated with purified SIMPL. GST-Cpne6 was able to pull-down SIMPL, showing that Copine 6 and SIMPL interact *in vitro.*

SIMPL is expressed in hippocampal neurons and its knockdown affects neuronal survival

The function of SIMPL was so far not addressed in neuronal cells, although Northern blot analysis from various mouse tissue indicated a strong expression of SIMPL in the brain (Vig et al., 2001). To confirm that SIMPL is expressed in hippocampal neurons, we performed PCR with SIMPL specific primers on cDNA isolated from rat primary hippocampal neurons. These results showed that SIMPL is strongly expressed in these cultures but in contrast to Copine 6 also in non-neuronal cells (COS7) (Figure 3A). To examine the role of SIMPL in neurons an shRNA-mediated knockdown was

performed. Two different shRNAs were generated and their knockdown efficiency tested in COS7 cells (Figure 3B). An shRNA targeting CD4 was used as control. Western blot analysis on lysates form these COS7 cells demonstrated that both shRNA constructs were able to reduce the amount of SIMPL (Figure 3B). Next, the most efficient shRNA construct was transfected at DIV7 into primary hippocampal neurons together with a GFP, whose expression was under the control of the synapsin promoter, to visualize the targeted neurons. Analysis of these neurons at DIV14 revealed that knockdown of SIMPL strongly affected the dendritic arborization and neuronal survival (Figure 3C). Previous data on the function of SIMPL in non-neuronal cells indicate a role in the regulation of NF-kappa B activity (Kwon et al., 2004; Luo et al., 2007; Vig et al., 2001); furthermore in non-neuronal cells it has been demonstrated that SIMPL can influence cell survival (Benson et al., 2010). As the tightly regulated control of NF-kappa B has been shown to be the key pathway in the regulation of neuronal survival (Sarnico et al., 2009), our results indicate that also in neurons SIMPL controls neuronal survival by influencing NF-kappa B activity.

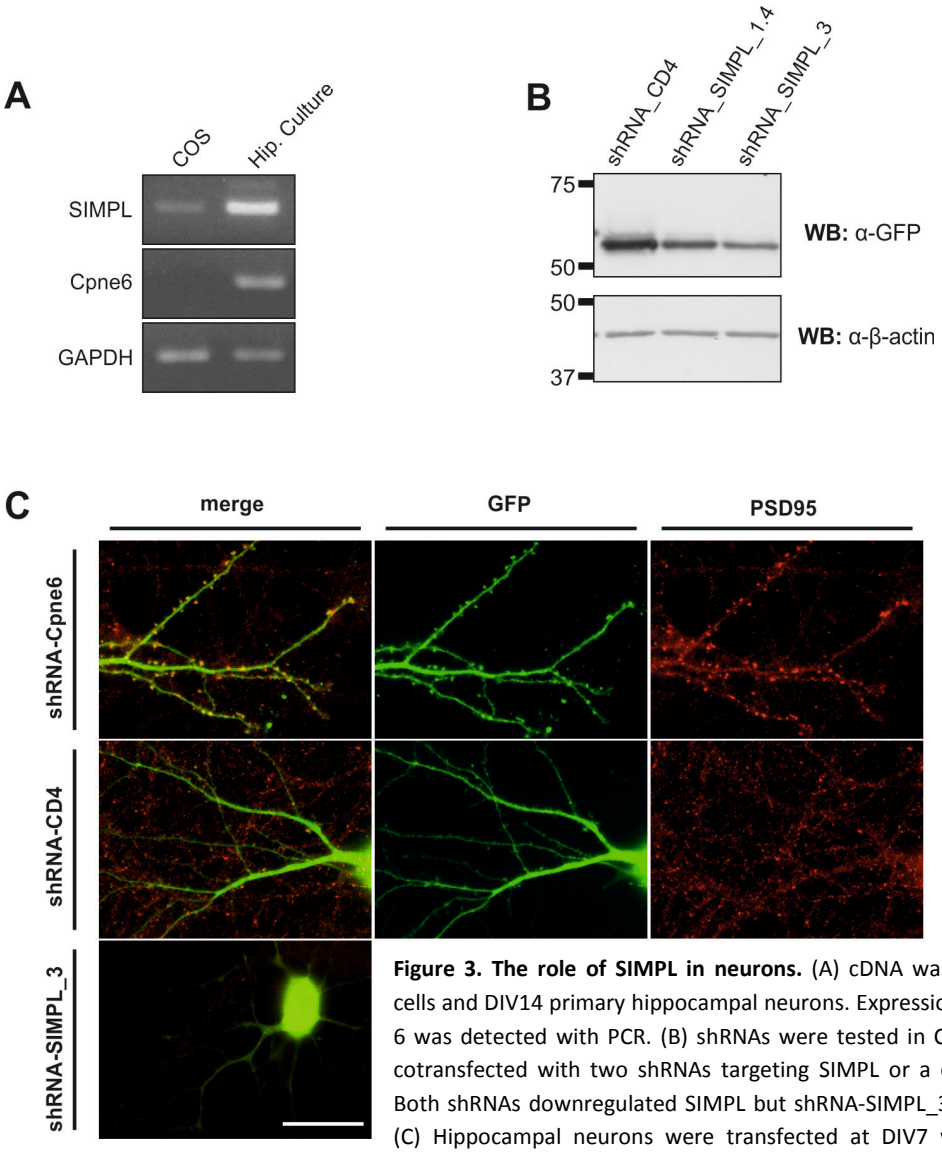

Figure 3. The role of SIMPL in neurons. (A) cDNA was isolated form COS7 cells and DIV14 primary hippocampal neurons. Expression of SIMPL or Copine 6 was detected with PCR. (B) shRNAs were tested in COS7 cells. Cells were cotransfected with two shRNAs targeting SIMPL or a control shRNA (CD4). Both shRNAs downregulated SIMPL but shRNA-SIMPL_3 was more effective. (C) Hippocampal neurons were transfected at DIV7 with a cytosolic GFP expression construct and indicated shRNA. At DIV14, neurons were fixed and stained with antibodies to PSD95. Knockdown of Copine 6 increased the amount of spines (colocalization of GFP (green) and PSD95 (red)). Knockdown of SIMPL leads to a collapse of the dendritic tree. Scale bar represents 20 µm.

Copine 6 affects the localization of SIMPL and thereby NF-kappa B activity

SIMPL has been shown to be present in the cytosol and to translocate into the nucleus via its nuclear localization signal (NLS) (Kwon et al., 2004). If present in the nucleus, SIMPL acts as a co-activator of NF-kappa B transcriptional activity (Vig et al., 2001). As Copine 6 directly interacts with SIMPL, we addressed whether the presence of Copine 6 could influence the subcellular localization of SIMPL. Hippocampal neurons were transfected at DIV7 with myc-SIMPL (red) together with a control shRNA (CD4) and an shRNA targeting Copine 6. The analysis of the transfected neurons at DIV14 revealed that knockdown of Copine 6 strongly increased the amount of SIMPL in the nucleus (Figure 4A). These data indicate that the presence of Copine 6 retains SIMPL in the cytoplasm whereas its absence allows the translocation of SIMPL into the nucleus. In an attempt to address if this change in the localization of SIMPL had functional consequences, we determined the NF-kappa B transcriptional activity in these neurons (Figure 4B). To this end, neurons were co-transfected at DIV7 with control shRNA (CD4) or an shRNA targeting Copine 6 together with firefly-luciferase that was under the control of NF-kappa B response elements. Four times more shRNA than reporter plasmid were transfected to make sure that luciferase-containing neurons were also transfected with the shRNA. After lysis of the cultures at DIV14, luciferase activity was determined. Quantification revealed a significant increase of firefly-luciferase and therefore NF-kappa B transcriptional activity in Copine 6 knockdown neurons (Figure 4B). Taken together, these data indicate that Copine 6 influences NF-kappa B activity by preventing the nuclear translocation of SIMPL.

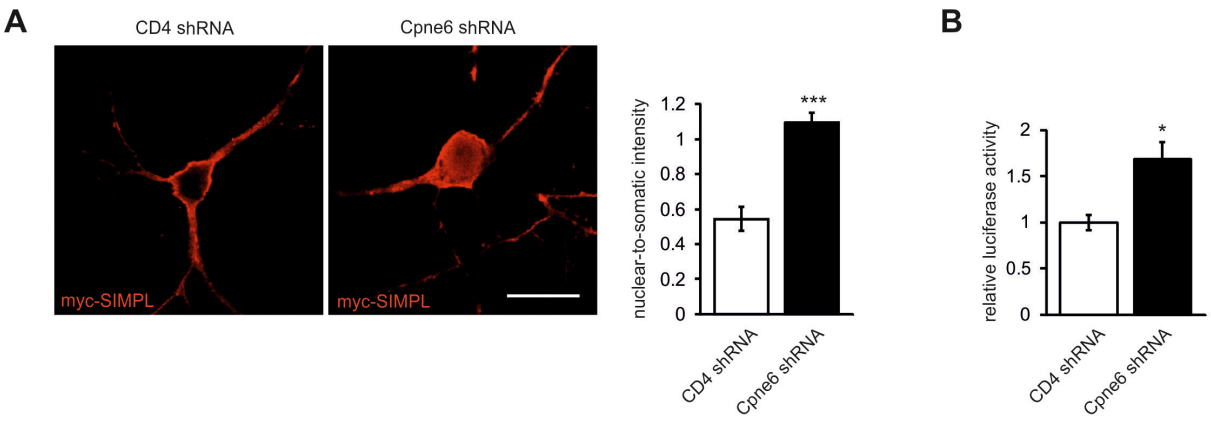

Figure 4. Copine 6 affects localization of SIMPL and NF-kappa B activity in neurons. (A) DIV14 hippocampal neurons that express myc-SIMPL (red) together with the indicated shRNA. Knockdown of Copine 6 increases the amount of SIMPL in the nucleus. Quantification is shown to the right. N=8 neurons per condition. Scale bar represents 20 µm. (B) Luciferase assay showed that knockdown of Copine 6 increases NF-kappa B transcriptional activity. N=4 wells per condition. *p < 0.05, **p < 0.001

Discussion

In this study, we screened for new Copine 6 interacting partners. We identified SIMPL as a novel binding partner of the postsynaptic calcium sensor Copine 6. Our results demonstrate that this direct interaction requires the C-terminal ending of Copine 6, that SIMPL is a Copine 6-specific binding partner and as it does not interact with other Copines (Figure 1, Figure 2). As consequence of this interaction, Copine 6 influences the subcellular localization of SIMPL. In particular, in the presence of Copine 6 SIMPL is retained in the cytoplasm whereas in its absence SIMPL translocates into the nucleus, which in turn increases the NF-kappa B activity (Figure 5).

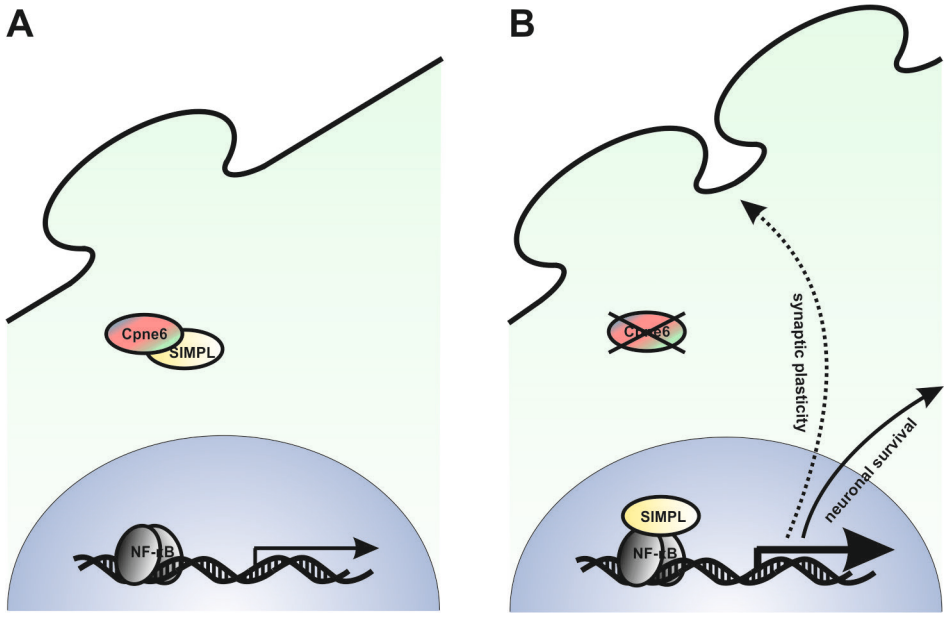

Figure 5. Model. (A) In the presence of Copine 6, SIMPL is retained in the cytoplasm. (B) Absence of Copine 6 leads to the translocation of SIMPL into the nucleus and this increases NF-kappa B transcriptional activity. Increase in NF-kappa B activity affects neuronal survival and plays a role in synaptic plasticity.

Copine 6 is involved in neuronal NF-kappa B signaling

Previously, Copine 6 was characterized as a postsynaptic calcium sensor that translates synaptic activity into local rearrangement of spines (Chapter 2). Hence, our finding that Copine 6 binds the co-activator of the transcription factor NF-kappa B and in turn, influences transcriptional activity was surprising. Compared to its well-described function in the immune system, the consequences of NF-kappa B activity in neurons are less understood. On the one hand, in neurons as in other cells NF-kappa B induces the expression of antiapoptotic genes to promote cell survival (Mattson and Meffert, 2006). In line with this, NF-kappa B has an important role in neuroprotection as its activation protects neurons against oxidative stress and ischemia-induced neurodegeneration (Fridmacher et al., 2003; Mattson and Meffert, 2006). In consequence, unbalanced NF-kappa B activity is found in

many pathophysiological conditions (Mattson and Meffert, 2006). NF-kappa B has been implicated in neurogenesis and differentiation and recently also in synaptic plasticity. Initially, it was observed that glutamatergic neurons in the CNS show a high level of basal NF-kappa B activity (Kaltschmidt et al., 1994) and this is especially true for neurons in brain regions of high plasticity as found in the hippocampus (Schmidt-Ullrich et al., 1996). Interestingly, the expression pattern of Copine 6 overlaps with constitutive NF-kappa B activity. Beside the constitutive NF-kappa B activity, several lines of evidence indicate that NF-kappa B activity is strongly responsive to neuronal activity. Specifically, to postsynaptic changes in intracellular calcium concentration (Lilienbaum and Israel, 2003; Meffert et al., 2003). If the NF-kappa B activity is determined by electrophoretic mobility shift assay (EMSA), it was demonstrated that neuronal activity increases the DNA-binding affinity of both p50:p65 and p50:p50 dimers (Meffert et al., 2003). At the synapse, neuronal activity increases the amount of p50:p65 dimers, which is mediated by Ca^{2+}/calmodulin-dependent protein kinases II (CamKII) (Meffert et al., 2003). The mechanisms responsive for the calcium-dependent p50:p50 activation in the nucleus remain elusive. It has been shown that SIMPL affects NF-kappa B activity by increasing the amount of p50:p50 dimers in the nucleus (Conner et al., 2010). As Copine 6 binds and affects the subcellular localization of SIMPL, this may in turn influence p50:p50 homodimer activity. Previously, we have shown that Copine 6 is responsible to changes in neuronal activity (Chapter 2). Here, we demonstrate that Copine 6 influences basal NF-kappa B activity (Figure 4B). Taken together, Copine 6 may translate neuronal activity into gene expression regulated by NF-kappa B activity. The translocation of Copine 6 into spines upon neuronal activity and subsequent calcium influx may release the cytosolic retained SIMPL to translocate to the nucleus, which in turn increases the NF-kappa B activity.

The role of SIMPL in neurons

SIMPL was so far mainly implicated in cellular responses to inflammation (Conner et al., 2010; Kwon et al., 2004; Vig et al., 2001) and its function in neurons has not been addressed. Our data demonstrate that SIMPL directly interacts with the neuronal protein Copine 6 (Figure 1 and Figure 2) and therefore provide first time evidence for a function of SIMPL in neurons. It has previously been shown that SIMPL is strongly expressed in the adult brain (Vig et al., 2001). Here we demonstrated that SIMPL is expressed in hippocampal cultures (Figure 3A). We observed that perturbation of SIMPL leads to a collapse of the dendritic tree and subsequent neuronal death (Figure 3B). This is reminiscent to previous data from non-neuronal cells showing that SIMPL knockdown affects cell survival (Benson et al., 2010). We propose that the SIMPL-mediated decrease in NF-kappa B activity is also responsible for the increase in apoptosis in neurons. However, the lethal effect of SIMPL knockdown in neurons prevented us from a more detailed evaluation of its neuronal function. In neurons, NF-kappa B is responsive to a variety of stimuli and its activity affects very diverse functions. The coactivator SIMPL may provide a mechanism to achieve specificity in response to certain stimuli.

The Copine 6-SIMPL interaction may mediate synapse-to-nucleus communication

To translate activity signals occurring at synapses into changes in gene expression the synapse-to-nucleus communication is of pivotal importance. Calcium-dependent regulation of gene expression occurs through spreading of calcium waves, signaling cascades, diffusion of molecules or active transport (Greer and Greenberg, 2008; Hardingham et al., 2001; Jordan and Kreutz, 2009). Several components of the postsynaptic density contain nuclear localization signals (NLSs), suggesting that these proteins are transported from the synapse to the nucleus (Hardingham et al., 2001; Jordan et al., 2007; Meffert et al., 2003). The NLS-mediated importin binding, has been shown to be required and sufficient for the translocation into the nucleus (Ambron et al., 1992) and it also mediates an active synapse-to-nucleus transport (Lai et al., 2008; Thompson et al., 2004). We provide evidence that in neurons under basal activity SIMPL is predominantly localized in the cytoplasm of dendritic shaft and the soma. We propose that presence of Copine 6 in the cytoplasm anchors SIMPL in the cytoplasm and suppresses its NLS-mediated nuclear translocation. In line with this, in absence of Copine 6 (shRNA-mediated knockdown) SIMPL is freed from its cytoplasmic anchor and is transported to the nucleus. Copine 6 senses neuronal activity by binding calcium and subsequent translocation into spines (Chapter 2). If this translocation effects SIMPL localization, the Copine 6-SIMPL interaction may provide an efficient mechanism to communicate between synapse and nucleus, as it would combine passive transport of Copine 6 along calcium gradients and active transport of SIMPL via its NLS. This may enable a neuron to change gene expression in response to subthreshold or locally restricted calcium signals rather than global activity.

Experimental procedures

Plasmids and antibodies

shRNAs were cloned into the pBluecript SK(+) vector under the control of the U6 promoter. The following 21 nucleotide sequences were used to specifically target Copine 6 and SIMPL. Cpne6: 5'-GGAGATCTATAAGACCAATGG-3'; SIMPL-1: 5'-GCCCACCTGAGTTCTATCACA-3' and SIMPL-3: 5'-GCCGAGGTCTGCATTACATTT-3'. For the overexpression in COS7 cells Copine 6 and SIMPL were subcloned into the pIRES2-EGFP or pEGFP(C1) vector, respectively. For the yeast two-hybrid experiments the bait construct were generated by cloning the full-length Copine 6 (corresponding amino acids 1-557), the full-length Copine 7 (1-557) or Copine 6 deletions mutants (Copine6ΔC2-domains (270-557), Copine6ΔAΔC-term (1-269), Copine6ΔC-term (1-539), Copine6C-term (540-557)) into the pNLexA vector (Origene).

The following antibodies were used: Anti-GFP (clone 7.1 and 13.1, Roche), anti-LexA (Milipore), anti-Copine 6 (clone 42, Santa Cruz), anti-SIMPL (IRAK1BP1 MaxPap polyclonal antibody, Anova), anti-myc (clone 9E10), anti-PSD95 (Affinity Bioreagents).

Yeast two-hybrid screen

For the yeast two-hybrid screen the DupLEX-A system from Origene was used. The full-length Copine 6 (corresponding amino acids 1-557) was cloned in frame with the C-terminal LexA-binding domain into the pNLexA bait vector. This bait construct was used to screen an adult mouse brain cDNA library (Origene) that was cloned into the pJG4-5 vector and transformed into the yeast strain EGY48. Positive clones were selected for growth on leucine-deficient media and expression of the LacZ reporter gene. Plasmids from positive clones were recovered and transformed into electro-competent KC8 E.coli and selected on tryptophan deficient plates. Isolated plasmids were retransformed into yeast to test their ability to induce reporter activation and afterwards sequenced. For further yeast-two hybrid analysis deletion mutants were transformed into the yeast stain RFY206 and mated with the strain EGY48 transformed with the full-length SIMPL in the pJG4-5 vector or the empty pJG4-5 vector. Interaction of the two proteins was tested by LacZ-reporter activation.

For Western-blot analysis of yeast cell extract, cells (OD_{600} = 0.8) were extracted with yeast sample buffer (0.06 M Tris-HCl pH 6.8, 10% (v/v) glycerol, 2% (w/v) SDS, 5% (v/v) 2-mercaptoethanol and 0.0025% (w/v) bromphenol blue), boiled for 5 min at 95°C, centrifuged at 14.000 x g for 5 min and supernatant loaded on SDS-PAGE.

Co-immunoprecipitation and GST-pull-down

COS7 cells were transfected with Lipofectamin 2000 (Invitrogen) and 24h later lysed on ice in lysis buffer (50 mM Tris pH7.5, 150 mM NaCl, 1% NP-40, 0.5% deoxycholate and protease inhibitors). Lysates were cleared by centrifugation at 16.000 x g for 15 min at 4°C and incubated overnight at 4°C

with 2 µg GFP antibody or total IgG as control. Washed Protein G sepharose beads (Sigma-Aldrich) were added and the incubation continued for 2 h at 4°C. Beads were pelleted by centrifugation and washed five times with lysis buffer. Finally beads were resuspended in sample buffer and boiled for 5 min. After centrifugation the supernatant was loaded on a SDS-PAGE.

For GST pull-down experiments the full-length Copine 6 was subcloned into the pGEX4T1 vector (N-terminal fusion of GST) and the full-length SIMPL in pET15b vector (N-terminal fusion of HIS). Proteins were expressed in BL21 bacteria by IPTG induction and solubilized by lysozyme, triton-X-1000 and sonication. GST-Copine 6 was purified via Glutathione sepharose beads (GE Healthcare) and HIS-SIMPL by HIS-Select Nickel Gel (Sigma-Aldrich). Purification was verified by SDS-PAGE and Coomassie staining. Purified Copine 6 bound to Glutathione sepharose beads was incubated with purified SIMPL for 4 h at 4°C. Beads were washed four times with lysis buffer, than proteins bound to beads were extracted by addition of sample buffer and boiling for 5 min at 95°C. After centrifugation supernatant was loaded on SDS-PAGE.

Primary hippocampal culture, transfection and immunostaining

Primary rat hippocampal neuronal cultures were prepared from E18-19 rat hippocampi. After dissection in HBSS, hippocampi were washed in ice-cold HBSS. For dissociation, hippocampi were incubated for 15 min in trypsin at 37°C followed by suspension in plating medium (MEM with glutmax, 0.6% glucose, fetal calf serum and pen/strep). Neurons were plated at a density of 750 cells per mm^2 on poly-l-lysine coated glass slides. After 3 h plating medium was exchanged by culture medium (Neurobasal medium, 0.5 mM glutamine, B27 supplement and pen/step).

Transfection was performed at DIV7 with Lipofectamin 2000 (Invitrogen) according to manufacturer's instructions with a total of 500 ng DNA per well (24-well plate). Neurons were fixed at DIV 14 with 4% paraformaldehyde in PBS with 120 mM sucrose. Permeabilization was performed with 0.5% Triton-X-100 in PBS for 15 min and subsequently incubated in primary antibody in blocking solution overnight at 4°C. After extensive wash with PBS neurons were incubated for 1 h at RT in appropriate secondary antibody (and DAPI). Coverslips were mounted with cervol.

Images were taken with a confocal Leica SPE system. For quantification of nuclear SIMPL intensity nuclei were identified by DAPI straining. Images from a single confocal plane with maximal nuclear diameter were acquired. These pictures were analyzed with ImageJ software. Identified nuclei (DAPI signal) were set as region of interest (ROI) and used as a mask for the measurement of the mean grey value of the SIMPL signal. This nuclear signal was normalized to the somatic mean grey value (ROI, defined as a band with a defined diameter adjacent to the nuclear DAPI signal).

Luciferase assay

NF-kappa B activity was measured with the NF-kappa B–Luc plasmid (Agilent Technologies) containing firefly luciferase driven by NF-kappa B response element $(TGGGGACTTTCCGC)_5$. Primary hippocampal neurons (in 24-well plate) were transfected at DIV7 with the following amount of DNA per well: 400 ng shRNA, 100 ng NF-kappa B–Luc and 10 ng RL-Luc (Renilla luciferase, Promega).

Renilla luciferase was co-transfected to control for transfection efficiency. At DIV14 luciferase activity was measured with the dual-luciferase assay system (Promega) according to manufacturer's instructions. In brief, neurons were washed and immediately lysed in passive lysis buffer (PLB). Firefly and renilla luciferase activity was determined with a plate-reading luminometer. NF-kappa B activity was calculated by the firefly luciferase activity normalized to the renilla luciferase activity.

Statistics

All data are shown as mean ± s.e.m. Statistical significance was tested with Student's t-test.

References

Ambron, R.T., Schmied, R., Huang, C.C., and Smedman, M. (1992). A signal sequence mediates the retrograde transport of proteins from the axon periphery to the cell body and then into the nucleus. J. Neurosci. *12*, 2813-2818.

Benson, E.A., Goebl, M.G., Yang, F.C., Kapur, R., McClintick, J., Sanghani, S., Clapp, D.W., and Harrington, M.A. (2010). Loss of SIMPL compromises TNF-alpha-dependent survival of hematopoietic progenitors. Exp. Hematol. *38*, 71-81.

Brose, N., Petrenko, A.G., Sudhof, T.C., and Jahn, R. (1992). Synaptotagmin: a calcium sensor on the synaptic vesicle surface. Science *256*, 1021-1025.

Conner, J.R., Smirnova, II, Moseman, A.P., and Poltorak, A. (2010). IRAK1BP1 inhibits inflammation by promoting nuclear translocation of NF-kappaB p50. Proc. Natl. Acad. Sci. U. S. A. *107*, 11477-11482.

Fridmacher, V., Kaltschmidt, B., Goudeau, B., Ndiaye, D., Rossi, F.M., Pfeiffer, J., Kaltschmidt, C., Israel, A., and Memet, S. (2003). Forebrain-specific neuronal inhibition of nuclear factor-kappaB activity leads to loss of neuroprotection. J. Neurosci. *23*, 9403-9408.

Greer, P.L., and Greenberg, M.E. (2008). From synapse to nucleus: calcium-dependent gene transcription in the control of synapse development and function. Neuron *59*, 846-860.

Hardingham, G.E., Arnold, F.J., and Bading, H. (2001). Nuclear calcium signaling controls CREB-mediated gene expression triggered by synaptic activity. Nat. Neurosci. *4*, 261-267.

Jordan, B.A., Fernholz, B.D., Khatri, L., and Ziff, E.B. (2007). Activity-dependent AIDA-1 nuclear signaling regulates nucleolar numbers and protein synthesis in neurons. Nat. Neurosci. *10*, 427-435.

Jordan, B.A., and Kreutz, M.R. (2009). Nucleocytoplasmic protein shuttling: the direct route in synapse-to-nucleus signaling. Trends Neurosci. *32*, 392-401.

Kaltschmidt, C., Kaltschmidt, B., Neumann, H., Wekerle, H., and Baeuerle, P.A. (1994). Constitutive NF-kappa B activity in neurons. Mol. Cell. Biol. *14*, 3981-3992.

Kwon, H.J., Breese, E.H., Vig-Varga, E., Luo, Y., Lee, Y., Goebl, M.G., and Harrington, M.A. (2004). Tumor necrosis factor alpha induction of NF-kappaB requires the novel coactivator SIMPL. Mol. Cell. Biol. *24*, 9317-9326.

Lai, K.O., Zhao, Y., Ch'ng, T.H., and Martin, K.C. (2008). Importin-mediated retrograde transport of CREB2 from distal processes to the nucleus in neurons. Proc. Natl. Acad. Sci. U. S. A. *105*, 17175-17180.

Lilienbaum, A., and Israel, A. (2003). From calcium to NF-kappa B signaling pathways in neurons. Mol. Cell. Biol. *23*, 2680-2698.

Lubin, F.D., and Sweatt, J.D. (2007). The IkappaB kinase regulates chromatin structure during reconsolidation of conditioned fear memories. Neuron *55*, 942-957.

Luo, Y., Kwon, H.J., Montano, S., Georgiadis, M., Goebl, M.G., and Harrington, M.A. (2007). Phosphorylation of SIMPL modulates RelA-associated NF-kappaB-dependent transcription. Am J Physiol Cell Physiol *292*, C1013-1023.

Mattson, M.P., and Meffert, M.K. (2006). Roles for NF-kappaB in nerve cell survival, plasticity, and disease. Cell Death Differ. *13*, 852-860.

Meberg, P.J., Kinney, W.R., Valcourt, E.G., and Routtenberg, A. (1996). Gene expression of the transcription factor NF-kappa B in hippocampus: regulation by synaptic activity. Brain Res. Mol. Brain Res. *38*, 179-190.

Meffert, M.K., Chang, J.M., Wiltgen, B.J., Fanselow, M.S., and Baltimore, D. (2003). NF-kappa B functions in synaptic signaling and behavior. Nat. Neurosci. *6*, 1072-1078.

Sarnico, I., Lanzillotta, A., Benarese, M., Alghisi, M., Baiguera, C., Battistin, L., Spano, P., and Pizzi, M. (2009). NF-kappaB dimers in the regulation of neuronal survival. Int. Rev. Neurobiol. *85*, 351-362.

Schmidt-Ullrich, R., Memet, S., Lilienbaum, A., Feuillard, J., Raphael, M., and Israel, A. (1996). NF-kappaB activity in transgenic mice: developmental regulation and tissue specificity. Development *122*, 2117-2128.

Thompson, K.R., Otis, K.O., Chen, D.Y., Zhao, Y., O'Dell, T.J., and Martin, K.C. (2004). Synapse to nucleus signaling during long-term synaptic plasticity; a role for the classical active nuclear import pathway. Neuron *44*, 997-1009.

Tomsig, J.L., and Creutz, C.E. (2000). Biochemical characterization of copine: a ubiquitous Ca2+-dependent, phospholipid-binding protein. Biochemistry (Mosc). *39*, 16163-16175.

Vig, E., Green, M., Liu, Y., Yu, K.Y., Kwon, H.J., Tian, J., Goebl, M.G., and Harrington, M.A. (2001). SIMPL is a tumor necrosis factor-specific regulator of nuclear factor-kappaB activity. The Journal of biological chemistry *276*, 7859-7866.

Whittaker, C.A., and Hynes, R.O. (2002). Distribution and evolution of von Willebrand/integrin A domains: widely dispersed domains with roles in cell adhesion and elsewhere. Mol. Biol. Cell *13*, 3369-3387.

Supplementary Figures

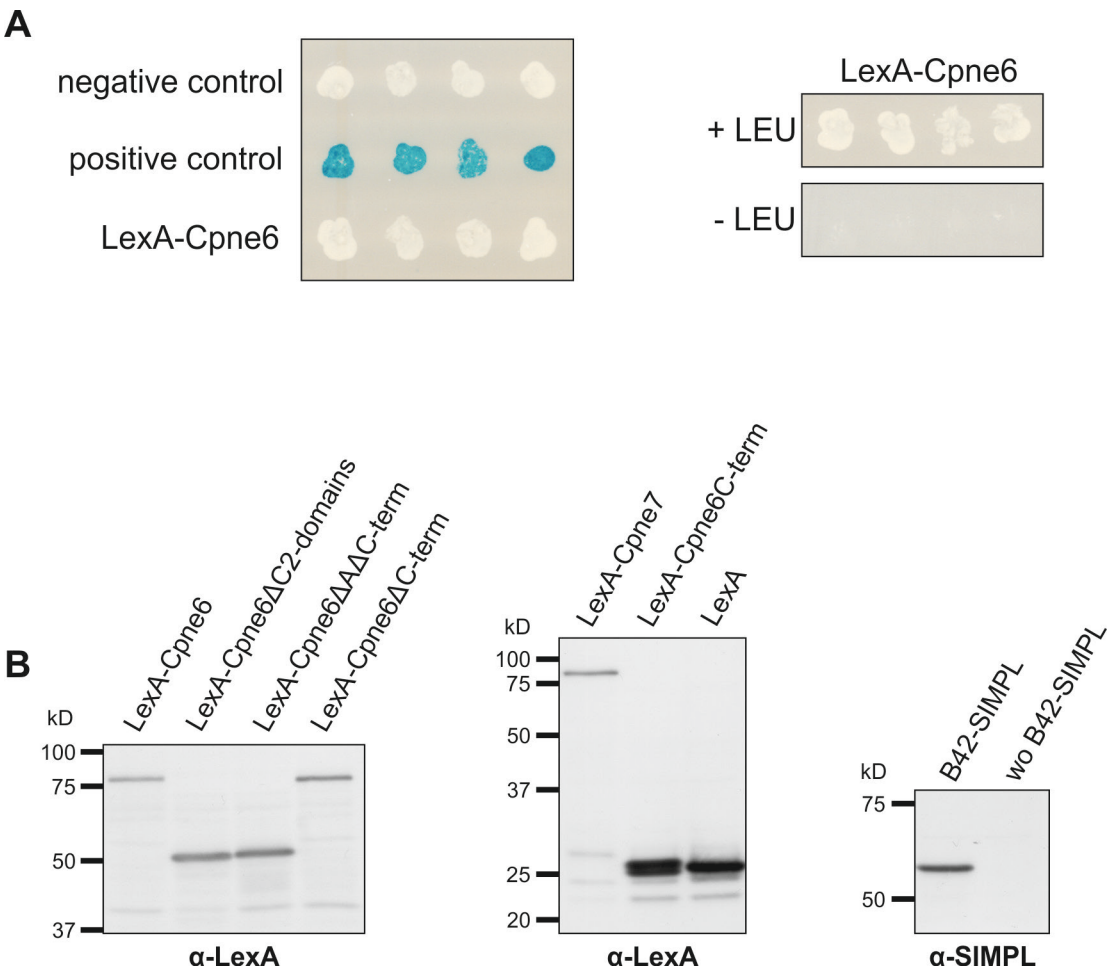

Supplementary Figure 1. Autoactivation and expression test of yeast expression constructs. (A) Testing the autoactivation potential of the Copine 6 bait construct (LexA-Cpne6). Yeast cells were transformed with indicated plasmids. The LexA-Cpne6 bait construct does not self-activate the lacZ reporter (left) or the leucine reporter (right). (B) The expression of the bait constructs was validated by Western blot analysis with LexA or SIMPL antibody.

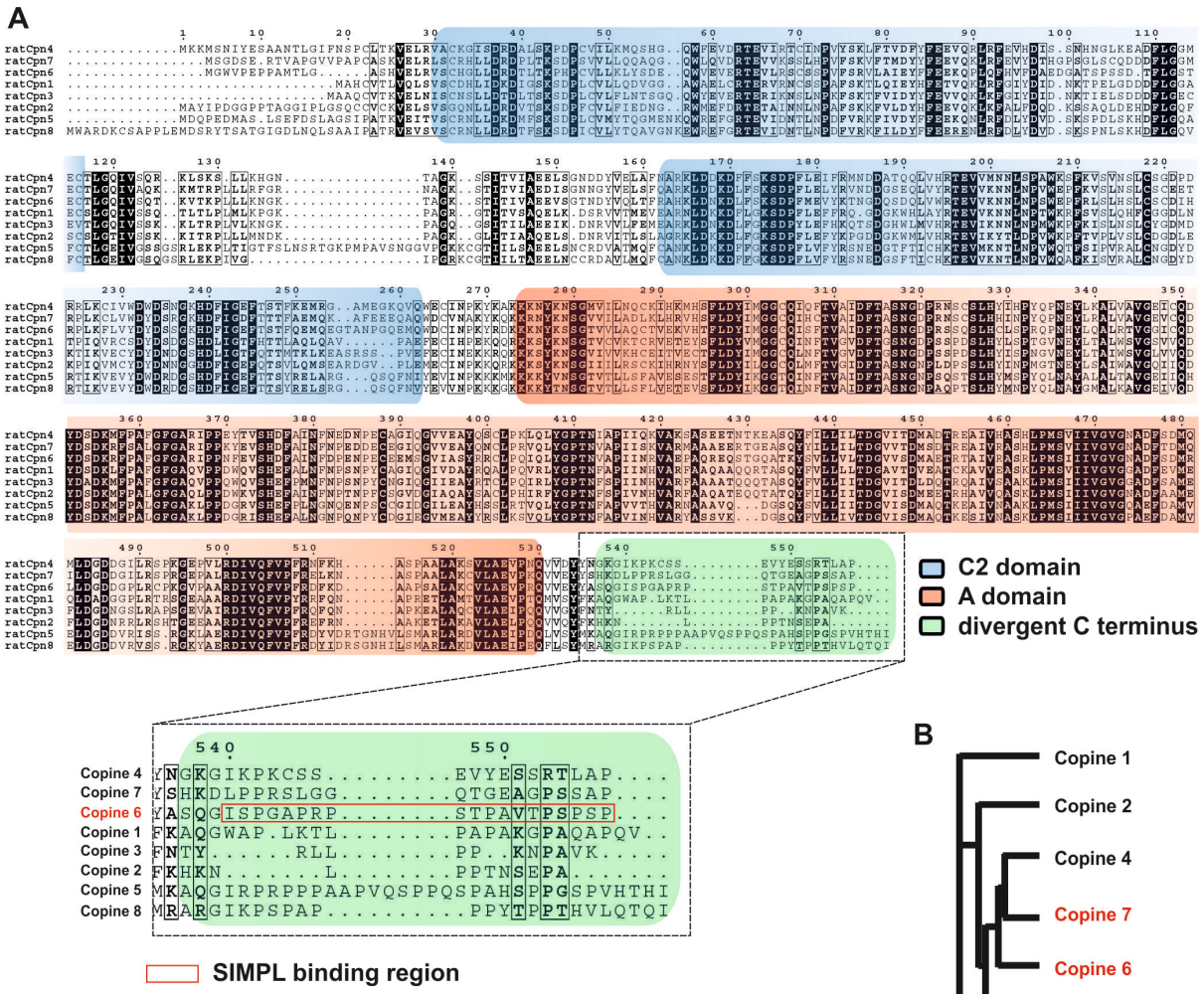

Supplementary Figure 2. The Copine family. (A) Amino acid sequences from Copine family members. Conserved residues are marked in black boxes. C-terminal region is magnified below. The SIMPL binding region is not conserved among Copine family members. (B) Relative homologies between Copine family members. Copine 7 is the most similar to Copine 6.

CHAPTER 5

Concluding discussion and perspectives

Discussion

This thesis aimed to characterize Copine 6 and to elucidate its putative involvement in synaptic plasticity. In Chapter 2, we extensively characterized the role of Copine 6 *in vitro* and provide evidence that Copine 6 acts as a calcium sensor that modulates spine number and stability upon changes in neuronal activity. We further identified Copine 6 to be essential for synaptic plasticity *in vivo* (Chapter 3). In an attempt to identify novel Copine 6 interacting partners, we performed a yeast-two hybrid screen (Chapter 4). We provide evidence that Copine 6 can influence transcriptional activity by preventing the translocation of its novel interaction partner, the NF-kappaB co-activator SIMPL (Chapter 4).

Copine 6 modulates spine number and plasticity

Loss of Copine 6 in culture increases the number of dendritic spines (Chapter 2 and 3). The formation and maturation of spines is caused by changes in the actin cytoskeleton (Luo, 2002). The supernumerous spines that are formed in absence of Copine 6 may therefore be caused by a perturbed regulation of the actin cytoskeleton. We demonstrate that Copine 6 changes its localization upon neuronal activity. Specifically, NMDA receptor activation and subsequent calcium influx recruits Copine 6 into the postsynaptic site (Chapter 2).

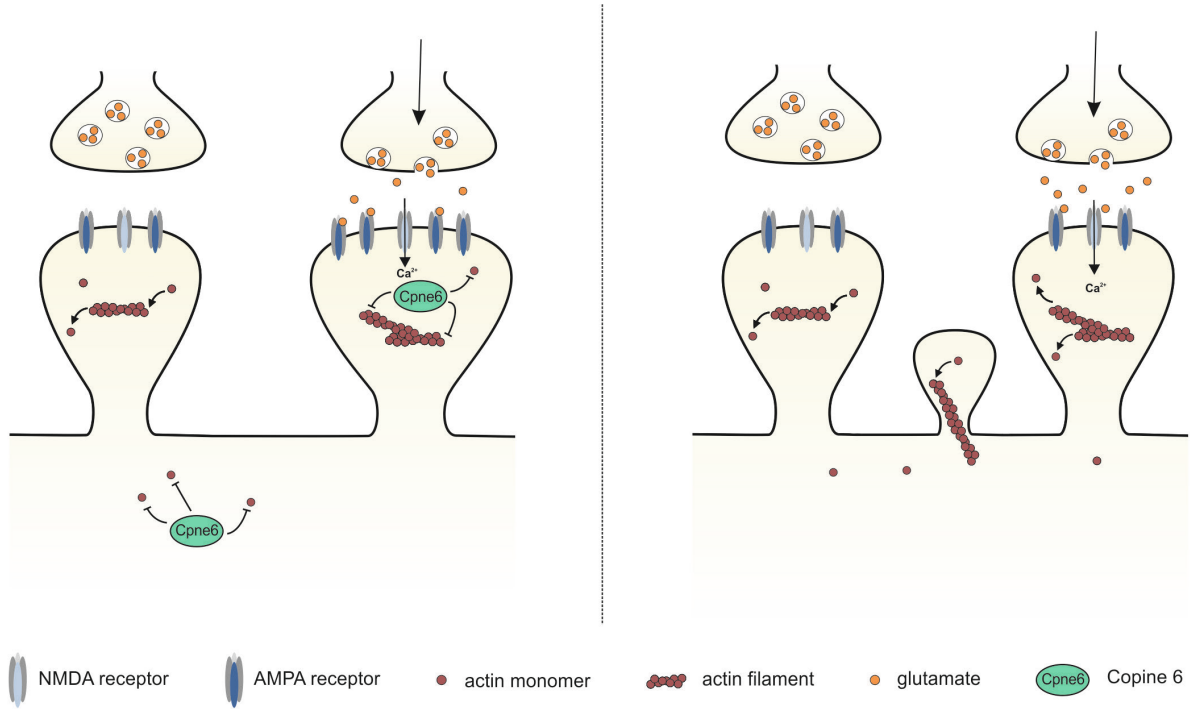

Figure 1. Model of Copine 6 function. (Left) In presence of Copine 6, actin remodeling is blocked in the dendritic shaft and existing filaments are stabilized in activated spines. (Right) Absence of Copine 6 increases actin remodeling in the shaft, which promotes spine formation (*in vitro*). In activated spines absence of Copine 6 leads to a failure in filament stabilization upon LTP (*in vivo*).

Due to its activity-dependent localization, Copine 6 has the potential to control the actin cytoskeleton at specific subcellular compartments in an activity-dependent manner. We propose a model in which the presence of Copine 6 in the dendritic shaft prevents actin polymerization and subsequent spine formation (Figure 1, right). Upon LTP induction, Copine 6 may be recruited into activated spines where it stabilizes actin filaments (Figure 1, right). Absence of Copine 6 *in vivo* prevents LTP because structural modification, such as insertion of additional AMPA receptor and increase in spine head are not consolidated after LTP induction (Figure 1, left).

The Copine 6-Rac1-Cofilin pathway links neuronal activity with actin remodeling

Spine formation and remodeling are both driven by modulations of the actin cytoskeleton (Dillon and Goda, 2005). The main pathways that control the actin cytoskeleton in neurons involve small GTPases with its family members Rac1, RhoA and Cdc42. Deregulation of the Rac1 pathway causes changes in overall neuronal morphology and, specifically, in dendritic spines (Dietz et al., 2012; Haditsch et al., 2009). The formation and maturation of the dendritic tree as well as spine formation occur during development also in absence of neuronal activity (Verhage et al., 2000). In contrast, spine remodeling during adulthood is governed by neuronal activity (Hotulainen et al., 2009). Since both processes involve Rac1-Cofilin signaling, it demands an upstream regulation specific for certain stimuli. We propose Copine 6 to be involved in this pathway and to provide specificity downstream of calcium signaling (Figure 2). In neurons, three guanine-nucleotide exchange factors GEFs that activate Rac1 have been identified. The GEF Tiam1 is present in developing neurons and its loss *in vitro* causes changes in the dendritic arborization and spine number, indicating a role during development (Tolias et al., 2005). A similar role has been proposed for the GEF βPIX (Saneyoshi et al., 2008). In contrast, the GEF kalirin-7 is mainly present in mature neurons and its absence mainly affects spine size (Xie et al., 2007). All these GEFs are phosphorylated and activated in an NMDA receptor-dependent manner (Saneyoshi et al., 2008; Tolias et al., 2005; Xie et al., 2007), providing a link between calcium signaling and Rac1 activation. Here, we show that Copine 6 is also involved in this signaling. We propose that Copine 6 differently from GEFs does not directly activate Rac1, but controls its localization. As it does this in an activity-dependent manner it can locally confine Rac1 activity and thus influence local actin remodeling.

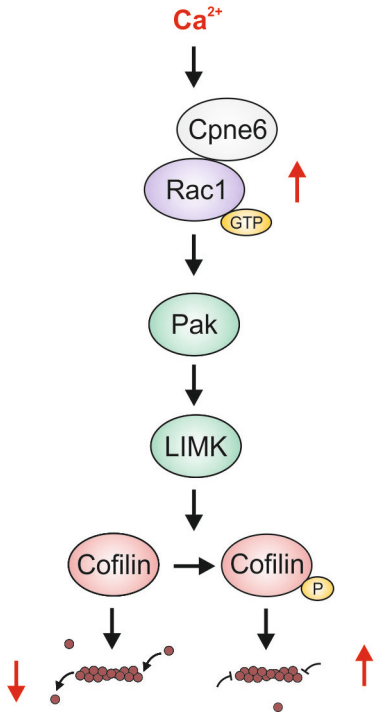

Figure 2. Copine 6-Rac1-Cofilin pathway. Presence of Copine 6 increases Rac1 activity, this in turn, induces phosphorylation of Cofilin. Phosphorylated Cofilin stabilizes actin filaments. As the localization of Copine 6 is dependent on the intracellular calcium concentration, Copine 6 spatially controls actin stabilization.

Perspectives

Copine 6-deficient mice, a novel animal model to study synaptic plasticity during adulthood

Spine remodeling upon changes in neuronal activity is a key mechanism of synaptic plasticity during adulthood (Bourne and Harris, 2008). *In vitro,* several molecules have been identified to mediate the translation of neuronal activity into structural changes of spines (Rex et al., 2010; Saneyoshi et al., 2008; Tolias et al., 2007; Xie et al., 2007). They all converge at the regulation of the actin cytoskeleton, finally responsible for morphological changes. Most of these spine regulators identified *in vitro* are not expressed only in the central nervous system and they are implicated in diverse neuronal processes. As a consequence, there is a lack of animal models with a confined deficit in synaptic plasticity. In contrast, Copine 6 expression is confined to mature excitatory neurons in the hippocampus (Chapter 3). In line with its expression, loss of Copine 6 *in vivo* does not interfere with the development of neuronal circuits but is critically involved in LTP expression. This makes Copine 6-deficient mice a very useful mouse model to specifically study synaptic plasticity during adulthood.

It is widely accepted that LTP is required for the formation of new memories (Morris, 1989; Morris et al., 1986). More specifically, LTP in the CA1 neurons of the hippocampus is essential for the formation of spatial memories (McHugh et al., 1996). Since Copine 6 KO mice lack LTP in CA1 neurons, one would expect that these mice have spatial memory deficits. This question will be addressed by testing the Copine 6 KO mice in hippocampus-dependent spatial memory test such as the Morris water maze.

The hippocampus of mice housed in standardized cages is not really challenged. In recent years, several lines of evidence indicated that housing mice in an enriched environment induces hippocampal remodeling (Bednarek and Caroni, 2011; Kondo et al., 2012; Lin et al., 2008; van Praag et al., 2000). As we propose that Copine 6 regulates activity-dependent spine remodeling, increasing hippocampal activity in Copine 6 KO mice by environmental enrichment might reveal changes in spine number/morphology and actin remodeling pathways.

Calcium signaling and subsequent actin remodeling in not only critical for LTP, but it is also essential for LTD expression (Collingridge et al., 2010). Thus future experiments should also address the role of Copine 6 in LTD.

Copines in the brain

In this thesis, we focused on only one member of the Copine family, which consists of nine members in mammals. In the adult mouse brain, different Copines are expressed in different brain areas (http://www.brain-map.org). It would be interesting to analyze if Copines share some roles and exhibit them only in restricted brain areas or if they are functionally diverse.

References

Bednarek, E., and Caroni, P. (2011). beta-Adducin is required for stable assembly of new synapses and improved memory upon environmental enrichment. Neuron *69*, 1132-1146.

Bourne, J.N., and Harris, K.M. (2008). Balancing structure and function at hippocampal dendritic spines. Annu. Rev. Neurosci. *31*, 47-67.

Collingridge, G.L., Peineau, S., Howland, J.G., and Wang, Y.T. (2010). Long-term depression in the CNS. Nat. Rev. Neurosci. *11*, 459-473.

Dietz, D.M., Sun, H., Lobo, M.K., Cahill, M.E., Chadwick, B., Gao, V., Koo, J.W., Mazei-Robison, M.S., Dias, C., Maze, I.*, et al.* (2012). Rac1 is essential in cocaine-induced structural plasticity of nucleus accumbens neurons. Nat. Neurosci.

Dillon, C., and Goda, Y. (2005). The actin cytoskeleton: integrating form and function at the synapse. Annu. Rev. Neurosci. *28*, 25-55.

Haditsch, U., Leone, D.P., Farinelli, M., Chrostek-Grashoff, A., Brakebusch, C., Mansuy, I.M., McConnell, S.K., and Palmer, T.D. (2009). A central role for the small GTPase Rac1 in hippocampal plasticity and spatial learning and memory. Mol. Cell. Neurosci. *41*, 409-419.

Hotulainen, P., Llano, O., Smirnov, S., Tanhuanpaa, K., Faix, J., Rivera, C., and Lappalainen, P. (2009). Defining mechanisms of actin polymerization and depolymerization during dendritic spine morphogenesis. J. Cell Biol. *185*, 323-339.

Kondo, M., Takei, Y., and Hirokawa, N. (2012). Motor protein KIF1A is essential for hippocampal synaptogenesis and learning enhancement in an enriched environment. Neuron *73*, 743-757.

Lin, Y., Bloodgood, B.L., Hauser, J.L., Lapan, A.D., Koon, A.C., Kim, T.K., Hu, L.S., Malik, A.N., and Greenberg, M.E. (2008). Activity-dependent regulation of inhibitory synapse development by Npas4. Nature *455*, 1198-1204.

Luo, L. (2002). Actin cytoskeleton regulation in neuronal morphogenesis and structural plasticity. Annu. Rev. Cell. Dev. Biol. *18*, 601-635.

McHugh, T.J., Blum, K.I., Tsien, J.Z., Tonegawa, S., and Wilson, M.A. (1996). Impaired hippocampal representation of space in CA1-specific NMDAR1 knockout mice. Cell *87*, 1339-1349.

Morris, R.G. (1989). Synaptic plasticity and learning: selective impairment of learning rats and blockade of long-term potentiation in vivo by the N-methyl-D-aspartate receptor antagonist AP5. J. Neurosci. *9*, 3040-3057.

Morris, R.G., Anderson, E., Lynch, G.S., and Baudry, M. (1986). Selective impairment of learning and blockade of long-term potentiation by an N-methyl-D-aspartate receptor antagonist, AP5. Nature *319*, 774-776.

Rex, C.S., Gavin, C.F., Rubio, M.D., Kramar, E.A., Chen, L.Y., Jia, Y., Huganir, R.L., Muzyczka, N., Gall, C.M., Miller, C.A.*, et al.* (2010). Myosin IIb regulates actin dynamics during synaptic plasticity and memory formation. Neuron *67*, 603-617.

Saneyoshi, T., Wayman, G., Fortin, D., Davare, M., Hoshi, N., Nozaki, N., Natsume, T., and Soderling, T.R. (2008). Activity-dependent synaptogenesis: regulation by a CaM-kinase kinase/CaM-kinase I/betaPIX signaling complex. Neuron *57*, 94-107.

Tolias, K.F., Bikoff, J.B., Burette, A., Paradis, S., Harrar, D., Tavazoie, S., Weinberg, R.J., and Greenberg, M.E. (2005). The Rac1-GEF Tiam1 couples the NMDA receptor to the activity-dependent development of dendritic arbors and spines. Neuron *45*, 525-538.

Tolias, K.F., Bikoff, J.B., Kane, C.G., Tolias, C.S., Hu, L., and Greenberg, M.E. (2007). The Rac1 guanine nucleotide exchange factor Tiam1 mediates EphB receptor-dependent dendritic spine development. Proc. Natl. Acad. Sci. U. S. A. *104*, 7265-7270.

van Praag, H., Kempermann, G., and Gage, F.H. (2000). Neural consequences of environmental enrichment. Nat. Rev. Neurosci. *1*, 191-198.

Verhage, M., Maia, A.S., Plomp, J.J., Brussaard, A.B., Heeroma, J.H., Vermeer, H., Toonen, R.F., Hammer, R.E., van den Berg, T.K., Missler, M.*, et al.* (2000). Synaptic assembly of the brain in the absence of neurotransmitter secretion. Science *287*, 864-869.

Xie, Z., Srivastava, D.P., Photowala, H., Kai, L., Cahill, M.E., Woolfrey, K.M., Shum, C.Y., Surmeier, D.J., and Penzes, P. (2007). Kalirin-7 controls activity-dependent structural and functional plasticity of dendritic spines. Neuron *56*, 640-656.

Acknowledgments

First of all, I would like to thank Markus Rüegg for providing an ideal environment to learn how to perform scientific research. I very much appreciate his always “open door”, his willingness for advice and critical discussion, his support and guidance, his confidence and resulting grant of liberties to attain self-reliance.

Thanks to all the past and current Rüegg lab members that were part of our team during the last four years: Alexander Kriz, Andrea Erni, Andrin Wacker, Anna Rostedt Punga, Anny Schäfer, Barbara Kupr, Cyrille Delley, David Hollinger, Dimitri Cloëtta, Filippo Oliveri, Florian Bentzinger, Klaas Romanino, Leonie Enderle, Lionel Tintignac, Manuel Schweighauser, Manuela von Arx, Marcin Maj, María Fernández, Nathalie Rion, Nathalie Wenger, Nico Angliker, Regula Lustenberger, Sarina Meinen, Shuo Lin, Venus Thomanetz and Verena Albert for being on hand with help and advice.

I would like to thank Bernhard Bettler for accepting to be co-referee of this thesis and Heinrich Reichert for chairing the exam.

Thanks to all the people working in the animal facility for taking care of all mice involved in this project.

I am thankful to my parents and brothers for always remaining steadfastly at my side.